UNIVERSITY OF ROSTOCK

FUCULTY OF AGRICULTURAL AND ENVIRONMENTAL SCIENCES

EVALUATION OF THE IMPACT OF CLIMATE CHANGE ON HYDROPOWER GENERATION IN ETHIOPIA, A CASE OF UPPER AWASH RIVER BASIN

Keneni Elias Shoro

THESIS SUBMITTED FOR THE DEGREE

DOCTOR OF ENGINEERING (Dr.-Ing.)

University of Rostock, Germany

Rostock, 2020

https://doi.org/10.18453/rosdok_id00002974

Reviewer

Prof. Dr. Konrad Miegel, University Rostock, Professor for Hydrology and Applied Meteorology

Prof. Dr. Markus Disse, Technical University of Munich, Chair of Hydrology and River Basin Management

Prof. Dr. Hartmut Wittenberg, Leuphana University Lüneburg, Institut for Ecology

Submitted 2019

Defence 2020

Declaration and Copyright

I, Keneni Elias Shoro, declare that this thesis entitled "***EVALUATION OF THE IMPACT OF CLIMATE CHANGE ON HYDROPOWER GENERATION IN ETHIOPIA, A CASE OF UPPER AWASH RIVER BASIN***", is an original report of my research, has been written by me and has not been submitted for any previous degree. The experimental work is almost entirely my own work; the collaborative contributions have been indicated clearly and acknowledged. Due references have been provided on all supporting literatures and resources. I declare that this thesis was composed by myself, that the work contained herein is my own except where explicitly stated otherwise in the text, and that this work has not been submitted for any other degree or professional qualification.

ACKNOWLEDGEMENTS

Blessed be the LORD for He hath showed me His marvellous kindness in a strong city. For I said in my haste, I am cut off from before thine eyes; nevertheless, thou heardest the voice of my supplications when I cried unto thee.

What words shall I use to express my deepest and sincere appreciation to you Dear Professor Miegel? Lo to your patience! Eight solid years are in fact beyond patience. Whatever the reasons behind my sufferings, including my own weaknesses, it is amazing and quite unique that you didn't lose your trust on me. God bless you to the rest of your life together with all your family members.

I really admire Professor Konrad Miegel, my main supervisor, for his advice, suggestions, encouragement, guidance and support for the realization of my research work from the beginning to the end. He devoted his precious time and energy in offering me constructive suggestions, and also in coming to my study area, which indeed required him to bear the hardship of unpleasant infrastructures.

My sincere appreciation also goes to Dr. Semu Ayalew Moges, my co-supervisor, for his initiation of the idea of the study and his advice, comments, and in granting me so many useful documents and data, right from the beginning. By the way, Dr Semu also played a great role when I attended my second degree in Arba Minch University, Ethiopia.

Professor Dr. Eng. Alemayehu Gebisa, one of the VIP's, helped me a lot in communicating with my Supervisor, Prof. Dr Konrad Miegel. Apart from this, he gave me frequent and consistent advices during my sufferings and temptations. He played the major role in arranging accommodations and also in all processes required to be enrolled to the University of Rostock. God bless you and thank you a lot dear Professor.

I would like to express my appreciation to Dr. Kassa Tadele, Dr. Habtamu Etefa, Dr Belete Berhanu, Dr. Tamene Adugna and Dr. Fisiha Behulu for their kind support during the research work, which was of course full of many temptations and challenges.

So many institutions and individuals were helpful for the accomplishment of the research. Ethiopian Capacity Building Program (ECBP), DAAD, Ministry of Education of the Federal Democratic Republic of Ethiopia and Jimma University played great role in my journey of completing the PhD study. I thank all of them.

Many institutions offered me data and information that I used as inputs for the realization of the research. Among others, Ministry of Water, Irrigation and Energy, Ethiopian Electric Utility, National Meteorology Agency, Koka Hydropower Station, Awash II and Awash III Hydropower stations and Wonji Shoa Sugar Factory played their roles in delivering me useful information that I used as inputs for my research in one way or another. Mr Mohammad, a Hydrologist in the Ministry of Water, Irrigation and Energy, was one of the individuals who helped me in delivering many useful data and information, both as a staff of the Ministry as well as personally. I want to say thank you all.

ABSTRACT (Deutsch)

Das Ziel dieser Studie besteht darin, die Auswirkungen des Klimawandels auf die Generierung von Wasserkraft in Äthiopien zu bewerten. Dies erfolgte beispielhaft im oberen Teil des Awash River Einzugsgebietes, das als Kerngebiet und bezüglich der Generierung von Wasserkraftenergie als repräsentativ für Äthiopien angesehen werden kann. Die Ergebnisse verdeutlichen den Einfluss veränderter Klimavariablen auf die lokalen hydrologischen Verhältnisse und davon ausgehend auf die Energiedargebot durch Wasserkraft. Genauso wie Klimaexperten versuchen Projektionen für das künftige Klima zu entwickeln, indem sie die das Klima der Vergangenheit und Zukunft simulieren, ist es bedeutsam und erforderlich, auf dieser Grundlage Aussagen zur Verfügbarkeit von Wasserkraftenergie zu machen. In diesem Zusammenhang ist der Niederschlag der wichtigste Parameter, da er für die Abflussbildung und somit die Energieproduktion auf der Grundlage von Wasserkraft entscheidend ist. Entsprechende Ergebnisse machen es den Wissenschaftlern, Fachleuten, Planern und politischen Entscheidungsträgern möglich, gut begründete Strategien zu entwickeln und implementieren, um nachteilige Entwicklungen und negative Auswirkungen des Klimawandels auf den Energiesektor zu lindern

In dieser Studie werden gut begründet zwei Klimaszenarios mit ihren Auswirkungen auf die Produktion von Wasserkraftenergie betrachtet, nämlich die Szenarien RCP4.5 und RCP8.5, definiert durch das IPCC in seinem fünften Synthesebericht AR5. Dies erfolgte mit einer dafür geeigneten Modellkette, durch die Klima, Hydrologie und Wasserkraft miteinander verknüpft werden. Dabei kam das physikalisch begründete Modell SWAT zu Einsatz, um die hydrologischen Prozesse und insbesondere das Abflussgeschehen zu simulieren. Die verwendeten meteorologischen Eingangsgrößen sind Maximum- und Minimumtemperatur, Niederschlag, Globalstrahlung, relative Luftfeuchte und Windgeschwindigkeit, aufgezeichnet an verschiedenen Klimastationen innerhalb des Einzugsgebietes.

In den Aufzeichnungen waren an allen Stationen etliche Datenlücken zu verzeichnen. Sie zu füllen war mit einem hohen Aufwand verbunden. Dafür kam mit dem Statistical Downscaling Model SDSM ein Werkzeug zum Einsatz, das ein Tool zur Generierung von Wetterdaten und Szenarios aufweist.

Die Software SWAT-CUP wurde für die Modellkalibrierung von SWAT und die Analyse von Modellunsicherheiten verwendet. Maßgebliches Kriterium war dabei die Überein-

stimmung von simulierten und beobachteten Abflüssen, wobei letztere durch das zuständige Ministerium bereitgestellt worden sind. Für die Verarbeitung der Klima- und hydrologischen Daten kam weitere, zugehörige Software zum Einsatz. Dazu gehören pcpSTAT.exe, dew.exe and dew02.exe, die u. a. verwendet worden sind, um langjährige Monatsmittelwerte von Klimavariablen, insbesondere von Temperatur und Niederschlag, zu generieren.

Im Anschluss an die hydrologische Modellierung kam das Modell WEAP zum Einsatz, um die monatliche Wasserkraftenergie des Koka-Speichers zu berechnen, und zwar für die Vergangenheit, als auch in Form der Szenarios für die Zukunft. Vor dem Modelleinsatz war nachzuweisen, dass die Modelle geeignet sind, um das Geschehen im Untersuchungsgebiet zielgerichtet (siehe oben) und ausreichend genau abzubilden.

Durch Anwendung der Modelle liegen Ergebnisse zum Abfluss, zur Speicherfüllung, zur Evaporation und zur Wasserkraft bis zum Jahr 2100 vor. Für die Auswertung der Ergebnisse wurde der Projektionszeitraum in die Teilzeiträume 2019 – 2040, 2041 – 2070 und 2071 – 2100 unterteilt. Die Ergebnisse verdeutlichen im Vergleich zum Referenzzeitraum, dass beim Szenario RCP8.5 die Wasserkraftenergie in den letzten beiden Dekaden vor 2100 um ca. 15 % geringer ausfallen würde. Dieses Szenario entspricht dem „business as usual“, bei dem keine Maßnahmen des Klimaschutzes eingeleitet werden. Die Ergebnisse machen deutlich, dass durch die Weltgemeinschaft ein Weiterso nicht akzeptiert werden kann.

Auch wenn nicht einheitlich, so ergibt das RCP4.5-Szenario in allen drei Perioden im Vergleich zur Referenzperiode eine Zunahme der Energieproduktion durch Wasserkraft. Der Zuwachs beträgt 7,8 %, 1,5 % und 0,9 %. Die Zahlenwerte zeigen insbesondere bei diesem Szenario an, dass der anfänglich stärkere Zuwachs ab etwa der Mitte des 21. Jahrhunderts wieder rückläufig ist.

ABSTRACT

The core aim of this study is to evaluate the impact of climate change on hydropower generation in Ethiopia, taking a river basin, which can be considered as the nucleus of the country, Upper Awash River Basin, as a bench mark. The research work addresses the influence of global climate change on local hydrology and as a result on hydropower. Just as professionals in the science of climate change try to project future climate variables based on the past and current situation of climate pattern, it is important that future hydropower energy is also projected as it is directly dependent on precipitation, one of the most important climate variable. This enables the planners, researchers, related professionals and policy makers to implement reasonable policies to mitigate the adverse and negative effects of climate change on energy sector.

In this study, two scenarios of hydropower generation were developed based on two scenarios of climate change, namely RCP4.5 and RCP8.5, formulated by IPCC in the fifth assessment report, AR5. It is considered reasonable to relate the projection of climate change with future hydropower production. Sequences of related software were utilized to associate climate and hydrology with hydropower. A physically-based, semi-distributed hydrological model, SWAT, was used to simulate hydrological responses in general and streamflow in particular. The input data used for SWAT model were weather data: maximum and minimum temperature, precipitation, solar radiation, relative humidity and wind speed recorded at meteorological stations located in the river basin. There are so many missing values in the raw data obtained from almost all meteorological stations that required a lot of energy and time to be filled. A decision support tool, Statistical Downscaling Model (SDSM) was used for this purpose, as it has a weather and scenario generation function.

SWAT-CUP software was used for calibration and uncertainty analysis of the distributed watershed model. The simulated streamflow was compared with the observed streamflow data, obtained from Ministry of Water, Irrigation and Energy. For the detail processing of climate and hydrological elements, other related software's were also used. Some of them include pcpSTAT.exe, dew.exe and dew02.exe, which are used to generate long-years monthly averages of climate variables, in particular temperature and precipitation.

Having completed the hydrological processes part, WEAP model was used to simulate monthly hydropower generation from Koka Reservoir for the current as well as for future

period. The performances of these and other models have been accordingly evaluated to work with them. Thus, having ensured the applicability of the models to the study area, climate change scenarios and the resulting future hydropower production were used to reveal the impact of climate change.

The streamflow, reservoir storage, evaporation and hydropower, using the respective models, were simulated till 2100, dividing the century into three long periods, of course excluding the reference period. The three future periods were 2019 – 2040, 2041 – 2070 and 2071 – 2100. The results of simulation revealed that there will be a decrease in energy by 15.1% in the last two decades of the 21st Century under RCP8.5 scenario as compared to the reference period of 2006 – 2014. This scenario is the extension of the business as usual scenario under which there is no policy for alleviating the harsh effect of climate change. This certainly calls for special attention of the world community.

As to RCP4.5 scenario, though variable, it was seen that there will be an increase in energy production in all the three periods as compared to the reference period. The increase in energy for the periods 2019 – 2040, 2041 – 2070, and 2071 – 2100 was predicted to be respectively, 7.8%, 1.5% and 0.9%. But as can be seen from the percentages, the increment itself has a decreasing tendency going further in the future even for this middle concentration scenario.

TABLE OF CONTENTS

ABBREVIATIONS

95PPU	95 percent prediction uncertainty
AR4	fourth assessment report
AR5	fifth assessment report
ARMA	autoregressive moving average model
ARS	Agricultural Research Service
BASINS	Better Assessment Science Integrating Point and Nonpoint Sources
BUA	business as usual
CGCM	coupled general Circulation Model
CLIVAR	climate variability
CM	climate modellers
CMIP5	coupled model intercomparison project phase 5
CMS	Cubic meter per second
CN	Curve Number
CORDEX	Coordinated Regional Downscaling Experiment
CREAMS	Chemicals, Runoff, and Erosion from Agricultural Management Systems
DEM	Digital Elevation Model
DWSM	Dynamic Watershed Simulation Model
EEU	Ethiopian Electric Utility
EPIC	Environmental Impact Policy Climate
EU	European Union
FAO	Food and Agriculture Organization
GCAM	Global Change Assessment Model
GenScn	Generation and analysis of model simulation Scenarios
GHG	greenhouse gases
GIS	Geographic Information System
GLEAMS	Groundwater Loading Effects on Agricultural system
GLUE	Generalized Likelihood Uncertainty Estimation
HBV	Hydrologisika Bayraans Vattenbalans-avediling
HEC	Hydrologic Engineering Center
HEC-ResSim	Hydrologic Engineering Center Reservoir simulation model
HRU	Hydrologic Response Units
HSPEXP	Expert System for HSPF hydrology calibration

HSPF	Hydrological Simulation Program-FORTRAN
IAM	Integrated Assessment Models
IFPRI	International Food Policy Research Institute
IIASA	International Institute for Applied Systems Analysis
IMAGE	Integrated Model to Assess the Global Environment
IMPLND	HSPF parameter for Impervious Land
IPCC	Intergovernmental Panel on Climate Change
IR	infra red
IS92	emission scenarios report of 1992
ITCZ	Inter-Tropical Convergence Zone
IWRM	Integrated Water Resources Management
JGCRI	Joint Global Change Research Institute
LH-OAT	Latin Hypercube One at a Time
LSMs	Land Surface Models
masl	meter above sea level
MCM	million cubic meter
MCMC	Markov Chain Monte Carlo
MESSAGE	Model for Energy Supply Strategy Alternatives and their General Environmental Impact
MIKE SHE	European Hydrological System model (From Danish Hydraulic Institute)
MIWE	Ministry of Irrigation, Water and Energy
NASA	National Aeronautics and Space Administration
NCEP	National Centre for Environmental Prediction
NIES	National Institute for Environmental Studies
NMA	National Meteorology Agency
NSE	Nash-Sutcliffe efficiency
ParaSol	Parameter Solution
PBIAS	percent bias
PERLND	HSPF parameter for Pervious Land
ppmv	part per million by volume
PSO	Particle Swarm Optimization
RCHRES	Stream Reaches
RCP	Representative Concentration Pathways

RMSE	Root Mean Square Error
RSR	RMSE standard deviation ratio
SCS	Soil Conservation Service
SDSM	Statistical Downscaling Model
SEI	Stockholm Environmental Institute
SRES	Special Report on Emission Scenarios
SUFI-2	Sequential Uncertainty Fitting version 2
SWAT	Soil and Water Assessment Tool
SWAT-CUP	SWAT Calibration and Uncertainty Programs
SWRRB	Simulator for Water Resources in Rural Basins
TOPMODEL	Topographic-Based Model
UARB	Upper Awash River Basin
UNDP	United Nations Development Program
USDA	United States Department of Agriculture
USI	User Control Input
VIC	Variable Infiltration Capacity
WDM	Watershed Data Management
WDMUtil	Watershed Data Management Utility
WEAP	Water Evaluation and Planning
WinHSPF	Windows version of HSPF
WQ	Water quality
WM	Water movement
WWDSE	Waterworks Design and Supervision Enterprise

SYMBOLS

CO_2	Carbon dioxide
°C	Degree Celsius
W/m^2	Watt per square meter
°F	Degree Fahrenheit
CH_4	Methane
N_2O	Nitrous oxide
CFCs	Chlorofluorocarbons
O_3	Ozone
OH	Hydroxide
HCFCs	Hydrochlorofluorocarbons
SO_2	Sulphur dioxide
Q	Discharge
S	Storage
I	Inflow
t	Time
Δ	Change (delta)
Ω	Ohm
kVA	kilovolt ampere
kWh	kilowatt-hour
R^2	coefficient of determination
GWh	Gigawatt-hour

LIST OF FIGURES

LIST OF TABLES

CHAPTER 1

1. INTRODUCTION

1.1 Background

The observational evidence from all continents and most oceans shows that many natural systems are being affected by regional climate changes, particularly temperature increases (IPCC, 2007). Climate change can occur naturally as well as because of anthropogenic activities. In the natural cause of climate, the complex interactions between components of the climate system maintain the equilibrium of the change naturally. However, since mankind started agriculture about eight thousand years ago, their activities began influencing the climate system (Jung, 2006). The most energy source, on which the world population at large is relying on so far, in order to meet the energy demand, is fossil fuel. The extravagant use of the fossil fuels as primary energy sources has led to the rise in carbon dioxide (CO_2), the most prominent greenhouse gas (GHG).

As the most important component GHG forcing, global CO_2 concentrations have increased from a preindustrial level of 280 ppmv to 370 ppmv at the beginning of the 21st century (Jung, 2006). Apart from using fossil fuels for transportation as well as for industries, human being also expanded agriculture, which is mostly characterized by clearing land. Burning down of forests releases enormous amount of CO_2 to the atmosphere.

The greenhouse effect is actually essential to life on Earth. The problem, however, is that by releasing huge amounts of carbon dioxide (from the burning of fossil fuels) into the atmosphere, humans are increasing the amount of greenhouse gases in the atmosphere. In fact humans have increased the amount of CO_2 in the atmosphere from around 600 giga-tonnes to almost 800 giga-tonnes in the last century. The big question of course is: what effect will this have on the total greenhouse effect (Burrows, 2009).

All the basic chemistry and physics of the interactions of the greenhouse gases with the atmosphere have been studied in great detail. It is known very well how the gases interact with the infra red (IR) radiation from the Earth and the thermodynamics of the Earth's energy balance is also well known. Laboratory experiments and observations of both the Earth and other planets confirm the basic science. Furthermore, the biggest science

experiment in human history is being run by pouring massive amounts of carbon dioxide into the atmosphere and waiting to see what happens! Unfortunately, however, humans can't wait to run the real experiment to the end because that will a) take many centuries to run its course, and b) most likely result in catastrophic and irreversible changes (for mankind) to the climate (Burrows, 2009).

Every year these emissions add to the carbon already present in atmospheric carbon dioxide a further seven thousand million tonnes, much of which is likely to remain there for a period of a hundred years or more (Houghton, 2004). Because carbon dioxide is a good absorber of heat radiation coming from the Earth's surface, increased carbon dioxide acts like a blanket over the surface, keeping it warmer than it would otherwise be. With the increased temperature the amount of water vapour in the atmosphere also increases, providing more blanketing and causing it to be even warmer. The Intergovernmental Panel on Climate Change (IPCC) has reported in the fifth assessment report (AR5) that the globally averaged combined land and ocean surface temperature data as calculated by a linear trend, show a warming of 0.85 [0.65 to 1.06] °C, over the period 1880 to 2012. The panel further indicated that for the longest period when calculation of regional trends is sufficiently complete (1901 to 2012), almost the entire globe has experienced surface warming (IPCC, 2013).

Given the apparent change in climate due essentially to anthropogenic interferences, the traditional simple computation of streamflow for the purpose of hydropower generation is not adequate. Also, given the extraordinary concern offered to the climate change by the world community, very few or no decision makers are unaware of the subject matter. There is clear recognition that climate change information ought to be considered, but there is little experience with how to incorporate the seemingly complex science into design and operational decisions (Block and Brown, 2008). Not only do future hydropower projects require special attention of climate change patterns, but the existing hydropower schemes in Ethiopia need to be evaluated against their design discharge, taking climate change as another very essential hydropower "parameter".

It is anticipated that climate change may result in water shortages for settlements, industry and societies; reduced hydropower generation potentials; and it may cause population migration.

1.2 Problem Statement

In Ethiopia, where more than 90% of the energy supplies are from hydropower, the study of the impact of climate change on hydropower generation has no substitute. Many studies related to water resources have been conducted in river basins level in Ethiopia, especially in Upper Awash and Blue Nile River Basins. While the effect of landuse landcover and climate changes on hydrological regime, watershed sediment yield modelling and modelling of hydrological processes themselves and many other similar researches have been carried out, (for example, Kinfe, 1999; Dilnesaw, 2006; Habtom, 2009; Block, 2010; Habtamu, 2011; International Food Policy Research Institute (IFPRI), 2011), it is hardly possible to get studies revealing the impact of climate change on hydropower generation, particularly of Upper Awash River Basin.

Major Rivers such as Akaki, Mojo, Melka Kunutre and Teji are the sources of water in Koka reservoir. These rivers are highly exploited for other purposes, for example, for irrigation and water supply. Since Koka hydropower plant has been established, the population of Ethiopia increased nearly four times. Upper Awash River Basin is very densely populated area, including the capital Addis Ababa and nearby city of Bishoftu. The demand for water is highly increasing upstream of the plants and limited water reaches the reservoir. Furthermore, even between Koka Hydroelectric power and Awash II and III Hydroelectric power plants, Wonji Shoa Sugar Factory is located. Sugarcane plantation is irrigated using the water from Koka Dam. Apart from the plantation, many farmers privately use the water from the dam for irrigation purpose. Still, before it reaches the downstream Awash II and III hydropower plants, for the purpose of water supply, much amount of water is abstracted from the reservoir to Adama; a densely populated city located 100 km southeast of Addis Ababa. Even though these factors related to water use are so serious, they can be handled to some extent with a good water resources management and with improved technology. But the case of climate change impact is worldwide, and the best water resources management and utilization of the latest improved technologies are not adequate in alleviating the negative impact of climate change.

Additionally and most importantly, the previous design of the hydropower plant didn't take into account the possible impact of climate change, the subject matter of this research. The impact of climate change on the River Basin is two-sided. On the one hand, the hydropower plants and the population in general suffer from lack of adequate water during

water stress seasons. On the other hand, during rainy season, especially when there are events such as El Nino and floods, the areas downstream of Koka Dam are highly affected by flood; in extreme cases, loss of life of some inhabitants and animals, and serious damage to properties may occur. The issue of climate change is as equally important as management issue of utilization of water for various purposes. The situation of climate change should not be taken for granted. It is global issue and requires a special attention.

This study deals with the impact of climate change on hydropower generation of the country, taking this River Basin as a case. Unfortunately, the issue of landuse changes, irrigation and the management of water allocation are beyond the scope of this research.

1.3 Significance of the Study

The demand for energy is expected to grow at an alarming rate in Ethiopia. In the past twenty years, many industries have been established in different parts of the country. In those two decades, the population of the country doubled, i.e., it grew from about 42 million to more than hundred million. The awareness and living standard of the people is being greatly improved, thanks to science and technology. Infrastructures have been greatly developed in almost all regions of the country. More than fifty universities have been commissioned to date. About ten new sugar factories are ongoing currently. Many radical changes can be pointed out. All of these and other multitudes of activities seriously need energy.

About 90% of the energy required for all of these activities comes from hydropower. Of course, the country is endowed with huge hydropower potential. On the other hand, the current global issue of climate change came to be a big challenge for this huge potential clean energy source. In order to tackle the negative impact of climate change, the knowledge of it is compulsory. Thus, scientists and decision makers are busy day in and day out to look for solution so that sustainable development is ensured without compromising the life of the current and future generation.

As one country suffering from the negative impact of climate change and global warming, Ethiopia has already designed a clean energy strategy to alleviate the impacts to the extent possible. This requires making researches including projection of climate future scenario based on global situations. In this study, it is believed that some contribution can

be made to the country's effort to some extent, taking the research output from the River Basin as an example to extend further.

1.4 Scope of the Study

This study will explore the climate change processes, the natural factors behind the climate change and the human activities that worsen this global event in the context of Ethiopia. It associates the hydrological aspects of climate change with hydroelectric power generation. The study proceeds further and will develop time series of hydropower energy from Koka Reservoir till the end of the 21st Century, as related to climate scenarios established by IPCC. The main focus of the research is relating current and future precipitation to streamflow, the core parameter of hydropower generation.

The effect of the change of precipitation on streamflow and in turn the fluctuation of streamflow on hydropower generation will be the nucleus of the study. In fact many other factors such as landuse changes may affect streamflow and hydropower generation. But this study is confined to the impact of climate change.

1.5 Objectives of the Study

The aim of this study is to quantitatively assess the powerful effect a climate change poses on hydropower generation in Ethiopia, taking Upper Awash River Basin as a case. To realize the success of the core objective of this research, the existing hydrological processes in the basin will be investigated, relating observations with hydrological model output results. The study envisages that understanding climate change impact and relating it with hydrological processes will serve a lot in guiding decision makers and experts towards making an appropriate design of water resources mega projects in the future. The research specific objectives here follow:

1. To associate the hydrological aspects of climate change with hydroelectric power generation in the Upper Awash River Basin
2. To analyse the impact of climate change on dependable flows available for hydropower generation
3. To assess the impact of climate change on Koka Reservoir thereby develop its projected future evaporation and storage capacity
4. To develop projected future hydropower production from Koka Reservoir under two Representative Concentration Pathways (RCP) emission scenarios

1.6 Outline of the Thesis

The thesis consists of five chapters, and related references and appendices. In chapter one background, problem statement, significance of the study, scope and objectives of the study have already been presented. Chapter two presents the theoretical basics and literature review. Climate and climate change, the global climate system, anthropogenic causes of climate change, observed changes in Ethiopia and future projections, will be highlighted in this second chapter. Also, hydrological processes and models will be reviewed. In chapter three, working flow and methodology will be presented. Study area will be dealt with in this chapter. Modelling, climate scenarios, consideration of the impact of climate change on hydropower production are also among the topics that will be covered in the third chapter.

Chapter four reveals the results of the research carried out followed by the discussion of the results. The objectives of the study will be brought to the front here. Chapter five finalizes the documentation with conclusions and recommendations. Last but not least, the document will have references and appendices at the end.

CHAPTER 2

2. THEORETICAL AND PRINCIPAL BASICS

2.1 Climate and climate change

The earth's climate is a complex system, affected by natural events and by man-made interference. Since the second half of the eighteenth century, the concentration of CO_2 in the atmosphere has increased. It is also asserted that the increase in the atmospheric CO_2 has brought about heating of the earth through the additional man-made GHG effects. Major sources of CO_2 emissions include different forms of transport services and the burning of fossil fuels for the purpose of generating electricity. There are indications that climate is changing at a rate greater and faster than the usual natural variations. Among all others, the rise in temperature and the change in precipitation patterns are observed almost all over the entire globe.

2.1.1 The global climate system

A simple definition of climate is the average weather. A description of the climate over a period (which may typically be from a few years to a few centuries) involves the averages of appropriate components of the weather over that period, together with the statistical variations of those components (Houghton et. al., 1990). Climate variations are caused by the interaction of the atmosphere with those other components of the climate system, which include the oceans, land, snow and ice, and hydrological systems.

Fluctuations and variations of climate take place on many scales as a result of natural processes. This kind of fluctuation of the climate is usually referred to as climate variability. The climate change which most climate scientists, experts, professionals and the world community are concerned with is that which occur currently and in the future due to human activities.

The climate variables which are commonly dealt with are usually related with the atmosphere. However, in dealing with the climate system it is not sufficient to look at the atmosphere alone. Processes in the atmosphere are highly coupled to the land surface, to the oceans and to those parts of the Earth covered with ice. There is also very strong coupling to the biosphere, i.e., the vegetation and other living systems on the land and in the ocean. The five components that make the climate system are atmosphere, land, ocean, ice and biosphere (Houghton et. al., 1990).

The Earth's climate is driven by the output of the Sun. The variations in the Sun's output, together with the rotation and orbit of the Earth, influence the climate. This means that the source of energy which drives the climate is the radiation from the Sun. Much of the energy from the Sun is in the visible section of the electromagnetic spectrum. The amount of energy falling on a surface of one square meter directly facing the sun in a second is about 1370 W/m^2. Because of the spherical shape of the Earth, at any time half the Earth is in night. The average incident solar energy on a level surface outside the atmosphere is about one-fourth of this, i.e., 342 W/m^2. About 31% of this energy is scattered or reflected back to space by molecules, aerosols, clouds and the Earth's surface. This accounts for about 106 W/m^2. The rest 236 W/m^2 heats the Earth's surface and the atmosphere. To balance the incoming energy, the Earth must radiate back the same amount of energy. The energy that is radiated back to space by the Earth is the long-wave radiation in the infrared band of the electromagnetic spectrum. The amount of thermal radiation emitted depends on the temperature of the emitting surface and on its absorbency. If a completely absorbing surface would emit a radiation of 236 W/m^2, its temperature would have to be about – 19^{0}C. However, the average surface temperature on Earth is approximately 14^{0}C (Houghton et. al., 1990); but it varies because of so many factors.

The main factors include the time of day, the time of year, and where the temperature measurements are being taken, in particular the latitude. There are also other minor factors of limited importance. Given that the Earth has an inclined axis (approximately 23° towards the Sun's equator), the Northern and Southern Hemispheres of the Earth are either tilted towards or away from the Sun during the summer and winter seasons, respectively. Further, given that equatorial regions of the Earth are closer to the Sun, and certain parts of the world experience more sunlight and less cloud cover, temperature ranges widely across the planet. However, not every region on the planet experiences all the four seasons. At the equator, the temperature is on average higher and the region does not experience cold and hot seasons in the same way the Northern and Southern Hemispheres do. This is because the amount of sunlight that reaches the equator changes very little, although the temperatures do vary somewhat during the rainy season (Williams, 2016).

Therefore the temperature of the Earth can be very cold or very hot. For instance, the hottest temperature ever recorded on Earth was 70.7°C (159°F), which was taken in the

Lut Desert of Iran. These measurements were part of a global temperature survey conducted by scientists at NASA's Earth Observatory during the summers of 2003 to 2009. For five of the seven years surveyed (2004, 2005, 2006, 2007, and 2009) the Lut Desert was the hottest spot on Earth (Williams, 2016).

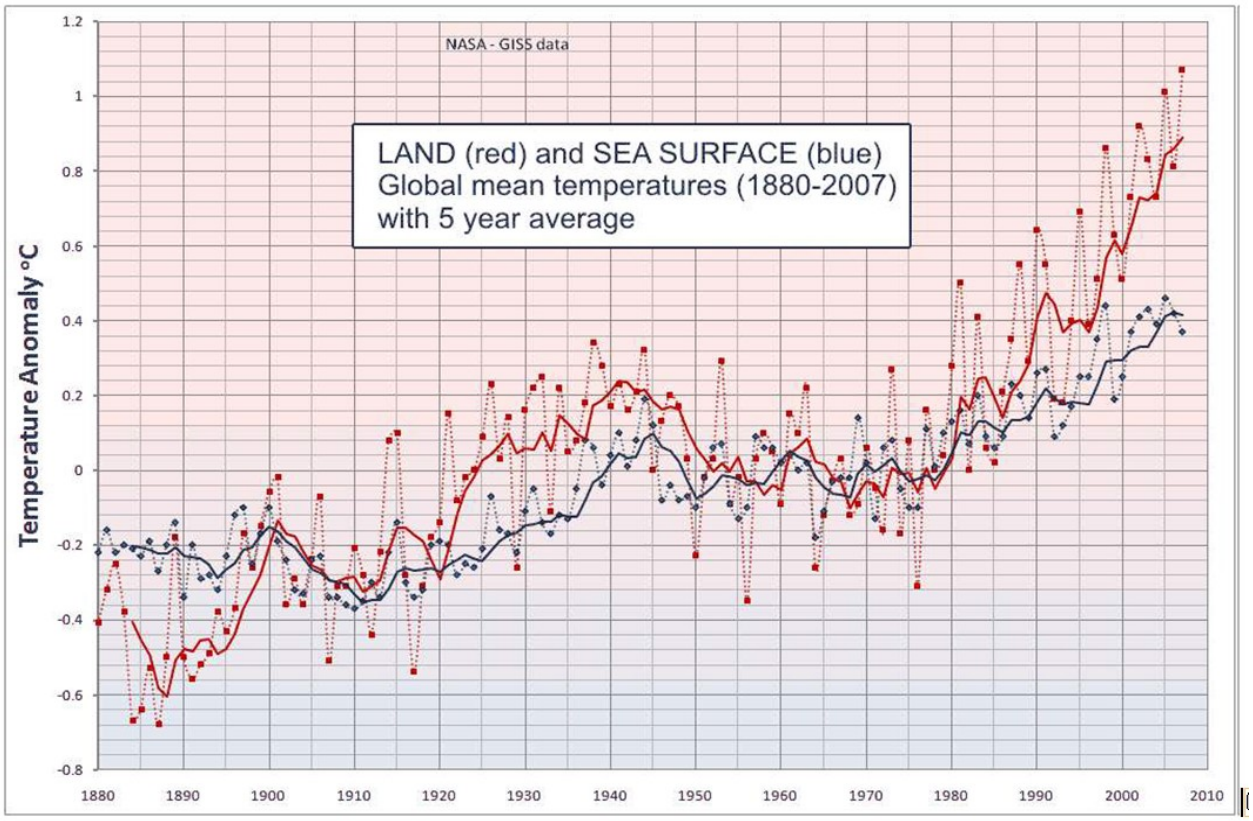

Figure 2.1 Five-years average of land and sea surface global temperature for the period 1880 - 2007 (Burrows, 2009)

However, it was not the hottest spot for every single year in the survey. In 2003, the satellites recorded a temperature of 69.3°C (156.7°F), the second highest in the seven-year analysis, in the shrub lands of Queensland, Australia. And in 2008, the Flaming Mountain got its due; with a yearly maximum temperature of 66.8°C (152.2°F) recorded in the nearby Turpan Basin in western China (Williams, 2016).

Meanwhile, the coldest temperature ever recorded on Earth was measured at the Soviet Vostok Station on the Antarctic Plateau. Using ground-based measurements, the temperature reached a historic low of – 89.2°C (– 129°F) on July 21st, 1983. Analysis of satellite data indicated a probable temperature of around – 93.2 °C (– 135.8 °F; 180.0 K), also in Antarctica, on August 10th, 2010. However, this reading was not confirmed by ground measurements, and thus the previous record remains (Williams, 2016).

2.1.2 The natural green house effect

Referring back to the solar energy reaching the Earth's surface, the temperature of – 19^0C required for emitting the 236 W/m^2 of thermal radiation is very cold as compared to the condition that actually exists near the Earth's surface. As the Earth's surface is on average 33^0C warmer, the atmosphere is warming the Earth (Harrison, 2001). This naturally warming is caused by the blanketing effect of greenhouse gases (GHG). The warming effect of the greenhouse gases in the atmosphere was first recognised in 1827 by the French scientist Jean-Baptiste Fourier (Houghton, 2004).

The atmospheric emissions to space occur either from the tops of clouds, or by gases present in the atmosphere. The atmosphere consists of about 78% nitrogen and 21% oxygen. These two bulk atmospheric air components are transparent to infrared radiation. On the other hand, water vapour, which varies in amount from 0 to about 2%, carbon dioxide, and some other minor gases present in the atmosphere in much smaller quantities, are responsible for the blanketing and warming effect. These gases are known as greenhouse gases because they act partially as a blanket for thermal radiation from the surface and enable it to be substantially warmer than it would otherwise be (IPCC, 1990). On the one hand, the GHGs are transparent to the incoming shortwave solar radiation. On the other hand, they absorb and re-emit longwave radiation that emanates from the surface of the Earth. The re-emission occurs in every direction available; some downwards direction of the emission warms the air near the ground, land surface and water bodies. The process is natural and has been occurring for at least two billion years, with small quantities of mainly water vapour and carbon dioxide trapping sufficient heat to allow water to exist in the liquid phase and creating conditions suitable for life (Harrison, 2001).

Great efforts have been exerted to evaluate the rising concentrations of some GHGs, with special attention to CO_2, and to relate them to global warming and the rise in mean temperature of the World, since the early nineteenth century. The enhanced greenhouse effect, caused by the gases present in the atmosphere due to human activities such as the burning of fossil fuels and deforestation led to more detailed investigation of the possible causes and possible effects on the rise of temperature. The increase in CO_2 has contributed about seventy percent of the enhanced greenhouse effect, methane (CH_4) about twenty-four per cent, and nitrous oxide (N_2O) about six per cent, ignoring the effects

of chlorofloro carbons (CFCs) and of changes in ozone, since these vary over the globe and thus difficult to quantify (Houghton, 2004).

2.1.3 The Enhanced Anthropogenic Greenhouse Gases Effect

Even though water vapour and carbon dioxide are the most important of the GHGs, they are not the only ones. In addition to these gases, there are other natural and man-made substances that have the potential to enhance the greenhouse effect. The importance of the gases depends on their absorbing power of infrared radiation. Besides, different compounds absorb radiation in particular wavelength bands. Some of the important greenhouse gases are presented in Table 2.1.

Table 2.1 The composition of the atmosphere, the mean constituents and the greenhouse gases in the atmosphere (Houghton, 2004)

Gas	N_2	O_2	H_2O	CO_2	CH_4	N_2O	CFCs	O_3
Mixing ratio or mole fraction expressed as fraction of ppm	0.78	0.21	0–0.02	370	1.8	0.3	0.001	0–1000

Methane (CH_4) is produced naturally, but anthropogenic sources including fuel production, landfill and deforestation, cattle farming etc. are increasing its atmospheric concentrations by about 5 ppb annually (Houghton, 2004). This gas has a much shorter atmospheric residence time and is removed from atmosphere due to reactions with the hydroxyl radical (OH). Therefore, the atmospheric lifetime of methane is dominantly controlled by a single process, oxidation by OH in the atmosphere. Anthropogenic activities are responsible for about 60 – 80% of current methane emissions. Methane emissions from natural wetlands appear to contribute about 20% to the global methane emissions to the atmosphere (Houghton, 2004).

Nitrous oxide (N_2O) is a naturally occurring, chemically active trace gas produced from a wide variety of biological sources in soils and water. However, its concentrations have also risen through fertilizer use and fossil combustion.

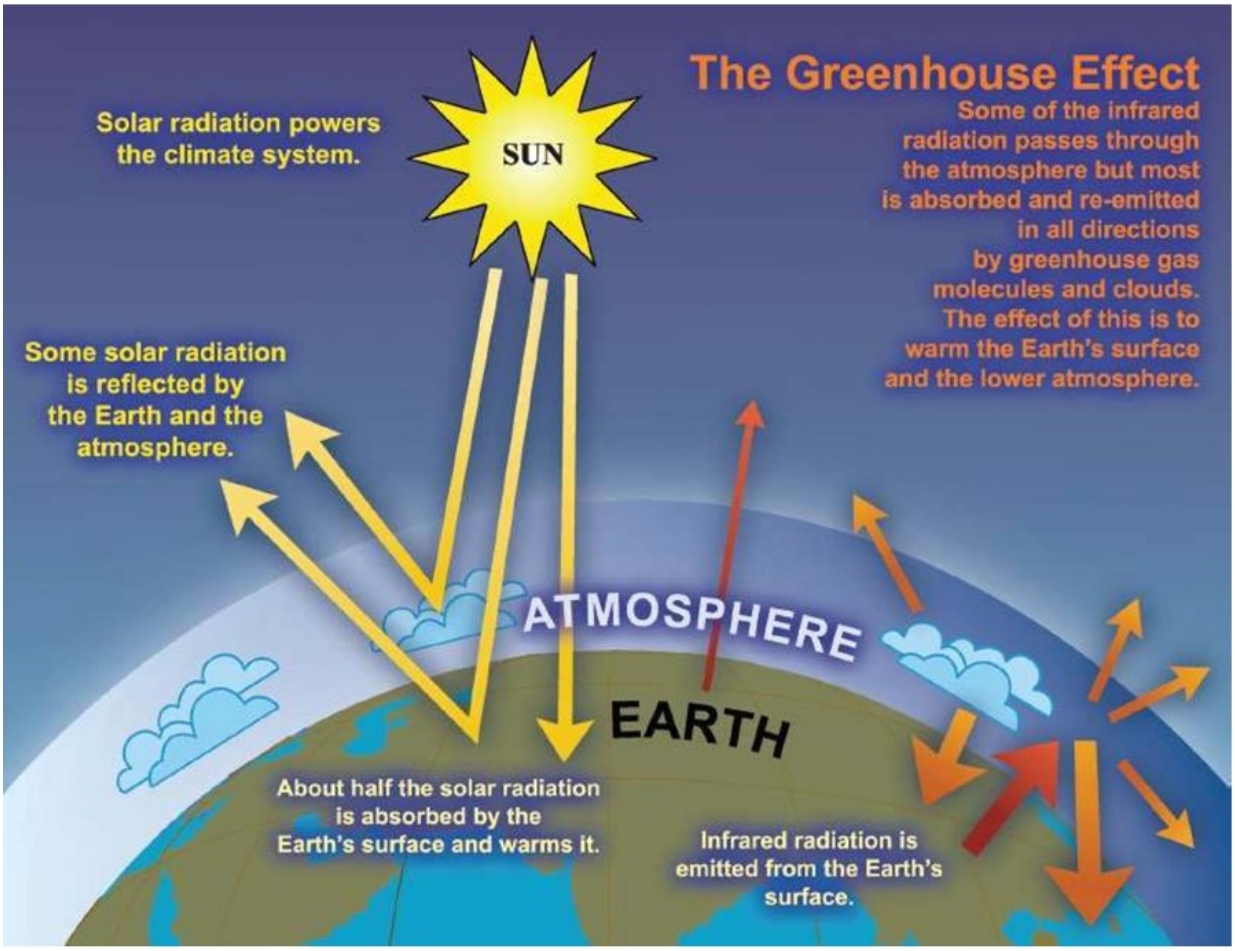

Figure 2.2 The greenhouse effect (Burrows, 2009)

Water vapour is an important greenhouse gas. A major source of stratospheric water vapour is the oxidation of methane, and it is anticipated that increased atmospheric concentrations of methane will lead to increases in stratospheric water vapour (Houghton et. al., 1990). As the atmosphere warms its ability to hold water increases, so the natural quantities of water vapour will increase enhancing the warming.

Aerosols are suspended particles in the atmosphere that can alter the energy balance by absorbing or scattering the incoming solar radiation. They tend to cool the atmosphere. The natural sources of aerosols include dust that is blown from various areas such as from land surface, from fossil fires, and rarely from volcanic eruptions. On the other hand, the anthropogenic sources include biomass burning. They are dominated by sulphate particles that arise from the formation of sulphur dioxide (SO_2). Aerosols have short residence time in the atmosphere. Therefore their effects are rather regional than global. Their effect on climate is indirect, since they influence the formation of clouds.

In particular, water vapour and CO_2 absorb some of the long wavelength IR radiated away from the Earth as part of the energy balance pointed earlier (Burrows, 2009). The water vapour (H_2O) and carbon dioxide (CO_2) molecules in the atmosphere don't just hang on to the IR energy they absorb. They re-radiate it. This re-radiated IR goes off in random directions. Some will go up (out into space) – and some will head back down to where it came from. Some will also be converted to heat in the atmosphere. So instead of escaping out into space some of the IR radiated by the Earth ends up being trapped back on Earth.

Just as a glass 'greenhouse' traps some of the heat of the sunlight that comes in, so the 'greenhouse gases' H_2O and CO_2 trap some of that outgoing IR radiation. The mechanism is a little different, but the effect is similar and so the expression 'greenhouse effect' has become well established as shorthand for this process by which H_2O and CO_2 molecules keep us warm. In fact, they trap heat to the extent that the Earth stays 33 degrees warmer than it would without them. The Earth would be at that frozen -19^0C if it weren't for the HO and CO in the atmosphere (Houghton et. al., 1990)!

2.1.4 Causes of Climate Change

Human beings have always influenced their environment. Since the beginning of the Industrial Revolution in the mid-18^{th} century, however, the impact of human activities on the environment has begun to extend to a much larger scale. The combustion of fossil fuels for domestic and industrial usage and biomass burning produced greenhouse gases and aerosols which affect the composition of the atmosphere. One of the greenhouse gases emitted to the atmosphere as a result of human activity is chlorofluorocarbon (CFC). CFCs are recent man-made gases and were used in refrigeration and as a propellant. The emission of this gas and other chlorine and bromine compounds has not only exaggerated the radiative forcing but even more dangerously led to the depletion of stratospheric ozone layer. CFCs have the ability to trap radiation tens of thousands of times greater than CO_2 does (Houghton et. al., 1990). The two most important compounds of CFCs, in terms of their warming contribution are CFC-11 and CFC-12. The fully halogenated CFCs are primarily removed by photolysis in the stratosphere, and have atmospheric lifetimes of more than fifty years.

CFC-11 and CFC-12 have been banned by the Montreal Protocol due to damage to the ozone layer, and their concentrations reduced. However, hydrofluorocarbons (HFCs) and

hydrochlorofluorocarbons (HCFCs) are introduced to replace CFCs, and their concentrations are increasing. These have similar radiation trapping properties, although they do not damage the ozone layer (Houghton et. al., 1990). Landuse and landcover change, due to urbanization and clearing of forests for agriculture affect physical and biological properties of the surface of the earth. The changing landuse is particularly pronounced in tropical regions.

While the anthropogenic fluxes of fossil fuel combustion and deforestation are by far less than that caused by natural processes, their effects are sufficient to alter the natural balance. The demand for agricultural land was in response to increasing population, until the middle of the twentieth century. But more recently, it is the exploitation of minerals and timber that has resulted in the clearance of enormous areas of forest.

The amount of carbon dioxide, for example, as indicated earlier, has increased by more than 30% since pre-industrial times and is still increasing at an unprecedented rate of on average 0.4% per year, mainly due to the combustion of fossil fuels and deforestation (Mimikou and Baltas, 2009). The concentration of methane (CH_4) and nitrous oxide (N_2O), is increasing as well due to agricultural, industrial and other activities. Human industrial, energy related, and land-use activities also increase the amount of aerosol in the atmosphere, in the form of mineral dust, sulphates and nitrates and soot. Their atmospheric lifetime is short because they are removed by rain. The increases in greenhouse gas concentrations and aerosol content in the atmosphere result in a change in the radiative forcing to which the climate system must act to restore the radiative balance.

An increase of greenhouse gas concentrations leads on average to an additional warming of the atmosphere and the Earth's surface. Many greenhouse gases remain in the atmosphere and affect climate for a long time.

2.1.5 Observed Climate Changes in Ethiopia

The average annual temperature (1961 – 1990) was 23.08'C (Ndaruzaniye, 2011). Ethiopia is characterized by diverse climates which translate into diverse vegetation zones. According to the Koeppen-Geiger climate classification system, Ethiopia has 10 climate types, including: the Hot Arid, Hot Semi-Arid, Tropical Rainy with distinct dry winter, Tropical Monsoon Rainy with short dry winter, Warm Temperate Rainy with dry winter, and Warm Temperate Rainy without distinct dry season.

Ethiopia has historically suffered from climatic variability and extremes. Absence of sufficient rain has contributed to failures in crop production, deaths of livestock, hunger and famines in the past. The country has experienced at least five major national droughts since 1980, along with literally dozens of local droughts. Cycles of drought create poverty traps for many households, constantly thwarting efforts to build up assets and increase income.

Droughts have repeatedly inflicted damage on Ethiopia, as a concomitant consequence of which the countrymen and women numbering in the tens of thousands have been subjected to famine. Neither have the rivers and vegetation resources been spared the damage caused by climate change. Not only has the water volume of the rivers diminished, but the headwater themselves have shown signs of desiccation. It may not be simple to demonstrate the situation in financial terms, but it can generally be said that the negative impact of climate change on Ethiopia has been extreme.

Analysis of observed temperature data indicates that there has been an increase in seasonal mean temperature in many areas of Ethiopia over the last fifty years (NMA, 2006). This is in agreement with the global trends (e.g., Gates et. al., 1990). For the past forty years the average annual temperature in Ethiopia has been increasing by 0.37 ^{0}C per decade. Consistent with the global trend, as regards the warmest decade of the 20th century, the majority of warming occurred during the second half of the 1990s.

With regard to precipitation, the country experiences high inter-annual and inter-seasonal rainfall variability too. A number of studies have showed that changes in rainfall are non-uniform and highly sensitive to the region and period of analysis.

Available studies clearly indicate that the projected changes in climate and its variability would have serious implications on natural resources, economy and welfare. Both instrumental and proxy records have shown significant variations in the spatial and temporal patterns of climate in Ethiopia. According to NMA (2006) the country experienced 10 wet years and 11 dry years over 55 years analyzed, demonstrating the strong inter-annual variability. Between 1951 and 2006, annual minimum temperature in Ethiopia increased by about 0.37°C every decade. The UNDP Climate Change Profile for Ethiopia (McSweeney et al., 2008) also shows that the mean annual temperature increased by 1.3°C between 1960 and 2006, at an average rate of 0.28°C per decade.

The temperature increase has been most rapid from July to September (0.32°C per decade).

2.1.6 Future Climate Change projections

Prior to briefing the bird's eye view of future climate change projections, it is worthwhile to introduce three fundamental efforts of the scientific community related to the new projection of future climate change: CMIP5, RCP and CORDEX.

2.1.6.1 Coupled model intercomparison project (CMIP5)

Human activity has changed the climate over the past century, and further change is inevitable over the next several decades, even if strong mitigation actions are taken. Climate Change and Variability (CLIVAR), which is a component of the World Climate Research Programme, therefore, found it crucial to promote and facilitate a state of the art predictive science that aims to assist adaptation decisions. Included under this new insight is the improvement of the ability of the scientific community to simulate the likely states of the climate system, including variations in the likelihood of extremes and precipitation, on near and long-term time horizons.

CLIVAR had the objective to understand and describe the dynamics of the coupled ocean-atmosphere system. Additionally, it had the deep objective to identify the processes leading to climate variability, change and predictability on different time frames. The time frames were seasonal, interannual, decadal, and centennial scales. Indeed, all these far-fetched plans, programs and activities were in cooperation with other relevant climate-research and observation programmes. In so doing, CLIVAR made unreserved devotion to put into effect, a multi-model experimental framework of unprecedented scale. The new set of coordinated climate experiments comprised what was then called The Coupled Model Intercomparison Project (CMIP5).

CMIP5 included more metadata describing model simulations than previous CMIP phases. It is of an enormously ambitious coordinated model intercomparison exercise involving most of the climate modelling groups worldwide (Meehl and Bony, 2011).

CMIP5 builds on the successful earlier phases of CMIP (Stouffer et al., 2011). It is anticipated that much of the new climate science emerging over the next few years will be connected to this activity. One prominent example was AR5. The scientific community and the climate modelling centers around the world brought together their activities in the

CMIP5, providing the basis for most of the assessment of future climate change in AR5 (IPCC, 2013). In order to perform future global and regional projections of climate change, a new set of scenarios, the Representative Concentration Pathways (RCPs), was used for the new climate model simulations carried out under the framework of this CMIP5 of the World Climate Research Programme. More details of CMIP5 can be found on Taylor et al. (2011).

2.1.6.2 Representative Concentrated Pathways (RCP)

In spite of the fact that the previous IPCC scenarios and processes have been productive in so many respects as far as climate change is concerned, new scenarios and new processes for selecting and using them are needed (Moss et al., 2010). For instance, IS92 scenarios and scenarios from the Special Report on Emission Scenarios (SRES) (Leggett et al., 1992) have performed decisive role (Nakicenovic et al., 2000). The research community needed new scenarios because of changes, especially in terms of landuse and landcover.

First of all, by far more detailed information and data are required for running the current climate models than those provided by any previous scenario sets. Secondly, there is an increasing concern in scenarios that clearly investigate the impact of different climate policies in addition to the no-climate-policy scenarios explored so far. Finally, there is also an increasing curiosity in investigating the role of adaptation in more detail. This requires further integration of information for scenario development across the different disciplines involved in climate research. The need for new scenarios motivated the Intergovernmental Panel on Climate Change (IPCC) to request the scientific communities to develop a new set of scenarios to facilitate future assessment of climate change (IPCC, 2007). The IPCC also decided such scenarios would not be developed as part of the IPCC process, leaving new scenario development to the research community.

The community thus designed a process of three phases (Moss et al., 2010):

i) Development of a scenario set containing emission, concentration and land-use trajectories—referred to as “representative concentration pathways” (RCPs).
ii) A parallel development phase with climate model runs and development of new socio-economic scenarios.
iii) A final integration and dissemination phase.

The core objective of the first phase, i.e., development of the RCPs was to make available information on possible development trajectories for the major forcing agents of climate change, consistent with the current scenario literature allowing ensuing analysis by both climate models (CMs) and Integrated Assessment Models (IAMs). Climate modellers will use the time series of future concentrations and emissions of greenhouse gases and air pollutants as well as simulations of land-use change from the RCPs in order to carry out new climate model experiments and assemble new climate scenarios as part of the parallel phase.

At the same time, IAMs will also investigate a range of different technological, socio-economic and policy futures that could lead to a particular concentration pathway and magnitude of climate change.

Therefore, the development of the RCPs in the first phase allowed climate modellers to move forwards with experiments in parallel to the development of emission and socio-economic scenarios, expediting the overall scenario development process (Moss et al., 2010).

The word “representative” signifies that each of the RCPs represents a larger set of scenarios in the literature. In fact, as a set, the RCPs should be compatible with the full range of emissions scenarios available in the current scientific literature, with and without climate policy.

The words “concentration pathway” are meant to emphasize that these RCPs are not the final new, fully integrated scenarios (i.e. they are not a complete package of socio-economic, emission and climate projections), but instead are internally consistent sets of projections of the components of radiative forcing that are used in subsequent phases.

The use of the word “concentration” instead of “emissions” also emphasizes that concentrations are used as the primary product of the RCPs, designed as input to climate models. Coupled carbon-cycle climate models can then as well calculate associated emission levels (which can be compared to the original emissions of the IAMs) (Hibbard et al., 2007).

In total, a set of four pathways were produced that lead to radiative forcing levels of 8.5, 6.0, 4.5 and 2.6 W/m^2, by the end of the century. Each of the RCPs covers the 1850 – 2100 periods, and extensions have been formulated for the period thereafter (up to 2300).

The Representative Concentration Pathways (RCPs) correspond to four greenhouse gas concentration (not emissions) trajectories adopted by the IPCC for its fifth Assessment Report (AR5) in 2014. It supersedes the Special Report on Emissions Scenarios (SRES) projections published in 2000.

The pathways are used for climate modelling and research. They describe four possible climate futures, all of which are considered possible depending on how much greenhouse gases are emitted in the years to come. The four RCPs, RCP2.6, RCP4.5, RCP6, and RCP8.5, are named after a possible range of radiative forcing values in the year 2100 relative to pre-industrial values (+2.6, +4.5, +6.0, and +8.5W/m^2 respectively).

The four IAM groups responsible for the four published scenarios that were selected as "predecessors" of the RCPs, generated the basic data sets from which the final RCPs were developed. The RCP8.5 was developed using the MESSAGE model and the IIASA Integrated Assessment Framework by the International Institute for Applied Systems Analysis (IIASA), Austria. This RCP is characterized by increasing greenhouse gas emissions over time, representative of scenarios in the literature that lead to high greenhouse gas concentration levels (Riahi et al., 2007).

The RCP6.0 was developed by the AIM modelling team at the National Institute for Environmental Studies (NIES) in Japan. It is a stabilization scenario in which total radiative forcing is stabilized shortly after 2100, without overshoot, by the application of a range of technologies and strategies for reducing greenhouse gas emissions (Fujino et al., 2006; Hijioka et al., 2008).

The RCP4.5 was developed by the GCAM modelling team at the Pacific Northwest National Laboratory's Joint Global Change Research Institute (JGCRI) in the United States. It is a stabilization scenario in which total radiative forcing is stabilized shortly after 2100, without overshooting the long-run radiative forcing target level (Clarke et al., 2007; Smith and Wigley, 2006; Wise et al., 2009).

RCP6.0 and RCP4.5 are medium stabilization scenario with minor difference that the latter corresponds to more stabilization of the greenhouse gases as compared to the former.

The RCP2.6 was developed by the IMAGE modelling team of the PBL Netherlands Environmental Assessment Agency. The emission pathway is representative of scenarios

in the literature that lead to very low greenhouse gas concentration levels. It is a “peak-and-decline” scenario; its radiative forcing level first reaches a value of around 3.1 W/m^2 by mid-century, and returns to 2.6 W/m^2 by 2100. In order to reach such radiative forcing levels, greenhouse gas emissions (and indirectly emissions of air pollutants) are reduced substantially, over time (van Vuuren et al., 2007a).

In summary, each RCP has associated emissions and concentration paths for each greenhouse gas. For CO_2, RCP8.5 follows the upper range of available literature (rapidly increasing concentrations). RCP6 and RCP4.5 show a stabilizing CO_2 concentration (close to the median range of the existing literature). Finally, RCP2.6 has a peak in CO_2 concentrations around 2050 followed by a modest decline to around 400 ppm CO_2 by the end of the century.

2.1.6.3 The Coordinated Regional Downscaling Experiment: CORDEX

There is a growing need for detailed, comprehensive and high-resolution regional information on the subject of future climate. Such information is needed by many scientists in fields that require climate information (e.g. hydrologists), decision makers, and by those working on the subject matters of assessment of climate change impacts, adaptation and vulnerability.

Even though climate change projections should necessarily be undertaken with global models, such models do not have an adequate spatial resolution for all applications. Limitations and gaps on existing computing resources constrain model resolution; therefore, various techniques have been developed for downscaling global climate projections and for generating fine-scale regional climate information. These techniques include statistical downscaling, nested regional climate models, variable resolution global models, global uniform high-resolution time-slice simulations, and/or combinations of these methods.

The familiarity with and the experience in the global climate modelling community has shown the enormous value of worldwide coordinated model experiments and the importance of the resulting multi-model ensemble in generating plausible climate change information and in evaluation of model uncertainties. Ensemble results from global coupled models have been used widely in the IPCC assessment reports, but similar ensemble results from regional models or other downscaling methods have not been

widely available for most regions of the world. This has limited the use of downscaling products in climate change impact assessment and adaptation studies.

Therefore it became mandatory that the World Climate Research Programme (WCRP) called for an international initiative that is able to provide regionally downscaled climate projections for most land regions of the globe, as a complement to the global climate model projections. Such an international initiative was called the Coordinated Regional Downscaling Experiment (CORDEX). CORDEX includes data from both dynamical and statistical downscaling. It is anticipated that the CORDEX dataset will provide a link to the impacts and adaptation community through its better resolution and regional focus (Evans, 2011).

The climate projection framework within CORDEX is based on the set of new GCM simulations of CMIP5. CORDEX focuses on the GCM experiments using RCP4.5 and RCP8.5 emission scenarios which represent a mid and a high-level emission scenario. Its simulations covered the period 1951 to 2100.

The first region targeted coordinated downscaling was carried out for Africa (Jones et al., 2011), and hence the project was called CORDEX Africa. Africa was selected for a number of reasons (Jones et al., 2011). First, Africa is particularly vulnerable to climate change because of the adverse impacts of changing climate variability on a number of vital sectors (e.g. agriculture, water management, health) and because of the relatively low adaptive capacity of its economies. Second, climate change may have significant impacts on temperature and precipitation patterns over Africa which in turn can interact with other environmental stressors such as land-use change, desertification and aerosol emissions, further exacerbating the stresses on human and natural populations.

While the CORDEX simulations are high resolution compared to the GCM simulations, they are still about 50 km resolution which remains too coarse for many impact and adaptation studies which in fact require very high resolution. Therefore, still the effort for more fine resolution remains. CORDEX simulations with resolution of 10 km have been currently released.

2.1.6.4 Future Climate Projections Based on CMIP5

A climate projection is a climate simulation that extends into the future based on a scenario of future external forcing. Such projections are very helpful for politicians and

policy-makers when assessing what to do about the problem of anthropogenic climate change, as they give an estimate of the likelihood of change given certain pollution scenarios (Collins and Senior, 2002). The projections of future climate change are obtained using climate models in which changes in atmospheric composition are specified. The models transform the changes in composition of the atmosphere into changes in climate based on the physical processes governing the climate system. The modelled climate change depends on projected changes in emissions, the changes in atmospheric greenhouse gas and aerosol concentrations that result, and the behaviour in which the models respond to these changes.

It is useful for purposes of analysis and description to consider the pre-industrial climate system as being in a state of climatic equilibrium with a fixed atmospheric composition and an unchanging sun (IPCC, 2013). Processes that occur naturally and the complex interactions that exist within the various components of the climate system lead to internally generated climate variability on several time scales in this theoretical state. Climate variations also result because of features outside of the idealized system. Some of the factors that give rise to externally forced climate variations include volcanic eruptions, solar variations, anthropogenic changes in the composition of the atmosphere and landcover change, etc. Therefore, for instance, climate system variables such as annual mean temperatures can be understood as the combination of internally generated and externally forced components.

It is worthwhile to distinguish climate projection from climate prediction. A climate prediction proceeds by integrating the governing fundamental physical equations forward in time from observation-based initial conditions. A decadal climate prediction combines aspects of both a forced and an initial condition problem (IPCC, 2013). At small time scales the evolution is basically dominated by initial state while at longer time scale the influence of the initial conditions shrink and the importance of the forcing increases. On the other hand, in contrast to predictions, projections are not initialized using observations; instead, they are initialized from historical simulations of the evolution of the climate from pre-industrial conditions up to the present (IPCC, 2013).

An updated ensemble, the Coupled Model Intercomparison Project phase 5 (CMPI5), was used for the IPCC 5th Assessment Report (AR5). CMIP5 promotes a standard set of model simulations and provides projections of future climate change on both near term (through 2035) and long-term (out to 2100) and beyond scales. The projections are

related to a reference period 1986 – 2005 Major use is made of CMIP5 model experiments forced by the Representative Concentrations Pathways (RCP) scenarios. Specifically projections presented here are based on RCP4.5 scenario. RCP4.5 was chosen because of its intermediate GHG forcing (IPCC, 2013).

According to AR5 findings (IPCC, 2013), the 5 to 95% range of the projected temperature anomaly under RCP4.5 scenario for the period 2016 – 2035, relative to the reference period 1986 – 2005, is 0.47^{0}C to 1.00^{0}C. This range represents the mean annual surface air temperature for the globe in the near-term as a whole. Considering decadal means, the 5 to 95% confidence interval for the projected temperature anomaly for the period 2016 – 2035 is 0.39 ^{0}C to 0.87 ^{0}C (IPCC, 2013).

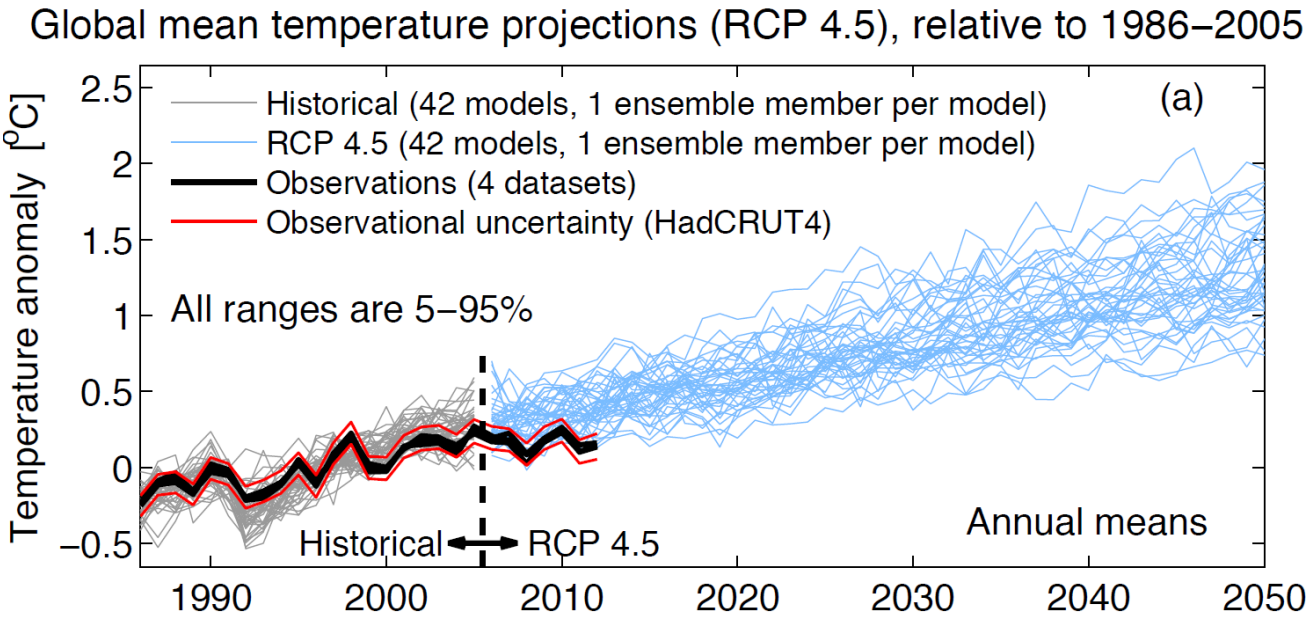

Figure 2.3 Projections of global mean, annual mean surface temperature 1986 - 2050 (anomalies relative to 1986 - 2005) under RCP4.5 from CMIP5 models (**IPCC, 2013**)

With regard to long-term future climate projections, a consistent and robust feature across climate models is a continuation of global warming in the 21st century for all RCP scenarios. For the first two decades after 2005, temperature increases are almost the same for all RCP scenarios. At longer time scales, the warming rate begins to depend more on the specified GHG concentration pathway, being highest (> 0.3^{0}C per decade) in the highest RCP8.5 and significantly lower in RCP2.6, particularly after 2050 when global surface temperature response stabilizes and declines thereafter. In the CMIP5 ensemble mean, global warming under RCP2.6 stays below 2°C above the levels in 1850 – 1900 throughout the 21st century, clearly demonstrating the potential of mitigation policies (IPCC, 2013).

As for the other pathways, global warming exceeds 2°C within the 21st century under RCP4.5, RCP6.0 and RCP8.5, in qualitative agreement with previous studies using the SRES A1B and A2 scenarios (Joshi et al., 2011). Global mean temperature increase exceeds 4°C under RCP8.5 in 2100 (IPCC, 2013).

In the fourth assessment report (AR4) of the IPCC, one finding (e.g., Held and Soden, 2006; Chou et al., 2009; Allan et al., 2010) was that the wet-get-wetter and dry-get-drier. This general pattern of wet-get-wetter (also referred to as rich-get-richer) and dry-get-drier has been confirmed, although with deviations in some dry regions at present that are projected to become wetter by some models, e.g., Northeast Brazil and East Africa (IPCC, 2013). The increase or change in precipitation in general is related to some extent with change in temperature and amount of CO_2 in the atmosphere. While the increase in global mean precipitation would be 1.5 to 3.5%/^{0}C due to surface temperature alone, it is reduced by about 0.5%/^{0}C due to the effect of CO_2 (Lambert and Webb, 2008).

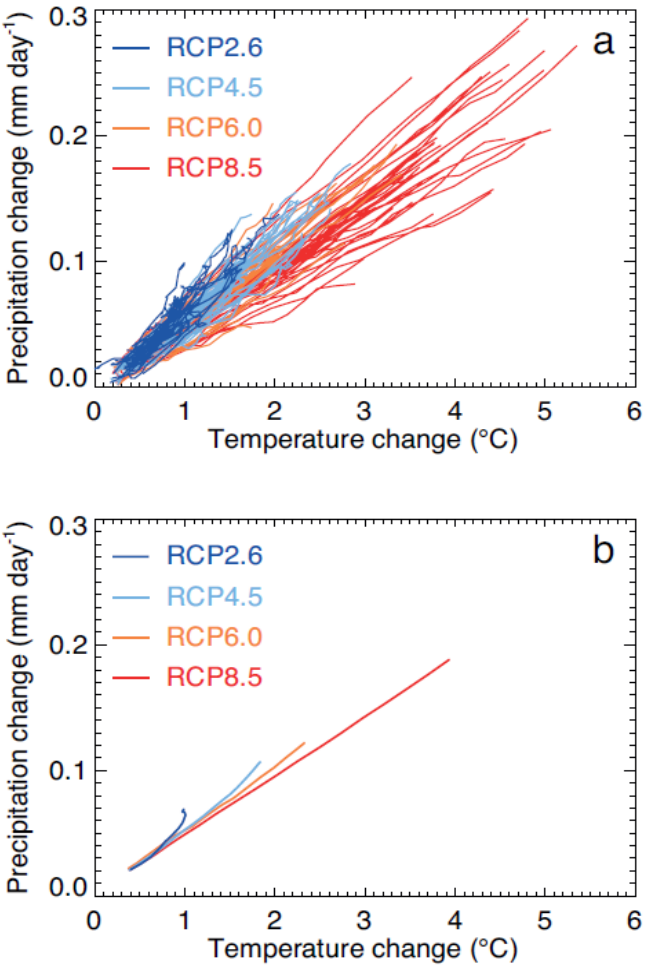

Figure 2.4 Global mean precipitation (mm/day) versus temperature (degree Celsius) changes relative to 1986 - 2005 baseline period CMIP5 concentrations-driven projections for the four RCPs. In the figure (a)

shows means over decadal periods (ten years) starting in 2006 and overlapped by 5 years (2011 – 2015). The decadal period continues as 2011 – 2020, 2021 – 2030, up to 2091 – 2100. In (a) each line on the figure represents a different model (one ensemble member per model). (b) shows the means of the corresponding multi-model for each RCP (**IPCC, 2013**).

Coming to the long-term precipitation projection, CMIP5 models (IPCC, 2013) on average project a gradual increase over the 21st century: change exceeds 0.05 mm/day (~2% of global precipitation) and 0.15 mm/day (~5% of global precipitation) by 2100 in RCP2.6 and RCP8.5 respectively. As is shown in Figure 2.4, the relationship between global precipitation and global temperature is approximately linear. The precipitation sensitivity, that is, the change of global precipitation with temperature, is about 1 to 3%/°C in most models, tending to be highest for RCP2.6 and RCP4.5 (IPCC, 2013). In the figure, it can be clearly seen that there is a steepening of the precipitation versus temperature relationship in RCP2.6 and RCP4.5 scenarios.

2.2 Hydrologic Processes

Hydrology encompasses the occurrence, distribution, movement and properties of waters of the earth. It is the science which deals with the various phases of the hydrologic cycle. Water and environmental issues are closely linked, and it is important to clearly understand how water is affected by and how water affects the ecosystem. Practical applications of hydrology are found in such tasks as the design and operation of hydraulic structures, water supply, wastewater treatment and disposal, irrigation, drainage, hydropower generation, flood control, navigation, erosion and sediment control, salinity control, pollution abatement, recreational use of water, and fish and wildlife protection.

A watershed can be considered as a hydrologic system (Figure 2.5). In this area of a watershed representing a hydrological system, precipitation is an input that is distributed spatially over the entire area. Streamflow is an output that is concentrated in the catchment outlet. Moreover, evaporation and subsurface flows are also outputs. It is worthwhile to note that prior to other courses of actions, the inputs and outputs are generally determined. Then, by using the system concept, the generalized model can be constructed. If the constructed model could relate inputs and outputs, indulging into extremely difficult tasks of trying to characterize the exact representation of the system is not important from practical point of view and could be avoided. On the other hand, though it is extremely difficult to model the entire hydrologic system, knowledge of the physical system is very important as it helps in developing a good model and validating its accuracy.

A hydrologic system model is an approximation of the actual system; its inputs and outputs are measurable variables and its structure is the concept of system transformation (Chow et al., 1988). In view of the land phase of the hydrologic cycle, any conceptual model bases on an expansion of the continuity equation (Chow et al., 1988) which relates the input, output and storage. A general model of the hydrologic system may be derived considering the input, *I* (precipitation), the output, *Q* (evaporation, streamflow and groundwater flow), and the whole process taking place in a time, *t*. The system performs a transformation of the input into the output. (Ω : TEXT)

$$Q(t) = \Omega I(t) \qquad (2.1)$$

By continuity, the time rate of change of storage *dS/dt* is equal to the difference between the input and the output

$$I - O = \frac{\Delta S}{\Delta t} \qquad (2.2)$$

where ΔS/Δt is the rate of change in the amount of water stored in the basin.

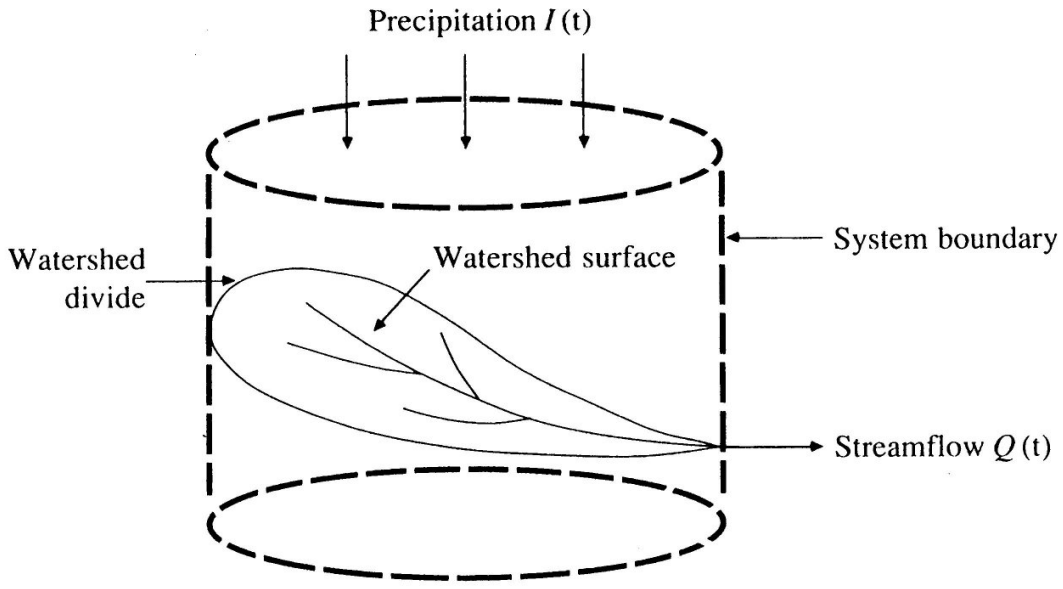

Figure 2.5 The watershed as a hydrologic system (Chow et al., 1988)

2.3 Hydrologic Models

In order to represent the hydrologic processes for the purposes of utilization of water and to define their nature to the extent possible, hydrologic models are very important. Watershed hydrologic models have a variety of forms because of the fact that they are developed for different reasons. Currently the existing watershed models range from simple conceptual lumped models to broad physically based distributed models. Conceptual lumped models employ an integrated interpretation of parameters signifying

an average value over the whole watershed. A catchment can be partitioned into a number of sub-basins where hydrologic parameters may differ from one watershed to another. Lumped models in such circumstances are said to be semi-distributed. However, they remain non-physically based, since they employ synthetic methods of transforming precipitation to runoff. A lumped model overlooks the distribution of the input variables in space, which describe the physical process.

On the other hand, physically based distributed watershed models can account for spatial variations in input parameters and state variables within the watershed. They include physical formulations of the various hydrologic processes. They incorporate data regarding the spatial distribution of variables together with computational algorithms to estimate the impact of the distribution on modelled behaviour. Thus, this class of models has the merit of simulating complex hydrologic systems and using distributed field hydrologic data. Apart from these, physically based distributed models are far more intricate to setup, have other rigorous data requirements, and as a result, may be subject to over-parameterization. Nevertheless, the promising availability of distributed data on precipitation and watershed properties, along with computational tools, has amplified the desire of research and application communities in the development and function of such models.

In addition, models can be explained as conceptual or empirical. Empirical models are occasionally known as black-box models or input-output models. They do not help in physical understanding. They have parameters that may play little role and have limited direct physical importance and can be approximated only by making use of concurrent measurements of input and output. Therefore some of their disadvantages are: they make assumptions that which in reality do not work; for example, they lack details and too simplistic; graphic models such as flow charts may be difficult for people to understand. Stochastic time series models are examples of empirical models. In many circumstances, however, these models can provide accurate answers and therefore can, serve as helpful tools in decision-making. The autoregressive moving average model (ARMA) and some other time series models are examples of empirical models.

Conceptual models are sometimes called grey-box models. They are intermediate between theoretical and empirical models. Conceptual models are models that are made of composition of concepts, which are used to guide people know, understand, or model a subject that the model stands for. Conceptual models are usually generalization of

things in the real world whether physical or social. In general, conceptual models consider physical laws but in a very simplified form. Some very significant outcomes may be skipped or missed.

Comprehensive and physically based watershed models have the capability of simulating hydrologic processes at a watershed scale. For watershed hydrologic modelling, careful attention should be given to select the appropriate model.

In reference to Borah and Bera (2003), different types of watershed models are summarized below differentiating between models representing long term simulation (continuous time step) and single event based simulation.

2.3.1 The HSPF Model

Hydrological Simulation Program—FORTRAN (HSPF) was designed to model the processes associated with the quantity and quality of water in watersheds scale, irrespective of their size and complexity. This comprehensive and continuous watershed hydrologic model was developed by the United States Environmental Protection Agency. In HSPF model, a watershed is categorized into pervious and impervious land areas. The pervious land area is intended to represent the agricultural activities whereas the impervious one is used to define urban areas. In addition, reaches and reservoirs are also represented in the model. The magnitudes of numerous parameters of the HSPF model can be considered to index the characteristics of specific factors that affect events such as water storage and fluxes in the land phase of the hydrologic cycle. Because of this reason, HSPF may be categorized under moderately physically based model. In other words, the simulation algorisms available within HSPF are a mixture of physically-based and empirical approaches. The model has the ability to simulate at temporal scales ranging from minutes to days. HSPF uses input meteorological forcing data and parameters that are related to system geometry, land use patterns, soil characteristics, and land use activities (e.g., agricultural practices) (Skahill, 2004).

The HSPF model is an integrated component of the Better Assessment Science Integrating Point and Nonpoint Sources (BASINS) system but it can be run stand-alone (Bicknel et al., 2001). The model is provided with three main modules which help to simulate different land segments. The modules are namely, PERLND, IMPLND, and RCHRES. As their name implies, the modules help to simulate pervious land segments, impervious land segments, and free-flow reaches and/or reservoirs, respectively. In

particular, PERLNDs and IMPLND application modules simulate runoff as well as water quality constituents from pervious and impervious land areas in the watershed.

The IMPLND application module is used for impervious land areas where little or no infiltration occurs, principally urban land categories. The RCHRES module is used to model the processes that occur in a single reach of an open channel or well-mixed impoundment. Within a given drainage area or sub-watershed, the RCHRES module is used to route runoff and water quality constituents simulated by PERLND and IMPLND.

The overland flow is estimated using the empirical outflow depth to the detention storage relation and the Chezy-Manning's equation. On the other hand, the interflow, percolation and groundwater flow are determined by the use of different empirical relations. Channel flow is estimated using the continuity equation as a basis, assuming that all the flows into the channel under consideration occur at one point upstream. The outflow from the outlet is computed on the basis of the volume of the reach.

Numerous component models of the BASINS system can be used as part of model development process with HSPF. For example, the Watershed Data Management Utility (WDMUtil) is used for pre-processing and, GENeration and analysis of model simulation Scenarios (GenScn) for post-processing. WDMUtil is a utility program for managing Watershed Data Management (WDM) files, which contain input and output time series data for HSPF. GenScn is a graphic user interface based program for creating simulation scenarios, analyzing the results and comparing scenarios. It facilitates the display and interpretation of output data derived from model applications. GenScn is not a model itself. It serves as a postprocessor for both the HSPF and SWAT models, as well as a tool for visualizing observed water quality data and other time series data.

The Expert System software was developed to assist less experienced modellers with calibration of a watershed model and to facilitate the interaction between the modeller and the modelling process not provided by mathematical optimization (Lumb et al., 1994). After the prototype was completed and tested, it was rewritten for portability and operational use and was named HSPEXP (Lumb et al., 1994). This software can be used during the process of modelling with HSPF.

At the present time, the Windows version of HSPF (WinHSPF) that is designed to work with version 12.0 of the HSPF model and integrates GIS for landscape data analysis including land use distribution, elevation data, and drainage stream network

characteristics may be employed to prepare many of the input data the model requires. Within the BASINS system, WinHSPF is intended to be used in conjunction with the interactive program GenScn. HSPF is capable of simulating a single watershed or a system of multiple hydrologically connected sub-watersheds and is designed for evaluating alternative management scenarios. Similar to SWAT, four types of digital spatial data are used in BASINS/WinHSPF to construct a User Control Input (UCI) file for an initial HSPF simulation run. The ability to efficiently construct and initially parameterize the UCI file, the main HSPF model input file, using readily available and/or project-specific GIS data coverage is the principal strength of the HSPF model interface in Watershed Modelling System (WMS). These are landuse data, DEM, user-specified outlet points (stream-gage locations), meteorological data, and user-specified sub-basin threshold-area size of concern in the watershed and its reaches.

The HSPF model has been extensively applied for different analysis with varied geographical characteristics. Researchers who used the applications for instance are Laroche, et.al. (1996); Jacomino and Fields (1997); Brun and Band (2000); Albek et al., (2004), and Singh et al., (2005). From calibration and validation of daily, weekly, and monthly stream flows, Laroche et al. (1996) found that as the time interval got smaller, the model became less precise. Bergman and Donnangelo (2000) used HSPF to regionalize its parameters in ungauged portion of a basin through calibration and validation on a few of the tributary watersheds. On the other hand, Gericke, et.al (2004) discussed the application of HSPF to model the hydrology of a River Basin in South Africa. They illustrated that the model can contribute for effective management of the hydrological cycles of the Basin and it can be used effectively to determine and evaluate environmental management and basin policies of watershed management agencies.

Borah and Bera (2003) reviewed and discussed the applications and performances of SWAT, HSPF, and DWSM. In the review, conceptual and mathematical bases of SWAT, HSPF, and DWSM were found to be sound, respectively, for long−term continuous simulations of predominantly agricultural watersheds, long−term continuous simulations of mixed agricultural and urban watersheds, and storm (rainfall) event simulations of agricultural and rural watersheds. Similarly, Singh et al., (2005) used SWAT and HSPF to simulate the hydrology of Iroquois River Watershed in the USA. They showed that calibrated SWAT and HSPF models can reproduce the average annual flows adequately

for period outside the calibration period. In most of the cases, HSPF was found to be robust in modelling hydrological processes of most watersheds worldwide.

2.3.2 MIKE SHE model

MIKE SHE is an integrated hydrological modelling system for building and simulating surface water and groundwater flows. This model has the capability to simulate the entire land phase of the hydrologic cycle and it allows components to be used independently and customized to local needs. MIKE SHE is among the distributed watershed hydrologic simulation models, and it was originally derived from the SHE (Systeme Hydrologique European).

As it is a physically based model, it requires extensive physical parameters. The model accounts various processes of hydrological cycle such as precipitation, evapotranspiration, interception, river flow, saturated ground water flow, unsaturated subsurface flow etc. It can simulate surface and ground water movement, their interactions, sediment, nutrient and pesticide transport in the model area and various water quality problems. It can also be applied for large watersheds.

Like other watershed hydrological models, MIKE SHE is provided with modules that serve specific but interrelated functions. It comprises two modules, namely water quality (WQ) and water movement (WM). The modules are based on the physical laws which are derived from the laws of conservation of mass, momentum and energy.

The evapotranspiration model is calculated using the Kristensen and Jensen (1975) methods although user input reference ET can be calculated in numerous ways. The unsaturated soil water infiltration and redistribution processes are modelled using Richard's equation or a simple wetland soil water balance equation (Zhang et al., 2008). Refsgaard and Storm (1995) have provided the detailed description of the structure and set up of the model. The code involves pre-processing and post processing modules and has various options for displaying results.

The properties of the MIKE SHE model make the model appropriate to cover a wide range of applications. For example, the physically based nature of the model provides the inclusion of natural topography and watershed characteristics such as vegetation, soil and weather parameter sets. The distributed nature of the model allows the user to spatially and temporally vary parameter sets, some of which are landuse conditions,

drainage practices, soil profiles, weather and evapotranspiration data sets, and overland flow values. The spatial distribution is accomplished through an orthogonal grid network that allows for horizontal or vertical discretization, as applicable within each parameter set (Abbott et al., 1996).

2.3.3 VIC model

Variable Infiltration Capacity model: It is a large-scale, semi distributed grid based hydrologic model which uses both energy and water balance equations. The main inputs are precipitation, minimum and maximum daily temperature and wind speed and allows many land cover types within each model grid. The processes like infiltration, runoff, base flow etc. are based on various empirical relations. Surface runoff is generated by infiltration excess runoff (Hortonian flow) and saturation excess runoff (Dunne flow). VIC simulates saturation excess runoff by considering soil heterogeneity and precipitation. It consists of 3 layers. Top layer allows quick soil evaporation, middle layer represent dynamic response of soil to rainfall events and lower layer is used to characterise behaviour of soil moisture.

Improvised VIC model has included both infiltration excess runoff and saturation excess runoff as well as the effects of variability of soil heterogeneity on surface runoff characteristics. It can deal with the dynamics of surface and ground water interactions and calculate ground water table (Gao et al., 2010).

The VIC model shares several basic features with other land surface models (LSMs) that are commonly coupled to global circulation models (GCMs). To mention some of its characteristics which resemble those of GCMs: the land surface is modelled as a grid of large, i.e., greater than 1 km, flat, uniform cells; the model inputs are time series of sub-daily meteorological drivers (e.g. precipitation, air temperature, wind speed, solar radiation, etc.; land-atmosphere fluxes, and the water and energy balances at the land surface, are simulated at a daily or sub-daily time steps; water can only enter a grid cell through the atmosphere.

In VIC model, routing of streamflow is performed separately from the land surface simulation, using a separate model, typically the routing model of Lohmann et al. (1996)

2.3.4 SWAT Model

SWAT (**Soil & Water Assessment Tool**) is a river basin scale model developed to quantify the impact of land management practices in complex watersheds. It is able to simulate the water balance from small catchments up to the continental scale. The model operates on a daily time step. It is characterized by its focus on land management, water quality loadings, and continuous simulation over long time spans.

SWAT was developed at USDA-ARS (Arnold et al., 1998) in a modelling experience that span roughly 30 years. It is semi-distributed, physically based simulation model and has the capability to predict the impact of landuse change and management practices on hydrological regimes in watersheds with varying soils, landuse and management conditions over long periods and primarily serves as a strategic planning tool. It incorporates features of several ARS models and is a direct outgrowth of the SWRRB model (Arnold and Williams, 1987). The specific models that contributed significantly to the development of SWAT were CREAMS model (Knisel, 1980), GLEAMS model (Leonard et al., 1987) and EPIC model (Izaurralde et al., 2006), which was originally called the Erosion Productivity Impact Calculator (Williams, 1990).

In SWAT, the impacts of spatial variations in topography, landuse, soil and other watershed characteristics on hydrology are considered in subdivisions. There are two-level scales of subdivisions: (1) a watershed is divided into a number of sub-watersheds based upon drainage areas of the tributaries, and (2) each sub-watershed is further divided into a number of Hydrologic Response Units (HRUs) based on landuse and land cover, soil and slope characteristics.

The SWAT model was built with state-of-the-art components with an attempt to simulate the processes physically and realistically. The model combines empirical and physically-based equations, uses readily available inputs, and enables users to study long-term impacts. It simulates eight major components: hydrology, weather, sedimentation, soil temperature, crop growth, nutrients, pesticides, and agricultural management (Neitsch et al., 2005). Major hydrologic processes that can be simulated by the model include evapotranspiration, surface runoff, infiltration, percolation, shallow aquifer and deep aquifer flow, and channel routing (Arnold et al., 1996). The simulation of the processes can be done in four subsystems: surface soil, intermediate zone, shallow and deep

aquifers, and open channels. Streamflow in a main channel is determined by three sources: surface runoff, lateral flow and base-flow from shallow aquifers.

Climatic inputs used in SWAT include daily precipitation, maximum and minimum temperature, solar radiation data, relative humidity, and wind speed data, which can be input from measured records and/or generated. Relative humidity is required if the Penman-Monteith (Monteith, 1965) or Priestly-Taylor (Priestly and Taylor, 1972) evapotranspiration (ET) routines are used; wind speed is only necessary if the Penman-Monteith method is used. Measured or generated sub-daily precipitation inputs are required if the Green-Ampt infiltration method (Green and Ampt, 1911) is selected. The average air temperature is used to determine it if precipitation should be simulated as snowfall. The maximum and minimum temperature inputs are used in the calculation of daily soil and water temperatures. Generated weather inputs are calculated from tables consisting of 13 monthly climatic variables, which are derived from long-term measured weather records.

Simulation of the hydrologic balance is foundational for all SWAT watershed applications and is usually described in some form regardless of the focus of the analysis. The majority of SWAT applications also report some type of graphical and/or statistical hydrologic calibration, especially for streamflow, and many of the studies also report validation results. As such, the model has been used to predict river flow which were compared satisfactorily with measured data for various watersheds (Govender and Everson, 2005; Van Liew and Garbrecht, 2003; Santhi et al., 2001; Saleh et al., 2000), to evaluate the impact of watershed scaling on the prediction of flow, sediment yield, and nutrient losses for watersheds (Jha et al., 2004), to predict various impacts of land management on water quantity (Srinivasan and Arnold 1994; Muttiah and Wurbs, 2002), to quantify the environmental benefits of conservation practices at both the national and watershed scales (Mausbach and Dedrick, 2004), to estimate base flow and/or groundwater flow (Arnold et al., 2000; Kalin and Hantush, 2006), to predict potential climate change impacts on water resource (Rosenberg et al., 2003; Jha et al., 2004; Gosain, et al. 2006) and assess the impact of land use changes on the annual water balance and temporal runoff dynamics (Fohrer et al., 2001; Fohrer and Frede, 2002; Fohrer et al., 2005).

A wide range of statistics has been used to evaluate SWAT hydrologic predictions. By far the most widely used statistics reported for hydrologic calibration and validation are the regression correlation coefficient (R^2) and the Nash-Sutcliffe model efficiency (NSE)

coefficient (Nash and Sutcliffe, 1970). Van Liew and Garbrecht (2003) evaluated SWAT's ability to predict streamflow under varying climatic conditions for three nested sub-watersheds in the 610 km^2 Little Washita River experimental watershed in south-western Oklahoma. After a calibration for relatively wet years in two of the sub-watersheds they found that SWAT could adequately simulate runoff for dry, average, and wet climatic conditions in another sub-watershed. Govender and Everson (2005) report relatively strong streamflow simulation results for a small (0.68 km^2) research watershed in South Africa.

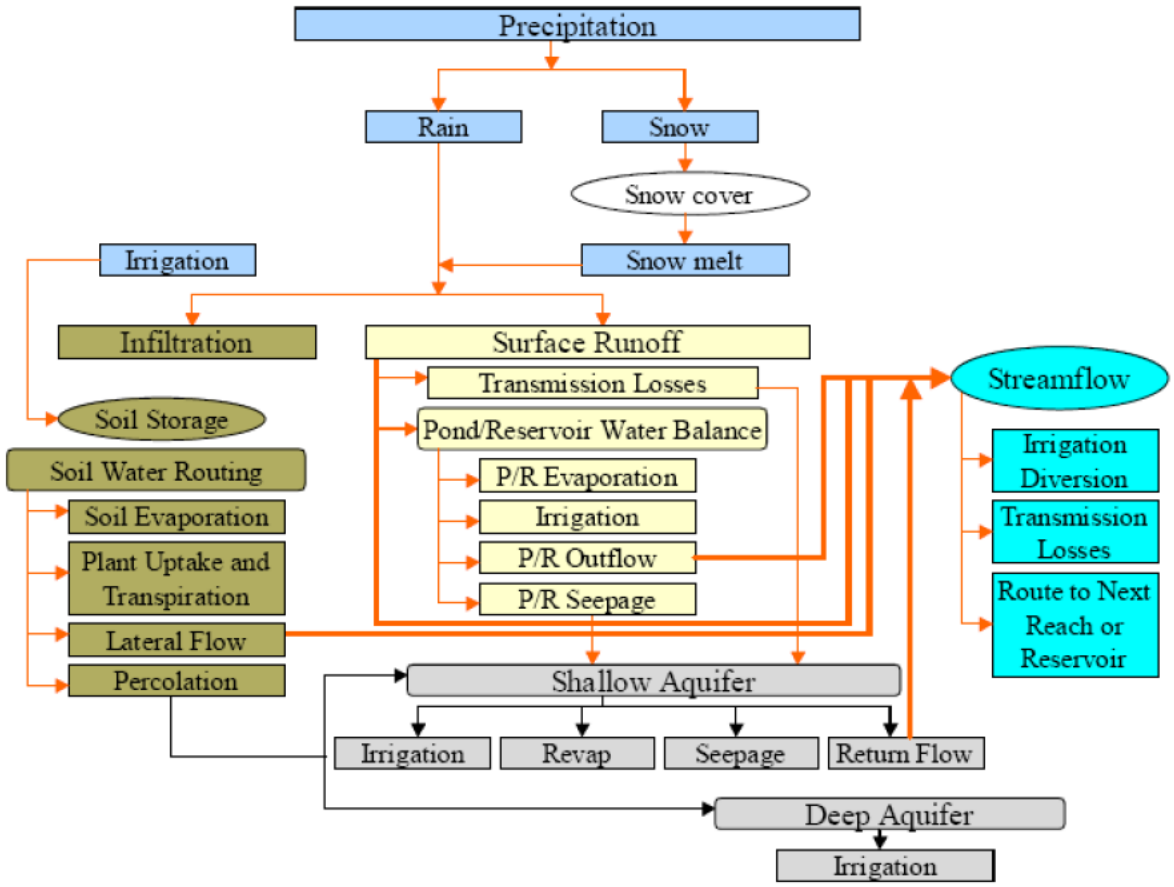

Figure 2.6 Pathways for water movement within SWAT (Neitsch, 2005)

In similar manner, SWAT has been effectively applied in several Ethiopian watersheds. To mention some, the model was used in central Ethiopia (Lijalem, 2006; Alamirew, 2006), Blue Nile Basin (Sirak, 2007; Shimelis, 2008) to model the hydrological process, sediment yield and to estimate water balance. In general, it was found that the overall performance of the model in most cases was reasonable.

Other researchers, Gosain et al. (2005), assessed the capability of SWAT to simulate return flow after the introduction of canal irrigation in a basin in Andra Pradesh, India.

SWAT could provide the assistance that the water managers needed in planning and managing their water resources under various scenarios. Santhi et al. (2005) describe a new canal irrigation routine that was used in SWAT. Volk et al. (2007) and van Griensven et al. (2006a) also described SWAT application approaches within in the context of the EU Water Framework Directive.

2.3.5 TOPMODEL

A simple approach to predicting spatial patterns of responses in a catchment is represented by TOPMODEL. TOPMODEL is a semi distributed conceptual rainfall runoff model that takes the advantage of topographic information related to runoff generation. But according to Beven and Kirby (1979), Beven et al. (1984), the TOPMODEL is considered as a physically based model as its parameters can be theoretically measured. In other words, it can be defined as a variable contributing area conceptual model in which the dynamics of surface and subsurface saturated areas is estimated from a simplified steady state theory for down slope saturated zone flows.

It can be used in single or multiple sub-catchments using gridded elevation data for the catchment area. It helps in the prediction of hydrological behaviour of basins. The major factors considered in this are the catchment topography and soil transmissivity. The main aim is to compute storage deficit or water table depth at any location. The storage deficit value is a function of topographic index (a/tanβ) (Beven 1986), where a is drained area per unit contour length and $\tan \beta$ is the slope of the ground surface at the location. Since the index is based on basin topography, the model gives calculations only for representative values of indices. It is obtained by manual analysis of contour maps. The model use exponential Green-Ampt method of Beven (1984) for calculating runoff and it is advised to reduce the number of parameters. The output will be in the form of area maps or simulated hydrographs.

The basic assumption of TOPMODEL is that all points in a catchment with the same value of the topographic index (or one of its variants) respond in a hydrologically similar way. It is then not necessary to carry out calculations for all points in the catchment, but only for representative points with different values of the index. The distribution function of the index allows the calculation of the responses at the catchment scale.

Having done the calculations, the results may then be mapped back into space by knowledge of the pattern of the index derived from a topographic analysis. The soil profile

is characterized by a set of stores. The upper part of the soil profile is designated as the root zone storage. Here, rainfall infiltrates until the field capacity is reached. When forest canopies appear, an additional interception and surface storage may be required. In this storage zone, evapotranspiration is assumed to occur at the potential rate to decline at a linear rate when the root zone becomes depleted. Once the field capacity is satisfied and exceeded, the second storage zone begins filling until the water content reaches saturation stage. The gravity drainage store links the unsaturated and saturated zones, according to a linear function that includes a time delay parameter for vertical routing via the unsaturated zone. Another approach on the basis of Darcian flux at the base of the unsaturated zone might be considered.

When the deficit in the gravity drainage store or the water table depth becomes nil, it means that the saturation condition is reached and the rainfall produces direct surface runoff. Therefore, the main goal of TOPMODEL is the computation of the storage deficit or the water table depth at any location for every time step. The theory associates the mean watershed storage deficit to the local storage deficits by making use of the local value of a function of the topographic index.

In general, in TOPMODEL streamflow is separated into surface runoff generated by surface water input on saturated contributing areas and subsurface downhill flow comprising base flow and return flow. In summary, TOPMODEL uses four basic assumptions to relate down slope flow from a point to discharge at a catchment outlet.

1) The dynamics of the saturated zone are approximated by successive steady state representations.
2) The recharge rate entering the water table is spatially homogeneous.
3) The effective hydraulic gradient of the saturated zone is approximated by the local topographic surface gradient (tan β is the notation most common in TOPMODEL descriptions).
4) The effective down slope transmissivity of a soil profile at a point is a function of the soil moisture deficit at that point. This is commonly based on an exponential decrease of hydraulic conductivity with depth.

2.4 Parameter optimization by SWAT-CUP: The SUFI-2 method

The SUFI-2 method in the SWAT-CUP interface is among the extensively used methods for parameter optimization. In this method all uncertainties (parameter, conceptual model,

input, etc.) are mapped onto the parameter ranges, which are calibrated to bracket most of the measured data in the 95% prediction uncertainty (Abbaspour et al., 2007). According to the same Authors, Various SWAT parameters related to discharge were estimated using the SUFI-2 algorithm. In SUFI-2, uncertainty is defined as the discrepancy between measured and simulated variables. SUFI-2 combines calibration and uncertainty analysis to find parameter uncertainties that result in prediction uncertainties bracketing most of the measured data, while producing the smallest possible prediction uncertainty band.

The SUFI-2 model starts by assuming a large parameter uncertainty (within a physically meaningful range), so that the measured data initially fall within the 95PPU. Two different indices are used to compare measurement to simulation: the P-factor and the R-factor. The *P*-factor is the percentage of data bracketed in the 95% prediction uncertainty (95PPU) calculated at the 2.5% and the 97.5% intervals of the simulated variables. This factor indicates how much of the uncertainty we are capturing and its maximum value is 100 %, and ideally one would like to bracket all measured data, except the outliers, in the 95PPU band. The *R*-factor, on the other hand, captures the goodness of calibration, as a smaller 95PPU band indicates a better calibration result (Abbaspour, 2007; Faramarzi et al., 2009). The R-factor is calculated as the ratio between the average thickness of the 95PPU band and the standard deviation of the measured data. It represents the width of the uncertainty interval and should be as small as possible. An ideal situation lead to an *R*-factor approaching zero but should be close to or smaller than a practical value of 1.

In each iteration, previous parameter ranges are updated by calculating the sensitivity matrix, and the equivalent of a Hessian matrix (Neudecker & Magnus, 1988), followed by the calculation of a covariance matrix, 95% confidence intervals of the parameters, and a correlation matrix. Parameters are then updated in such a way that the new ranges are always smaller than the previous ranges, and are centered around the best simulation (for more detail Abbaspour *et al*., 2007). Because this analytical approach considers a band of model solutions (95PPU) instead of a best fit solution, the goodness of fit and the degree to which the calibrated model accounts for the uncertainties are assessed by the above two measures instead of the usual R^2 or Nash-Sutcliffe coefficient (Nash & Sutcliffe, 1970), which only compare two signals.

2.5 Downscaling by SDSM

Prior to specifically dealing with SDSM, a brief description of downscaling methods are presented here. GCMS are powerful tools for simulating the global climate and its possible change in the future due to the increase in GHGs. These tools define the latitude-longitude grids on the entire globe and solve the prognostic equations of the atmosphere to obtain a trajectory of the global climate well-matched with the external forcings and the initial conditions supplied. Even though very complex, the governing physical equations are significantly simplified to be solved by a computer on the grid. GCMs have the capability to reproduce the main large-scale features of the current climate, the jet streams or the storm tracks. Unfortunately they can't provide detail information about regional climate. The coarse resolution of GCMs is not able to resolve small-scale physical processes, such as those related to cloud formation, precipitation or turbulence. Therefore, even though GCMs give information at their grid resolution, it can't be interpreted as local information for the region where the grid point is located. There should be a way through which large-scale atmospheric circulations are related to local scale climate variables. Downscaling is the combination of large-scaling forcing, called predictors, and the local climate variables, the predictands, to obtain information about regional climate. Generally, downscaling can be divided into dynamical and statistical downscaling.

Statistical downscaling

Statistical downscaling makes use of a strong observed empirical relationship between one or several large-scale predictors and a variable of interest at regional scale, the predictand. The relationship is then exploited to obtain information on the local variable out of the large-scale predictors. The need for a strong relationship explaining most of the variability of the local-scale variable is one of the main limitations for using statistical downscaling method. The area where the large-scale variable most influences the predictand must be selected.

Although statistical downscaling does not incorporate any physical knowledge about the underlying relationship between the large and regional scale variables under consideration, the driving physical principles behind the relationship can often be identified into the statistical results by means of the spatial signatures of the anomalies, for instance. This way, if the identified physical mechanism is plausible to remain

unchanged in an altered climate, the statistical downscaling model will likely perform correctly under such altered conditions.

Dynamical downscaling

Dynamical downscaling consists of increasing the spatial resolution of a GCM by means of a physical model which solves the governing equations on a grid with higher resolution than those used by GCMs. Due to computer power limitation it is not possible to run a GCM at the fine resolution needed to obtain the regional detail required for impact assessments. Moreover, resolution cannot be increased without solving more equations to explain the phenomena becoming resolved at those regional scales.

The Statistical downscaling model (SDSM)

Since statistical downscaling is very handy even though empirical, it has many advantages over dynamical downscaling and thus, here it is described in some more detail.

The Statistical Downscaling Model (SDSM), an empirical-statistical downscaling tool, was developed by Rob Wilby and Christian Dawson in UK. SDSM is described as a hybrid between a multivariate linear regression method and a stochastic weather generator. In their study of uncertainty analysis of statistical downscaling methods, Khan et al. (2006) showed that the SDSM is the most capable model to reproduce various statistical characteristics of observed data in its downscaled results with 95% confidence level. They compared SDSM with Long Ashton Research Station Weather Generator (LARS-WG) model and Artificial Neural Network (ANN) and found that SDSM was the most ideal software for downscaling.

The SDSM software statistically downscales daily weather series in seven discrete steps. The steps are briefly presented below.

1) Quality control and data transformation

There may be very few meteorological stations that have complete or fully accurate data sets. Handling of missing and imperfect data is necessary for most practical situations. The ‘Quality Control’ identifies gross data errors, specification of missing data codes and outliers prior to model calibration. In many instances it may be also necessary to transform predictors and/or the predictand prior to model calibration. Transformation

function will apply selected transformations for selected data files. The transformation can be logarithmic, power, inverse, lag or binomial.

2) Screening of predictor variables

Identifying empirical relationships between gridded predictors (such as mean sea level pressure) and single site predictand (such as minimum temperatures) is vital to all statistical downscaling methods. The main purpose of the screen variables operation is to decide and select appropriate downscaling predictor variables. The choice of predictors largely determines the character of the downscaled climate scenario.

3) Model calibration

The calibrate model operation takes user-specified predictand along with a set of predictor variables, and estimates the parameters of multiple regression equations via an optimization algorithm by either dual simplex or ordinary least squares methods.

It is needed to specify the model structure: whether monthly, seasonal or annual sub-models are required; whether the process is unconditional or conditional. In unconditional models a direct link is assumed between the predictors and predictand. In conditional models, there is an intermediate process between regional forcing and local weather. For example local precipitation is a conditional process because its amount depends on the occurrence of wet-days, and in turn the occurrence of wet-days depends on regional-scale predictors such as humidity and atmospheric pressure.

4) Weather generation

The weather generator operation generates ensembles of synthetic daily weather series given observed (or NCEP re-analysis) atmospheric predictor variables. This procedure enables the verification of calibrated models (using independent data) and synthesis of artificial time series for present climate conditions.

For this operation to take place selection of the calibrated model is required and the model automatically links all necessary predictors to model weights. Specification of the period of record to be synthesized and the desired number of ensembles are also needed.

5) Analyses of chosen statistical parameters

SDSM provides means of interrogating both downscaled scenarios and observed climate data with summary statistics and frequency analysis. This will allow the user to specify the sub-period and the chosen statistics. In return, SDSM displays a suite of diagnostics including monthly/seasonal/annual means, measures of dispersion, serial correlation and extremes.

6) Frequency analysis and visualization

This provides the options to analyze frequency analysis, compare results and time series analysis. The Frequency Analysis screen allows plot of extreme value statistics of the chosen data file. Analyses include Empirical, Gumbel, Stretched Exponential and Generalised Extreme Value distributions.

The Compare Results screen helps in plotting monthly statistics produced by the Summary Statistics screen. The graphing option allows simultaneous comparison of two data sets and hence rapid assessment of downscaled versus observed, or present versus future climate scenarios. The Time Series Analysis screen is used to produce time series plots for up to five variables.

7) Scenario generation

This scenario generation operation produces ensembles of synthetic daily weather variables given atmospheric predictor variables supplied by a climate model (either for present or future climate experiments), rather than observed predictors. This function is identical to that of the Weather Generator operation in all respects except that it may be necessary to specify a different convention for model dates and source directory for predictor variables.

2.6 The Water Evaluation and Planning Model (WEAP)

The Water Evaluation and Planning model is a software tool for Integrated Water Resources Management (IWRM) developed by the Stockholm Environmental Institute (SEI). WEAP has a long history of development and use in the water planning area (Yates et al., 2005). WEAP integrates physical hydrologic processes with the management of demands and infrastructure, as well as environmental and economic aspects of water planning. Simulations in WEAP are constructed as scenarios. Scenarios can be constructed and analyzed based on different trends in hydrology, water use and demands, demography, technology, operation rules and water management policies.

WEAP is developed with the purpose of being a flexible and transparent tool for aiding IWRM, and is not a tool for modelling detailed water operations, such as optimization of hydropower production.

WEAP is comprehensive, straightforward and easy-to-use, and attempts to assist rather than substitute for the skilled planner. As a database, WEAP provides a system for maintaining water demand and supply information. As a forecasting tool, WEAP simulates water demand, supply, flows, and storage, and pollution generation, treatment and discharge. As a policy analysis tool, WEAP evaluates a full range of water development and management options, and takes account of multiple and competing uses of water systems.

Reservoirs can be modelled either as online or offline. Moreover, it is possible for a reservoir to serve a single or multiple purposes in WEAP. Online reservoirs are instream and the river flows directly into the reservoirs. Runoff-river and river are the two categories of online reservoirs in WEAP. Unlike river reservoirs, runoff-river reservoirs do not provide storage. Also, they do not have a variable head for hydropower generation. Offline reservoirs are sometimes called local. In WEAP, local reservoirs receive water from the river through a transmission link or diversion. All demand sites linked to a local reservoir are assumed to be located downstream of the reservoir, and if the reservoir has hydropower plant, all releases are assumed to pass through the turbines. A river reservoir in WEAP delivers water to its demand sites through separate transmission links that are not connected to the turbines. Koka Reservoir is assumed as a local reservoir as there are three turbines through which the water passes and generates hydropower.

2.7 Optimal Storage Management on the Basis of HEC-ResSim model

HEC-ResSim is reservoir simulation software, which is under the public domain, developed by the hydrologic engineering center of the U.S. Army of corps of Engineers. HEC-ResSim represents a substantial progress in the decision support tools available to water managers. It is designed to simulate reservoir operations for flood management as well as flow augmentation.

HEC-ResSim has been developed to assist water resources engineers performing water resources studies in predicting the behaviour of reservoirs and to help reservoir operators plan releases in real-time during day-to-day and emergency operations (Klipsch and

Evan, 2007). The main advantage of the model is to support the reservoir regulator to take the right decision, i.e., to match the needs of real-time release targets.

HEC-ResSim makes use of an original rule-based approach to mimic the actual decision-making process that reservoir operators must use to meet operating requirements for power generation, irrigation, flood control, water supply, and environmental quality. The reservoirs constructed to meet the flow requirements may have multiple and/or differing and conflicted constraints on their operation. HEC-ResSim characterizes these flow requirements and constraints for the operating zones of a reservoir using a separate set of prioritized rules for each zone.

Basic reservoir operating goals are defined by flexible at-site and downstream control functions and multi-reservoir system constraints. As HEC-ResSim has evolved, advanced features such as outlet prioritization, scripted state variables, and conditional logic have made it possible to model more complex systems and operational requirements. The graphical user interface makes HEC-ResSim easy to use and the customizable plotting and reporting tools facilitate output analysis (Klipsch and Evan, 2007).

The software model consists of three modules: the watershed setup, the reservoir network and the simulation scenario module (Figure 2.7). The first module represents the watershed development which is the model configuration of the schematic elements. These elements include streams, projects, gauge locations, impact areas, time-series locations and hydrologic as well as hydraulic data for that specific area. Schematic elements allow the representation of watershed, reservoir network and simulation data usually in a geo-referenced content that interacts with associated data.

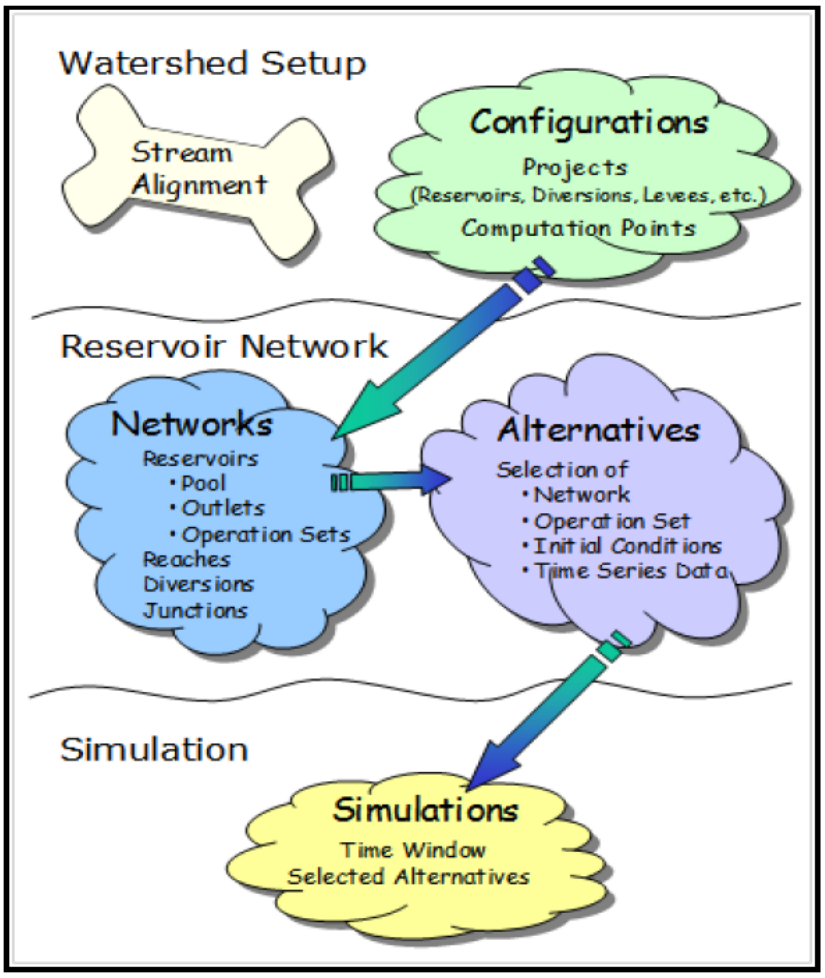

Figure 2.7 HEC-ResSim module concepts (Klipsch and Hurst, 2013)

The second module represents a reservoir network that characterizes a collection of watershed elements connected by routing reaches. The network includes reservoirs, reaches and junctions needed for the model and is where all the physical and operational data are entered and stored in the model. This module allows the model to describe the physical behaviour of reservoir systems with a combination of hydraulic computations for flows through control structures, and hydrologic routing to represent the lag and attenuation of flows through segments of streams. Hence, the model has options for the user to define alternatives and run their simulations simultaneously to compare the results until the target will be achieved. This improves the accuracy of the model; so this makes it unique among reservoir simulation models (Klipsch and Evan, 2007).

The third module is the Simulation module and its purpose is to isolate the output analysis from the model development process. Once the reservoir model is complete and the alternatives have been defined, the Simulation module is used to configure the simulation.

The computations are performed and results are viewed within the Simulation module (Klipsch and Hurst, 2013).

Reservoir operational management requires a set of operational rules that applies a certain procedure for release regulation, rules, schedules, policy or plans that best meet a set of goals. For this purpose, reservoir operation rules should be used to establish a guideline for responding to the questions how the reservoir storage should release during the operation time. The main purpose of reservoir operating rules is to guide release decisions for the reservoir operators based on the existing condition. In HEC-ResSim, every reservoir should have a target elevation. A reservoir's target elevation, presented as a function of time, is called its Guide Curve. It is the dividing line between the upper zones of the reservoir and the lower zones. Each zone can contain a different set of rules depending on the flow limits and requirements of that zone within the regulation plan. Hence, the guide curve is the principal logical criteria in HEC-ResSim to take release decision at any time.

CHAPTER 3

3. WORKING BASICS AND METHODOLOGY

3.1 General framework

This chapter is divided into sub-sections consisting of Hydrological modelling, Future Climate data and Scenarios, flow simulation and climate change Impact. Hydrological Modelling is carried out using SWAT model (see Subsection 2.3.4) to derive physiographic parameters of the watershed which need to be used in hydrological modelling. Thus, runoff processes are simulated on the sub-watershed system from the upstream to the watershed outlet throughout the streamflow network. Performance of the model was analysed using the SWAT-CUP model, via calibration, validation and uncertainty analysis. The statistical downscaling model (see Section 2.5) was used to specially produce the local climate change scenarios at the local scale and to fill the missing gaps in meteorological data using the model's weather and scenario generator

functions. The climate change downscaling results as well as those from RCPs (see Subsection 2.5.1.2) were used as input into rainfall-runoff SWAT modelling to forecast the future river flow.

This research involves connecting hydrology modelling to climate change downscaled output to understand the impact of climate change on hydropower generation. The method used for construction of climate change scenarios made use of change fields of rainfall and temperature from GCMs which were then superimposed on the baseline time series within SWAT. Beyond 2006, RCP climate data were used as input into the models to simulate the pertinent hydrological processes to assess the impact of climate change on hydropower generation of the study area, Upper Awash River Basin (UARB). The WEAP (Section 2.6) was used to simulate monthly, seasonal and annual hydropower generation for the current and future periods. Indeed, in some cases, specifically RCP4.5 and RCP8.5 emission scenarios climate data were used as input to model hydropower production for the period 2006 – 2014 to compare with the observed hydropower production data obtained from Ethiopian Electric Utility (EEU). Therefore, among the models described in Chapter two, Sections 2.3 and 2.4, SWAT, SWAT-CUP, SDSM and WEAP models were directly and frequently used for the realization of the research. Of course some other application software were used in addition under these core software models. For instance, Microsoft Excel, pcpSTAT.exe, dew01.exe, Dew02.exe, ArcGIS, ArcSWAT and other computer applications were used here and there, and now and then.

3.2 The Study Area

3.2.1 Awash River Basin

There are twelve major river basins in Ethiopia. The Awash River Basin is one of them covering a total area of about 110,000 km^2. The main River, Awash, starts from central Ethiopian highland, some 150 km west of the capital, Addis Ababa. From the source, tt flows in the south-east-direction for about 250 km. Then, it enters the Great East African Rift Valley, and follows the rift system in north-east direction for the rest of its course. It drains the northern part of the rift valley in Ethiopia. The Basin is located between $7^0 52' 12''$ N to $12^0 08' 24''$ N latitude, and $37^0 56' 24''$ E to $43^0 17' 02''$ E longitude.

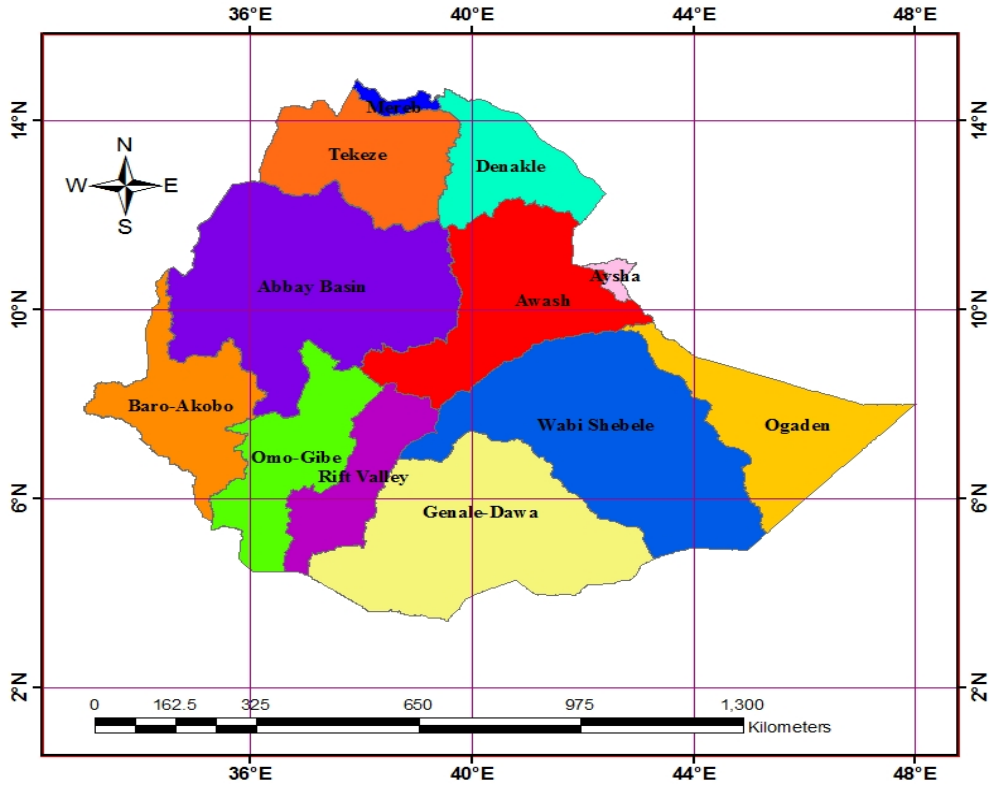

Figure 3.1 The Ethiopian major river basins

The total length of the main river is about 1200 km, and its final destination is Lake Abe, in the Danakil Depression near Ethio-Djibouti border. The basin is almost entirely within the boundaries of Ethiopia. The altitude of its source, the west-central highland, is about 3000 m.a.s.l, while that of its destination is as low as 250 m.a.s.l. Where it enters the Rift, the altitude is about 1500 m.a.s.l. About 70% of the country's irrigated agriculture is covered by Awash River Basin. Besides, the oldest hydroelectric power plants of Koka and Awash II and Awash III hydroelectric power, having a total installed capacity of 46 MW are located in this Basin.

The Awash Basin may be divided into three sub river basins, namely, Upper Awash, Middle Awash and Lower Awash. The elevation ranges from as high as 3554 meter above sea level in the west to as low as 116 meters below sea level in the east. The Upper Awash River Basin comprises south-east and east course of the river down to the point where it turns northwards along the line of the Rift. In this part of the main Awash River, the average slope exceeds 6%, and there are many falls, few of which have already been used for hydropower. The upper part has a length of about 300 km.

Middle Awash comprises the course northwards to a point downstream of the confluence of the Mile River, near Tendaho. In this section the general slope is less than 10%; there are numerous rapids where the river crosses bars of igneous rocks, between which occur

reaches of flood plain and swamp in places. The altitudes in the Middle Valley range from 1,000 m. at Metehara to about 500 m. at the rapids upstream of the confluence of the Mile. The length of this section is about 650 km.

Lower Awash has a short distance south of Tendaho. There occur a series of faults aligned generally northwest to southeast, which have caused the river to turn southeast wards across the alluvial plains. Its slope in this section is only about 0.39%; its course is meandering, deltaic, and unstable; extensive areas are flooded, and changes of course often occur. Several lakes exist, of which the largest is Lake Abe, which receives the remaining flows. The length of this part of the course, to the entrance of Lake Abe, is about 250 km. The research concerns the upper part of the river basin, Upper Awash River Basin (UARB).

3.2.2 The Upper Awash River Basin

3.2.2.1 Location

The geographical location of the Upper Awash Basin is between $8^0$16’ to $9^0$18’ N latitude and $37^0$57’ to $39^0$17’ E longitude. The River Basin has an area of about 11,140 km^2. The Berga, Holeta, Teji, Kela, and some other small tributaries join the plain of Becho at the upstream part of the UARB, the outlet being at Melka Kunture.

Downstream of Melka Kunture gauging station, there are other rivers that join the Awash River before it enters the plain surrounding Lake Koka. This low-lying plain at the west shore of Lake Koka that is also surrounded by volcanic hills has a mean elevation of 1590 m.a.s.l. The major rivers here are Akaki, Lemen, Dukem and some other smaller tributaries. When these rivers join together further downstream, and still upstream of Koka, they constitute River Hombole. The Mojo River forms a confluence with River Hombole and then flows to Koka.

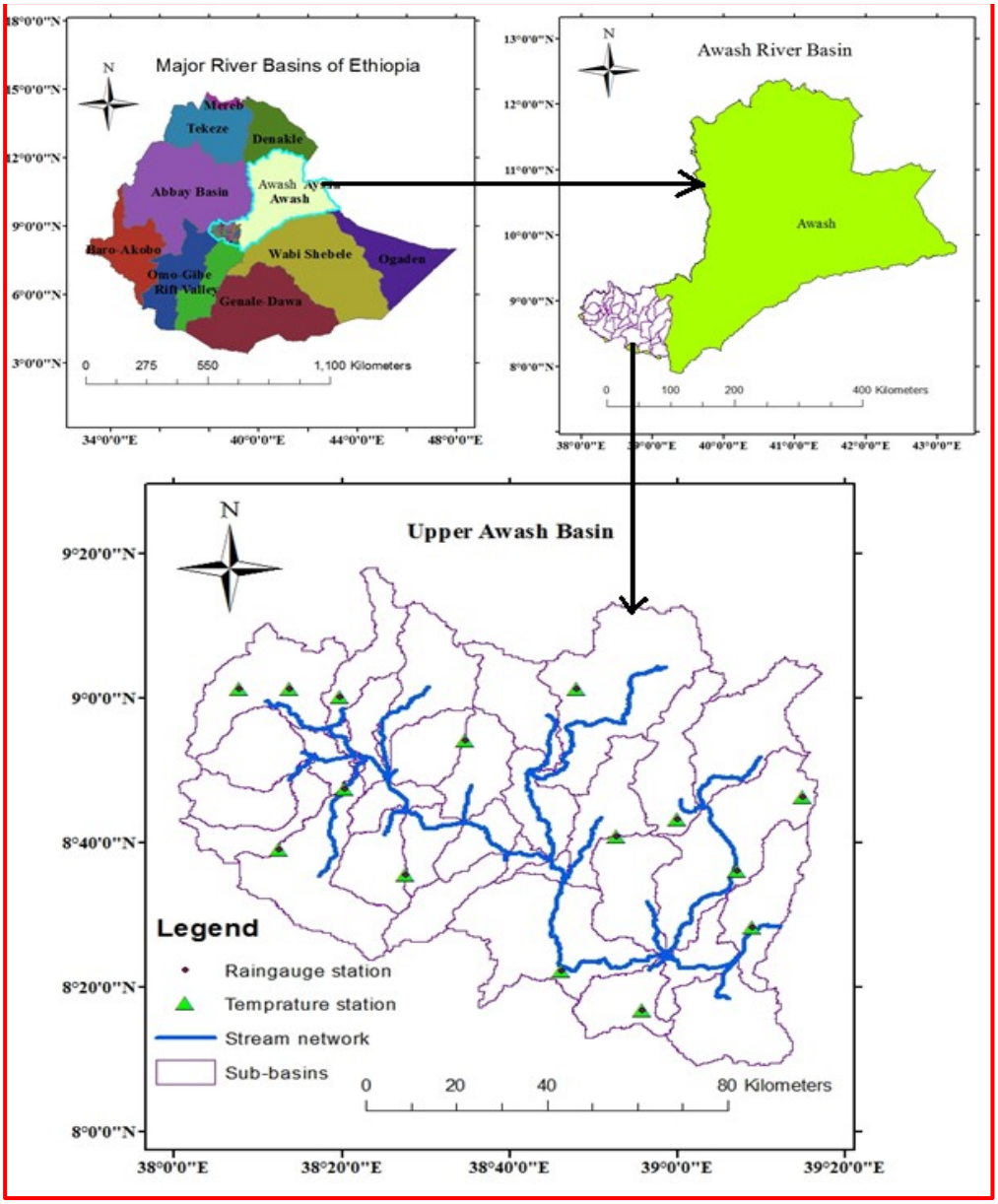

Figure 3.2 Map of the study area

3.2.2.2 Climate

The climate of the Awash basin is humid to sub-humid in the highlands and semi-arid to arid in the rift valley. The climate of the area is affected by the Inter-Tropical Convergence Zone (ITCZ). This Zone of low pressure marks the convergence of dry tropical easterlies and moist equatorial westerly. The explanation of the seasonal rainfall distribution (Figure 3.3) within the basin lies in the annual migration of the ITCZ across the basin. The ITCZ starts its advance across the basin from south in March, bringing the small or spring rains. In June and July the ITCZ reaches its most northerly location beyond the basin, which then experiences the heavy or summer rains throughout. The amount and distribution of rainfall over the highlands is influenced and modified by orographic features and shows

strong correlation with altitude (Halcrow, 1989; WWDSE, 2008). The ITCZ returns southwards during August, September and October, restoring a drier, easterly air stream that prevails until the ITCZ resumes its northward migration in March.

In plain areas of the basin, annual rainfall ranges from 800 mm to 1000 mm, and reaches about 1200 mm in peaks. 70 % to 75 % of the total rainfall occurs in the main wet season (Nederveen, 2013). The major rainy season is between June and mid September with a short monsoon rain in March to April. The mean annual temperature of the basin is about 16^0 C in the highlands and around 22^0 C in the lowlands. The lowest temperature occurs during the main rainy season; seasonal temperature variation is not pronounced. The average relative humidity is 77% in the wet season (June - September) and about 60% in the rest of the year (October - May).

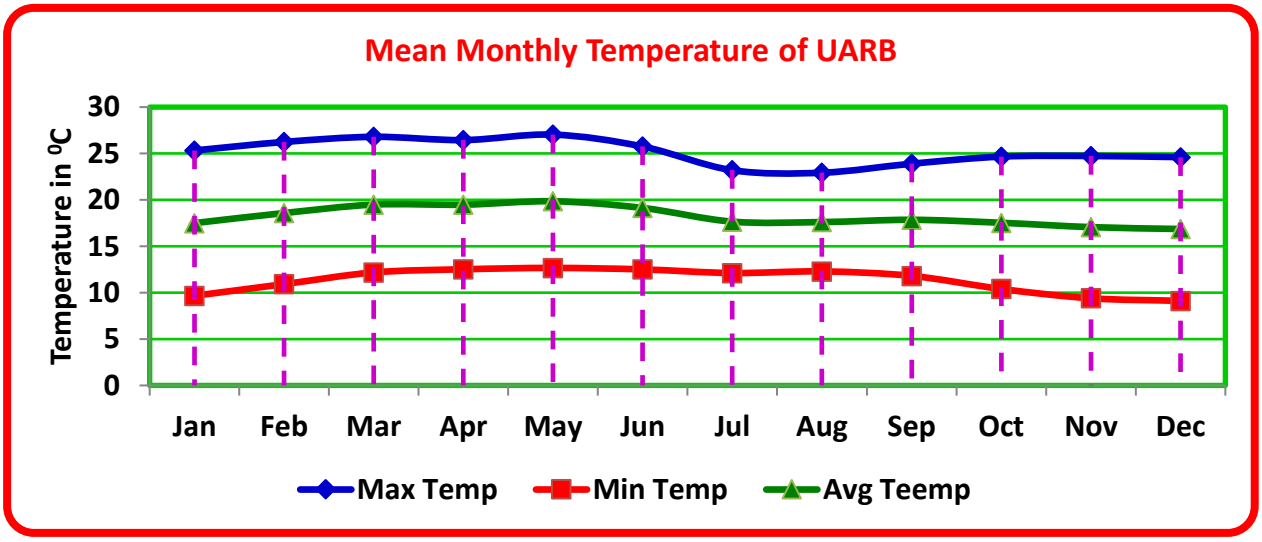

Figure 3.3 Mean monthly temperature of UARB

The average wind speed is 1.8 m/s; it is above 2 m/s for the months December to March, and below 2 m/s for the rest months. It shows that wind speed is more pronounced in dry season as compared to the wet season. This condition may be exploited for wind power during dry season when rainfall is sparse and therefore the runoff too. The lowest wind speed was recorded in the month of September, and the maximum one in December in almost all the study period of thirty years. The average pan evaporation is about 180 mm during the dry season and 75 mm in the wet season at Addis Ababa observatory (WWDSE, 2008).

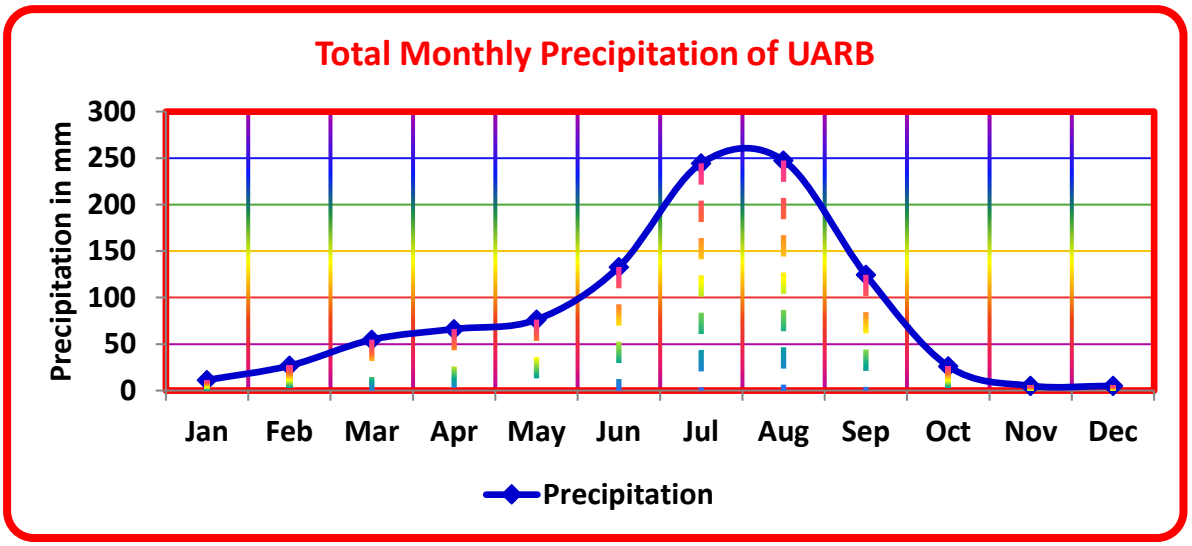

Figure 3.4 Mean total monthly precipitation distribution of UARB

3.2.2.3 Soil

Soils of the Ethiopian highlands are the outcome of the decomposition of the volcanic material. They are derived from lava rocks, are clayey in texture and are basically quite fertile.

Soils in the study area are classified by the FAO soil classification system (1990). There are four major soil types in the Upper Awash Basin; the deep red clay soil, Nitosol, and the dark clay soil, Vertisol, Luvisol, and Camibsol. The Nitosols are found in the upland areas, whereas the Cambisol and Luvisol are found in the escarpment and Vertisols are found in lowland areas with slopes ranging from 2 to 8%. Vertisols are by far the dominant soil classes, accounting for about 60% of the study area, and including the upland plains, all the seasonal swamps, and most of the alluvial cover flood plains and terraces (Nippon, 1996).

The vertisols in upper plains of the UARB are black clays that are dominated by montimorillonite clay mineral. This mineral expands when wet and contracts when dry, causing cracks at the surface in the dry season. These cracks are well developed in the inundated areas and back-swamps of the plains where they can be 10 cm wide and 70 cm deep.

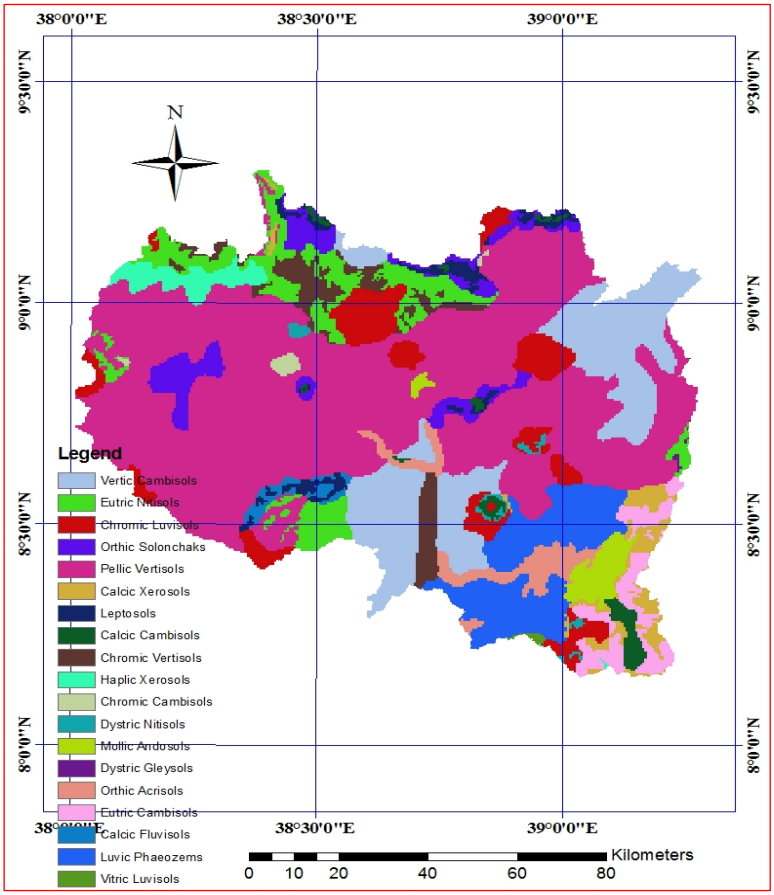

Figure 3.5 Soil map of UARB

The soils have a high water holding capacity, allowing flood recession agriculture where crops use the residual soil moisture. Although the clay rich soils hold water well, they are also impermeable for infiltration to deep aquifer. Moreover, most of the plains are inundated during floods especially in the months of August to Mid-September. The recharge of the deep groundwater in the UARB is restricted by the abundance of the vertisols (WWDSE, 2008).

3.2.2.4 Land use

The dominant landuse in the basin is rain-fed agriculture, covering an area of about 80%. The main crops grown are teff, wheat, barley and beans. Near to the capital Addis Ababa, there is also a considerable area of forest covering not less than 14%. The rest part of the basin is attributed to some range lands, pasture, grasslands with shrubs, some water bodies and urban area.

The main crops and agricultural practices differ in the upland areas from the inundated areas. Generally the higher areas are used for teff and other grains and the low-lying areas for pulses. The teff that is grown in the low-lying temporarily inundated areas gives

low yields, which is mainly caused by the lack of water in the grain formation phase. This water deficit is due to delayed planting caused by the inundation (Nippon, 1996).

Irrigation is highly practiced in the UARB. Of primary concern is that irrigation is intensively carried out by the government as well as by individual farmers and cooperatives. Most of the irrigation activity is accomplished downstream of Koka Lake, upstream of Awash II and III hydropower plants. This landuse system has highly hampered the power that would have been generated by the two downstream hydropower plants. Moreover, there is no promising way for upgrading the two hydropower plants because it is mandatory and fact that the irrigation farming will continue. The water supply service in Adama cannot be compromised as well.

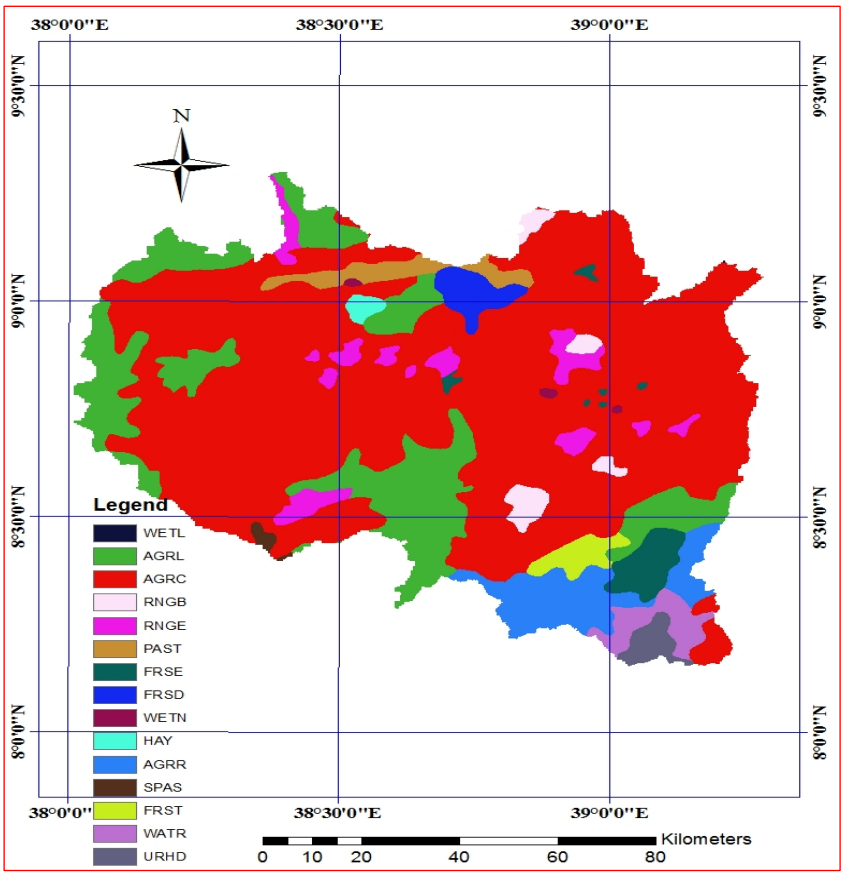

Figure 3.6 Landuse map of UARB

3.2.2.5 Topography

The topography of Upper Awash River Basin (UARB) is in general characterized by highlands and lowlands, like other river basins of Ethiopia. The highlands dominate in the north-west and, the lowlands are the major features towards the south-east of the river basin. Elevation ranges from 1545 to 3554 meters above sea level, as also defined by SWAT model. The topography of the study area generally increases in elevation from

downstream lowlands to upstream highlands. The North-west highlands have steeper slopes as compared to the middle and south-east part of the basin. However, large area of the basin has gentle slope, especially the regions surrounding the capital Addis Ababa and to the east. 57.4% (the green part in Figure 3.7) of the basin has a slope of less than 5% and the rest 42.5% (the part coloured pink in Figure 3.7) area is characterized by mild to steep slope of more than 5%.

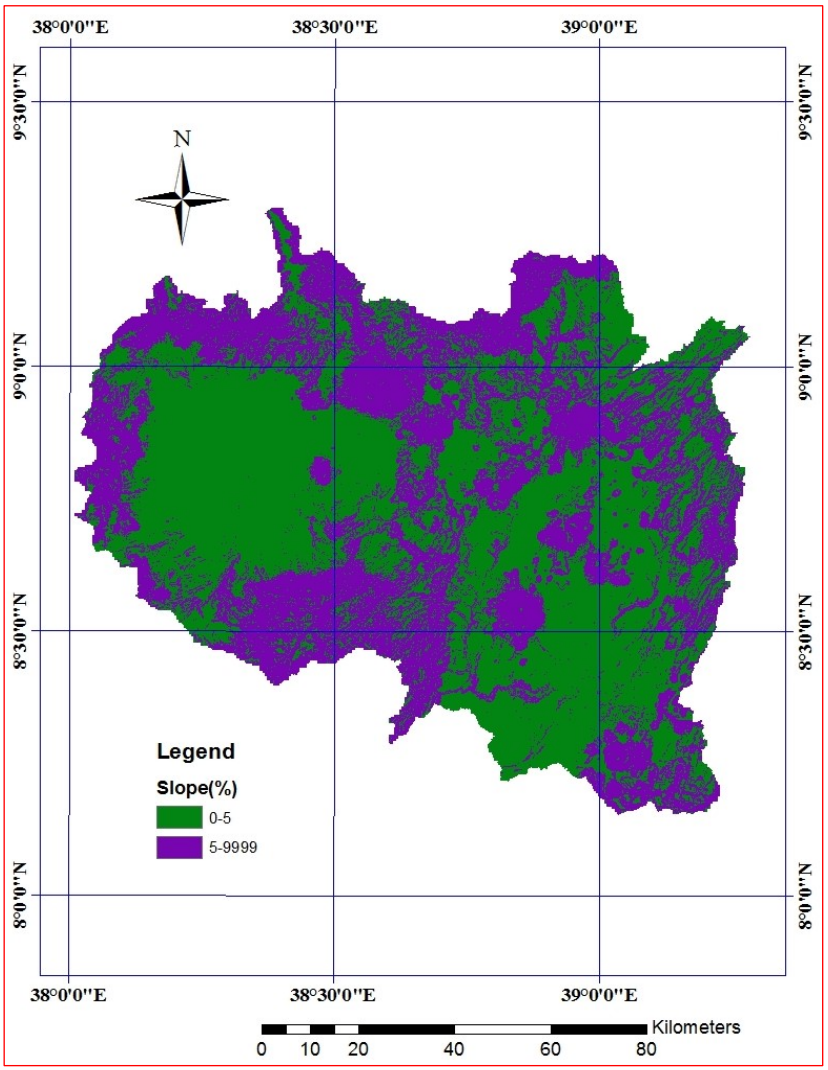

Figure 3.7 Slope classes of UARB

3.3 Koka Dam and Hydro-electric Power Plant

Koka Dam is located at a distance of about 81 km away from Addis Ababa, in the south-east direction on the Awash River course. From historic point of view, Koka Hydro-electric power plant is the most popular hydro-electric plant in Ethiopia. It is the second hydro-electric power plant that went into operation in 1960.

The discharge from Koka dam is regulated according to the needs of power production. Since the construction of the reservoir and hydroelectric station at Koka in the Upper Basin, the flows at that point have been largely controlled. On the average, the power plant can discharge about 40 m^3/s. As a result, further downstream the areas flooded are reduced, and the losses by evaporation correspondingly diminished. The volume of water discharged will become less irregular from one month to another. Such uniform regulation does not agree with irrigation requirements, which vary considerably at different seasons of the year.

Koka reservoir covers an area of 236 km^2. The maximum level of the reservoir is 1590.70 m.a.s.l, and its storage capacity at this level is 1.85 Mm^3. With a head of 32 – 40 meters, the installed capacity is 54,000 kVA comprising three generating units. The rated capacity at full load is 45,000 kW. The average production capacity is 110 GWh.

Figure 3.8 Few features of Koka Hydropower Plant

Koka Dam is also used for the operation of power cascade (Awash II and III power plants) and for irrigation and flood protection for the people at the downstream. In table 3.1, the salient features of Koka Reservoir, Dam and Hydropower Plant are presented.

Table 3.1 Salient features of Koka Reservoir, Dam and Hydropower Plant

Reservoir	
Maximum level	1590.7 m.a.s.l
Minimum level	1580.7 m.a.s.l
Total storage capacity at 1590.70 m	1.850 x 10^6 m^3
Usable storage capacity	1.680 x 10^6 m^3
Reservoir area at 1590.70 m	236 km^2
Regulated flow	42.3 m^3/s
Dam	
Type	Concrete gravity dam
Crest elevation	1.593.20 m.a.s.l
Crest length	458 m
Maximum height	23.8 m
Maximum spillway discharge at 1590.70 m	4 x 250 m^3/s
Water Conductors	
Pressure tunnel	
Length	71.50 m
Diameter	5.50 m
Concrete Pipeline	
Length	143.37 m
Diameter	5.50 m
Surge Tank	
Diameter	18 m
Height	20 m
Penstock	
Number	3
Diameter	3.5 m
Length	50.7/55.4/61.1 m
Production Capacity	
Average	110 GWh
Actual	101 GWh
Capacity	
Installed	43.20 MW
Firm	34.50 MW
Units	3 x 14.4 MW

Like other regions of the World, UARB faces many challenges as climate changes. Floods, droughts, rapid glacial melt, increasing temperatures, and variability in timing, location and amount of precipitation, are all symptoms of climate change that will affect hydroelectric generation by increasing water resources and hydropower potential in some regions and diminishing them in others (Blackshear et al., 2011). Developing countries such as Ethiopia are more vulnerable to the impact of climate change due to the fact that

they possess limited finance to spend on extreme climate events that may occur and on adapting to long-term alterations. The changes of the two most climate variables, temperature and precipitation patterns, have intense effects on river systems and runoff.

These impacts directly affect hydroelectric production. Hydropower entirely depends on river flow since it is directly proportional to the river discharge..

3.4 Modelling

3.4.1 Application of SWAT Model

SWAT simulates the hydrology of a watershed in two separate components. One is the land phase of the hydrological cycle and the other is routing phase of hydrologic cycle. The first controls the amount of water, sediment, nutrient and pesticide loadings to the main channel in each subbasin, and the second defines the movement of water, sediments, nutrients and organic chemicals through the channel network of the watershed to the outlet. A water balance model is simulated in the land component of SWAT (Arnold et al., 1998, Gassman et al., 2007).

The land phase of the hydrologic cycle as simulated by SWAT is based on the water balance equation:

$$SW_t = SW_o + \sum_{i=1}^{t}\left(R_{day} - Q_{sur} - E_a - w_{seep} - Q_{gw}\right) \text{ (mm)} \qquad (3.1)$$

where

SW_t = the final soil water content
SW_o = the initial soil water content on day i
T = the time (days)
R_{day} = the amount of precipitation on day i
Q_{surf} = the amount of surface runoff on day i
E_a = the amount of evapotranspiration on day i
w_{seep} = the amount of water entering the vadose zone from the soil profile on day i
Q_{gw} = the amount of return flow on day i

The subdivision of watershed enables the model to reflect differences in evapotranspiration for various crops and soils. Runoff is predicted separately for each

HRU and routed to obtain the total runoff of the watershed. This increases accuracy and gives much better physical description of the water balance.

The routing phase is generally accomplished through the main channels or reaches and the reservoirs. Routing in the main channel or reach can be divided into four components: water, sediment, nutrients and organic chemicals. Here, flood routing is briefed as it is, namely as routing of water associated with objectives of the thesis.

In flood routing, as water flows downstream, a portion may be lost due to evaporation and transmission through the bed of the channel. Another potential loss is removal of water from the channel for agricultural or human use. Flow may be supplemented by the fall of rain directly on the channel and by addition of water if tributaries discharge into the main river. Flow is routed through channel using a variable storage coefficient method developed by Williams (1969) or the Muskingum method.

Flow routing according to Williams is based on the continuity equation

$$I - O = \Delta S \tag{3.2}$$

which can be written as

$$\Delta t\left[\frac{I_1+I_2}{2}\right] - \Delta t\left[\frac{O_1+O_2}{2}\right] = S_2 - S_1 \tag{3.3}$$

where

Δt = time interval
I_1 = inflow rate at the beginning of routing interval
I_2 = inflow rate at the end of routing interval
O_1 = outflow rate at the beginning of routing interval
O_2 = outflow rate at the end of routing interval
S_1 = storage volume at beginning of time interval
S_2 = storage volume at end of time interval

Similarly, Muskingum routing is a storage routing method based on the storage equation which is an expression of continuity:

$$I - O = \frac{ds}{dt} \tag{3.4}$$

and this expression for storage in a reach or main channel of a stream in the Muskingum method is given as:

$$S = K[xI + (1-x)O] \tag{3.5}$$

where

I = inflow rate

O = outflow rate

S = storage

t = time

K = storage parameters

x = weighting parameter to consider the influence of I and O

SWAT subbasin components consist of hydrology, weather, sedimentation, crop growth, nutrients, pesticides and agricultural management. Hydrological processes include simulation of surface runoff, percolation, lateral flow and flow from shallow aquifers to streams, potential evapotranspiration, snowmelt, transmission losses from streams and water storage and losses from ponds.

SWAT provides two surface runoff computation methods; a modification of the Soil Conservation Service (SCS) Curve Number (CN) method (USDA SCS, 1972) or the Green & Ampt infiltration method (Green and Ampt, 1911).

The CN method is widely used (Arnold et al., 1998; Lukman, 2003; Garen and Daniel, 2005). In this method, the ratio of actual retention to maximum retention is assumed to be equal to the ratio of direct runoff to rainfall minus initial abstraction. This can be mathematically expressed as (USDA, 1985)

$$Q_{surf} = \frac{(R_d - I_a)^2}{(R_d - I_a + S)} \quad (3.6)$$

Ia ≅ 0.2 S

$$S = 25.4\left(\frac{1000}{CN} - 10\right) \quad (3.7)$$

Therefore,

$$Q_{surf} = \frac{(R_d - 0.2S)^2}{(R_d - 0.8S)} \quad (3.8)$$

where

Q_{surf} = the accumulated surface runoff (mm)

R_d = the rainfall depth for the day (mm)

I_a = initial abstraction (mm, surface storage, canopy interception, infiltration prior to runoff)

S = retention parameter (mm)

CN = curve number

3.4.2 Model input and model parameterization

The Hydrological Response Units (HRU) are the units within the watershed that dictate the standard ArcSWAT model set-up, including watershed delineation and their definition, on which calculations are based. The parameterization and the basic data sets required to develop the project for this study in the ArcGIS interface, the ARCSWAT, include the attributes of topography, soil, land-use, slope and climatic data. The data used in modeling for UARB are as follows:

1. A digital elevation model (DEM) taken from the website www.srtm.csi.org.
2. Soil map at a scale of 1:1 000,000, Soil and Land in East Africa (SEA)
3. Land-use maps, at a scale of 1:100,000, and other parameters were estimated using suggested values in the SWAT user manual and other sources.
4. Climate data records from 23 precipitation and seven air temperature gauges over a period of 30 years (1981 – 2010); data were obtained from the Ethiopian Metrological Agency
5. Stream flow data for 30 years have been obtained from MIWE.

Landuse and soil map along with their respective look up tables prepared earlier were supplied to the model for reclassification according to SWAT coding convention. Further entire watershed was classified into three slope categories using the interface. All the three maps were then overlaid to create HRU's with unique land cover/soil and slope class.

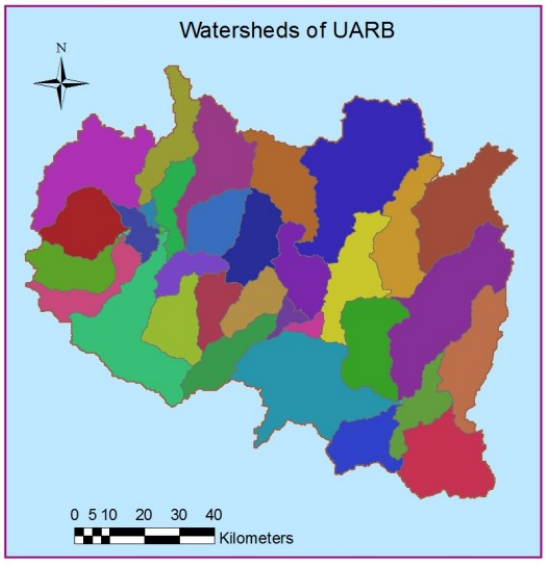

Figure 3.9 Sub-watersheds of UARB

Location table of Weather Data, Daily Precipitation Data Files, Maximum and Minimum Temperatures, Wind Speed, Relative Humidity were loaded to link them up with the required files already created for the purpose. After loading all the input data and generating the required database files, SWAT model was initially run on monthly basis using default parameter values.

The UARB was subdivided into 37 sub-basins and 388 HRUs. The soil map includes 15 types of soil. Soil texture, available water content, hydraulic conductivity, bulk density and organic carbon content information were available for different layers for each soil type. The simulation time period was 1981 – 2010. The first three years were used as a warm-up time for the model. Data from the Hombole station in the UARB were used for calibration and validation.

3.4.3 Parameter sensitivity

Sensitivity analysis demonstrates the impact that changes to an individual input parameter has on the model response and can be performed using a number of different methods (Veith and Ghebremichael, 2009). It is the process of determining the rate of change in model output with respect to changes in model inputs (parameters). Thus, it is important to identify the parameters that most significantly influence the model output. Sensitivity analysis from SUFI-2 provided partial information about the sensitivity of the objective function to model parameters. In this study, 19 water-related parameters (global parameters), were selected to do sensitivity analysis separately (Table 3.2). The sensitivity analysis is carried out by keeping all parameters constant to realistic values, while varying each parameter within the range assigned in the initial step. The t-test and the p-values were used to provide a measure and the significance of the sensitivity, respectively. A t-stat provides a measure of sensitivity (larger absolute values are more sensitive), and p values determine the significance of the sensitivity (a value close to zero has more significance).

Sensitivity analysis in SWAT is carried out based on the combined robust Latin Hypercube One at a Time (LH-OAT) method (van Griensven et al. 2006). *LH sampling procedure* is a sophisticated way to perform random sampling that allows a robust analysis requiring not too many runs (McKay et al., 1979). The concept of the LH is based on the Monte Carlo simulation but uses a stratified sampling approach that allows efficient estimation of the output statistics. After the sensitivity analysis was carried out in SWAT

model, eight most sensitive parameters were identified and then used as input in SWAT-CUP to carry out calibration and validation.

Table 3.2 Parameters and their ranges used in sensitivity analysis using SWAT model

S. No	Parameters	Description	Parameter range
1	ALPHA_BF	Base flow alpha factor (days)	0 – 1
2	CANMX	Maximum canopy storage (mm)	0 – 100
3	CH_K2	Channel effective hydraulic conductivity (mm/hr)	-0.01 – 500
4	CH_N	Manning's n value for main channel	0.01 – 0.3
5	CN2	SCS runoff CN for moisture condition II	35 – 98
6	EPCO	Plant uptake compensation factor	0 – 1
7	ESCO	Soil evaporation compensation factor	0 – 1
8	GW_DELAY	Groundwater delay (days)	0 – 500
9	GW_REVAP	Groundwater 'revap' coefficient	0 – 0.2
10	GWQMN	Threshold depth of water in the shallow aquifer for return flow to occur (mm)	0 – 5000
11	RCHR_DP	Groundwater recharge to deep aquifer (mm)	0 – 1
12	REVAPMN	Threshold depth of water in the shallow aquifer for 'revap' to occur (mm)	0 – 1000
13	SLOPE	Average slope steepness (m/m)	0 – 60
14	SLSUBBSN	Average slope length (mm)	10 – 150
15	SOL_ALB	Soil albedo	0 – 0.1
16	SOL_AWC	Available water capacity of the soil layer (mm/mm soil)	0 – 1
17	SOL_K	Saturated hydraulic conductivity (mm/hr)	0 – 2000
18	SOL_Z	Soil depth (mm)	0 – 3500
19	SURLAG	Surface runoff lag coefficient	1 – 12

3.4.4 Calibration setup and analysis

Model calibration and validation is a challenging and complex in hydrological model. The SWAT model was calibrated and validated for streamflow in the Upper Awash Basin. Monthly discharge records of a decade of the data period were selected in order to calibrate and subsequently validate water relative parameters. The first three years were used as warm-up period to mitigate the effect of unknown initial conditions, which were subsequently excluded from the analysis. Accordingly, the three years period from 1998 – 2000 was used as a warm-up time; the data years from 2001 – 2006 was used for calibration and the recorded data of the rest four years from 2007 – 2010 was used for validation.

SWAT Calibration and Uncertainty Program (SWAT-CUP) software was selected to do the auto-calibration because of its capability to perform calibration, validation, sensitivity analysis and uncertainty analysis – and also because its performance was better than the auto-calibration modulus embedded in the SWAT interface (Zhou et al., 2014). Currently, the program can run Sequential Uncertainty Fitting (SUFI-2) (Abbaspour, *et al*., 2007), Generalized Likelihood Uncertainty Estimation (GLUE) (Beven and Binley, 1992), and Parameter Solution (ParaSol) (van Griensven and Meixner, 2006), Particle Swarm Optimization (PSO) and Markov Chain Monte Carlo (MCMC) procedures. SUFI-2 was selected for this because it accounts for all sources of uncertainties, yet it is fast and relatively handy to use.

3.4.5 Objective functions

An objective function is used to evaluate model performance in hydrologic modelling. This is typically achieved by comparing simulated and observed results. Several objective functions have been used for estimating model performance models. The performance of the model in simulating hydrologic variables was evaluated with the help of statistical parameters such as coefficient of determination (R^2), Nash-Sutcliffe Simulation Efficiency (NSE), p-factor and r-factor.

Nash-Sutcliffe Efficiency (NSE)

The NSE is computed as the ratio of residual variance to measured data variances (Nash and Sutcliffe, 1970). NSE can range from -∞ to 1 with an efficiency of 1 corresponding to a perfect match of simulated streamflow to the observed data. The NSE was calculated using the following Equation.

$$NSE = 1 - \frac{\sum_{t=1}^{T}(Q_m^t - Q_O^t)^2}{\sum_{t=1}^{T}(Q_O^t - \overline{Q_O})^2} \qquad (3.9)$$

where $\overline{Q_O}$ is the mean of observed discharges, and

Q_m is modelled discharge.

Q_o^t is observed discharge at time *t*.

Coefficient of Determination (R^2)

Coefficient of determination R^2 is a measure of dispersion around the mean of the observed and predicted values and can be used as efficiency criteria. The range of R^2 lies between 0 and 1 which describes how much of the observed dispersion is explained

by the prediction. A value of zero means no correlation at all whereas a value of 1 means that the dispersion of the prediction is equal to that of the observation. A model which systematically over- or under-predicts all the time will still result in good R^2 values close to 1.0 even if all predictions were wrong. By weighting R^2 by the slope of regression line between observed and modelled, under or over-predictions are quantified together with the dynamics which results in a more comprehensive reflection of model results.

$$R^2 = \frac{\sum_{i=1}^{n}(Q_i - \acute{Q})(S_i - \acute{S})}{\sqrt{\sum_{i=1}^{n}(Q_i - \acute{Q})^2}\sqrt{\sum_{i=1}^{n}(S_i - \acute{S})^2}} \qquad (3.10)$$

where

Q_i = Observed streamflow

S_i = Simulated streamflow

$\acute{Q}$ = Mean observed streamflow

$\acute{S}$ = Mean simulated streamflow

n = Number of observation

p-Factor and r-Factor

The p- and r-factors are closely related to each other, which indicate that a larger p-factor can be achieved only at the expense of a higher r-factor. The Latin hypercube sampling method was employed for 95PPU and for obtaining the final cumulative distribution of the model outputs. During the initialization of model parameters, SUFI-2 assumed a large parameter uncertainty and then decreased this uncertainty through the p-factor and the r-factor performance statistics. The range of the p-factor varied from 0 to 1, with values close to 1 indicating a very high model performance and efficiency, while the r-factor was the average width of the 95PPU band divided by the standard deviation of the measured variable and varied in the range 0 –1 (Abbaspour et al. 2007; Yang et al. 2008). After balancing these two factors, and at an acceptable value of the r-and p-factors, the calibrated parameter ranges could be generated.

There were other statistics that indicated model performance, apart from those presented above. Two of them were percent bias (PBIAS) and root mean square error (RMSE).

Percent bias (PBIAS) measured the deviation between simulated and observed data. A score of 0.0 is the optimal PBIAS value and values of low magnitudes express accurate

model estimation. Positive PBIAS values indicate model underestimation, while negative values indicate the contrary. PBIAS was found using the following equation.

$$PBIAS = \frac{\sum_{t=1}^{n}(Q_i^{obs} - Q_i^{sim}) \times 100}{\sum_{i=1}^{n} Q_i^{obs}} \quad (3.11)$$

where

Q_i^{obs} = the ith observed value

Q_i^{sim} = the ith simulated value

The root mean square error (RMSE) is a commonly used statistical error index. RMSE standard deviation ratio (RSR) standardizes the RMSE by dividing it by the standard deviation of the observed data. RSR was computed using the following equation. Q_i^{obs}, Q_i^{sim} and Q_{mean} are of same meaning as in PBIAS and NSE.

$$RSR = \frac{RMSE}{STDEV_{obs}} = \frac{\sqrt{\sum_{t=1}^{n}(Q_i^{obs} - Q_i^{sim})^2}}{\sqrt{\sum_{i=1}^{n}(Q_i^{obs} - Q_{mean})^2}} \quad (3.12)$$

RSR values range from 0.0 to larger positive values. An RSR value of 0.0 is the optimum and indicates no residual variation and perfect model behaviour. The lower the RSR value is, the better the model performs. Based on an extensive literature review on methods of watershed model evaluation, Moriasi et al. (2007) defined model evaluation criteria for PBIAS, NSE and RSR. Table 3.3 lists the statistics and their recommended performance ratings.

Table 3.3 Performance rating for PBIAS, NSE and RSR (Moriasi et al., 2007)

Performance	**PBIAS (%)**	**NSE**	**RSR**
Very Good	PBIAS < ±10	0.75 < NSE ≤ 1.00 0.	00 ≤ RSR ≤ 0.50
Good	±10 ≤ PBIAS < ±15	0.65 < NSE ≤ 0.75	0.50 < RSR ≤ 0.60
Satisfactory	±15 ≤ PBIAS < ±25	0.50 < NSE ≤ 0.65	0.60 < RSR ≤ 0.70
Unsatisfactory	PBIAS ≥ ±25	NSE ≤ 0.50	RSR > 0.70

3.5 GCM Climate scenarios

Future climate projections from different models and for various emission scenarios and time periods are provided by the Intergovernmental Panel on Climate Change (IPCC, 2007). Although it is preferable to use the most up-to-date climate models for climate

change impact studies such as hydrological modeling, the raw output from low-resolution General Circulation Models (GCMs from Hadley Center) should not be used directly to force impact models (see Subsection 2.1.5). Instead, common practice is to increase the spatial variability of GCM output data by means of statistical or dynamical downscaling (Olsson et al., 2017 (see Subsection 2.1.5.3)). The GCM data were downscaled by SDSM (see Section 2.5) using the nearest observation station for the period of 1981 – 2010 in the UARB. With this specification, four grid points were within and near the study site.

SDSM, which is designed to downscale climate information from coarse-resolution of GCMs to local or site level was applied here to downscale the precipitation, maximum and minimum temperatures for the study area. In particular, SDSM was used to fill the missing gaps in meteorological data. SDSM uses linear regression techniques between predictor and predictand to produce multiple realizations (ensembles) of synthetic daily weather sequences. The predictor variables provide daily information about large scale atmosphere condition, while the predictand describes the condition at the site level.

The main reasons to apply the SDSM model for the study were; (i) It is widely applied in many regions of the world over a range of different climatic condition, (ii) It can be run on PC-based systems and has been tested on Windows 98/NT/2000/XP, (iii) The availability of the software (i.e. new users can register and download freely the software package at https://co-public.lboor.ac.uk/cocwd/SDSM/), (iv) Compared to other downscaling methods, the knowledge of atmospheric chemistry required by the SDSM is less, (v) The required time for simulating the surface weather parameter is low and the ability of the model to permit risk/uncertainty analyses by using the generated ensembles. Finally, one best quality of SDSM was that missing gap of the main meteorological data could be filled using its weather generator function. As long as the gaps were within reasonable limits, SDSM could fill the missing gaps in precipitation as well as temperature data.

On the other hand, SDSM has limitation in that the relationship between the predictor and predictand is achieved by only considering the statistical condition of the data, i.e. the model does not take into consideration the physical nature of the catchments. Moreover, it requires high quality data for model calibration and the model is highly sensitive to the choice of predictor variables and empirical transfer scheme.

3.5.1 Screening of Potential Downscaling Variables

The predictor variables were downloaded from the National Center for Environmental Prediction (NCEP) re-analysis data set. The data are already re-gridded to conform to the grid system of HadCM3. The Hadley Centre's coupled ocean-atmosphere GCMs (HadCM3) work at a spatial coverage of 2.5^0 latitude by 3.75^0 longitude. Screening of the potential predictors for the selected predictand (i.e. observed precipitation, minimum and maximum temperature) were used to select the appropriate downscaling predictors for model calibration and the most crucial and decisive part in statistical downscaling model. Identifying appropriate large scale gridded predictors results in good correlation between observed and downscaled climate variables during model calibration and scenario generation.

The recommended methods for screening the potential predictors is starting the processes by selecting seven or eight predictors at a time and analyzing their explained variance; then selecting those predictors which have higher explained variance. The significance level which tests the significance of predictor-predictand correlation was set to the default $P<0.05$ and the rest were dropped. For the selected predictors, their correlation matrix was analyzed and calculated with the observed predictand. This statistics identifies the amount of explanatory power of the predictor to explain the predictand and finally the scatter plot was carried out in order to identify the nature of the association (linear, non–linear, etc.), whether or not data transformation may be needed. This procedure is repeated by holding those predictors which fulfil the above criteria and new predictors are added from the rest of available predictors.

For UARB, climate data were collected from twenty three meteorological stations in and around the UARB, of which fifteen are found within the boundary of the sub-basin. Even though the downscaling was done for all the stations, five stations that can best represent the basin in all directions were selected for simulation of future climate.

Three main factors constrain the choice of predictors. Data should be (1) reliably simulated by GCMs, (2) readily available from archives of GCM output, and (3) strongly correlated with surface variables under consideration (Wilby et al., 1999). The best correlated predictor variables selected for precipitation, maximum temperature and minimum temperature are listed in Table 3.4.

It was expected from observation and experience of nature that some of the variables are relatively good predictors, because they are very closely related to precipitation and temperature. As an example, mean temperature at 2 m height (Table 3.4) from the ground is directly related to temperature, and thus it was possible beforehand that it could be a good temperature predictor. In similar manner, before using SDSM to identify potential predictors, it could be possible to guess that relative humidity and specific humidity (Table 3.4) would be direct predictors that could influence precipitation, especially in the study area. Therefore, it can be concluded that the everyday experience is very important apart from the software.

Table 3.4 Summary of predictor variables and their respective predictands

Predictors	
Maximum and Minimum Temperatures	Precipitation
Surface relative humidity (rhum) Mean temperature at 2 m height (temp) 500 hPa zonal velocity (p5_u) 500 hPa geopotential height (p500)	Mean sea level pressure (mslp) Surface airflow strength (p_f) Surface specific humidity (shum) Relative humidity at 850 hPa (r850) 500 hPa geopotential height (p500) Surface vorticity (p_z)

3.5.2 SDSM Model Calibration, validation and GCM Scenario generation

It is important to note that this scenario was generated using SDSM from previous HadCM3 GCM. As will be discussed later, the scenario defined for future hydropower generation was based on CMIP5 RCP4.4 and RCP8.5. As far as SDSM model is concerned, the model calibration operation takes a selected predictand along with a set of predictor variables, and computes the parameters of multiple regression equations via an optimization algorithm, either dual simplex of ordinary least squares. The SDSM was calibrated for each month for precipitation, minimum and maximum temperatures.

A regression equation is developed by SDSM based on the type of time selected. The model develops one regression equation for the whole month if monthly time step is selected. In similar manner, if annual model type is selected, again one regression equation is developed for the whole one year and so on. That one regression equation helps in generation of synthetic time series. For this particular study among the total period length of 1981 – 2010, the calibration was carried out from 1991 – 2000 and the withheld data from 2001 – 2010 were used for model validation. The model developed a better multiple regression equation parameters for the maximum and minimum

temperature than for precipitation. This result is mainly due to the conditional nature of precipitation

The Weather Generator operation generates ensembles (up to a maximum of 100) of synthetic daily weather series using the observed (or NCEP re–analysis) atmospheric predictor variables. The procedure enables the verification of calibrated models (using independent data) and the synthesis of artificial time series for present climate conditions. The use of the ensembles allows the evaluation of model uncertainties.

The Scenario Generator operation produces ensembles of synthetic daily weather series from the starting of the baseline period to the end of the 21st century (1961 – 2099) for a given daily atmospheric predictor variables supplied by a GCM (either under present or future greenhouse gas forcing). This function is identical to that of the Weather Generator operation in all respects except that it may be necessary to specify a different convention for model dates and source directory for predictor variables. Scenarios for A2 and B2 storylines are generated for the specified locations and for the period 1961 – 2099.

On the other hand, recalling and linking hydropower generation future scenario here, the monthly and annual hydropower generation data available in full from EEU was for the year 2006 – 2014. Therefore, for the purpose of future hydropower projection, and to be consistent, this period was selected as the reference period in WEAP for the research at hand. It was also assumed that the climate condition during this period may be more or less similar to the climate condition for the period 1986 – 2005 (IPCC, 2013), which is taken as the reference period by IPCC.

3.5.3 CORDEX Stations in UARB and RCP Scenarios

There are five grid points that lie within the UARB for which there are projected climate covering the whole 21st century under the RCP scenarios.

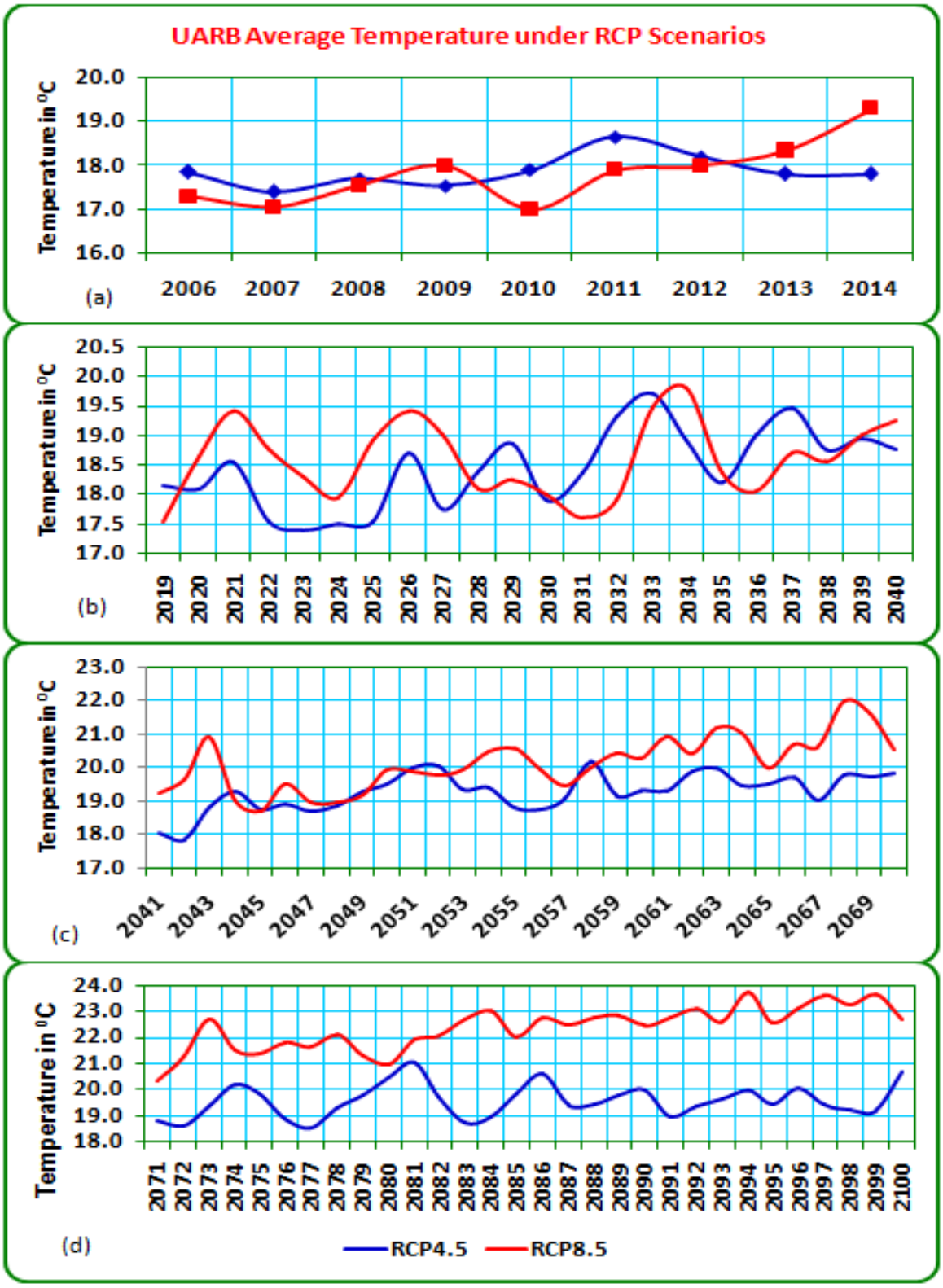

Figure 3.10 UARB projected annual average temperatures under RCP4.5 and RCP8.5 emission scenarios for the periods 2006 – 2014, 2019 – 2040, 2041 – 2070 and 2071 – 2100.

In this sub-section of the research, climate trends and hydrological trends have been discussed in brief. The climate projections are available for RCP2.6, RCP4.5 and RCP8.5 (see Subsection 2.1.5.2). RCP4.5 and RCP8.5 scenarios were used to simulate streamflow, reservoir evaporation and storage, and hydropower production. Comparison

of streamflow simulated by using these CMIP5 RCP4.5 and RCP8.5 climate scenarios with the streamflow modelled by using as inputs, climate variables (precipitation and temperature) downscaled from previous GCM (HadCM3 A2a) experiment using SDSM model was also carried out (see 4.4.1.1).

The results indicate that RCP4.5 and RCP8.5 lead to similar and very close outputs during the first decade of the century, but it is clearly visible that they diverge from each other as time proceeds towards the end of the century. Figure 3.10 shows one example comparing future temperature projection using RCP4.5 and RCP8.5, starting with the period 2006 – 2014. The tables and figures for the various hydrological and Climatological parameters as well as the resulting power production are presented in Appendix in detail.

3.6 Consideration of the impact of climate change on hydropower

Figure 3.11 (Blackshear et al., 2011) shows the complex ways in which changes in precipitation and temperature will affect hydropower.

Among existing hydropower plants, Koka Hydroelectric Plant is the oldest one which is located not far away from the Capital Addis Ababa. Of course the challenges of the plant are many-sided, ranging from sedimentation to overexploitation for various uses. One previous limitation with management of the water resource is that the impact of climate change was ignored. Being close to the Great East African Rift Valley, the evaporation from the reservoir is tremendous, even under the normal circumstance. When the effect of climate change is added, it becomes worse. The reservoir serves hundreds of thousands of people if not millions for different purposes, and will continue to do so, even with more stress. Due attention is needed to make close follow-up. Among others, reduction of evaporation by making use of appropriate techniques is found to be imperative, as the result of this research indicates.

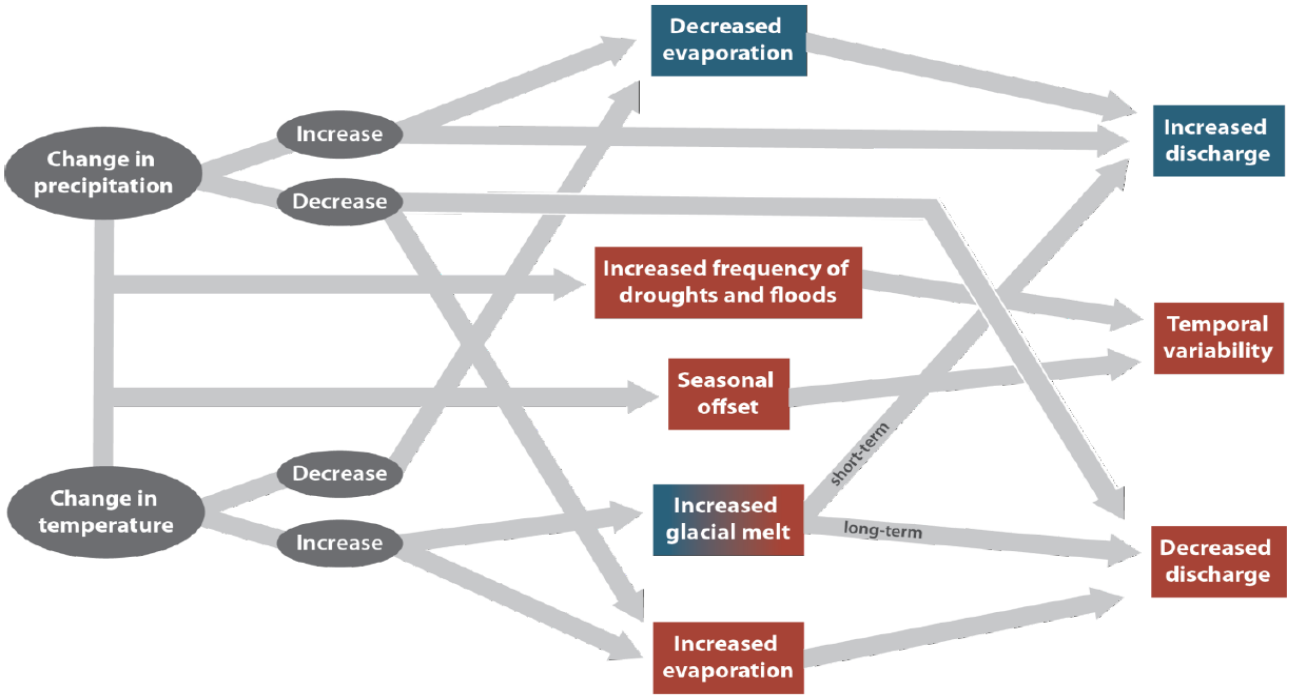

Figure 3.11 Flow chart of climate change effects: red indicates effects that are typically detrimental to hydroelectric production, and blue indicates effects that typically improve hydroelectric production potential (Blackshear et al., 2011)

3.6.1 Koka Reservoir and Hydropower Modelling

In WEAP, reservoir is divided into four zones (Figure 3.12): the flood control zone, the conservation zone, the buffer zone and the inactive zone.

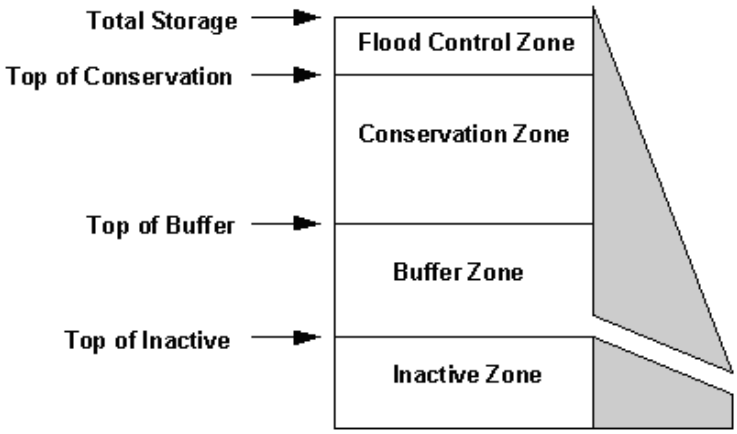

Figure 3.12 Reservoir zones in WEAP (Sieber and Purkey, 2016)

The conservation and buffer pools, together, constitute the reservoir's active storage. WEAP will ensure that the flood-control zone is always kept vacant, i.e., the volume of water in the reservoir cannot exceed the top of the conservation pool (Sieber and Purkey, 2016). WEAP uses the Buffer Coefficient to slow releases when the storage level falls

into the buffer zone. When this occurs, the monthly release cannot exceed the volume of water in the buffer zone multiplied by this coefficient.

According to Halcrow (1989), the monthly inflow into Koka Reservoir was estimated by a regression equation which was based on the gauge observation at Hombole and Mojo rivers. The regression equation was as follows:

$$Q_{Koka} = 1.065Q_{Hombole} + 1.180Q_{Mojo} \qquad (3.13)$$

Accordingly, the 30-years average monthly river flow at Awash River gauging station below their confluence is input into WEAP model. The schematic view of UARB in WEAP interface is shown in Figure 3.13 and, in Figure 3.14, the monthly inflow data input into the WEP model is presented. In all the computations and modelling of future hydropower from Koka Reservoir, it is assumed that the depth of Koka Reservoir stays the same as it is now till the end of the century.

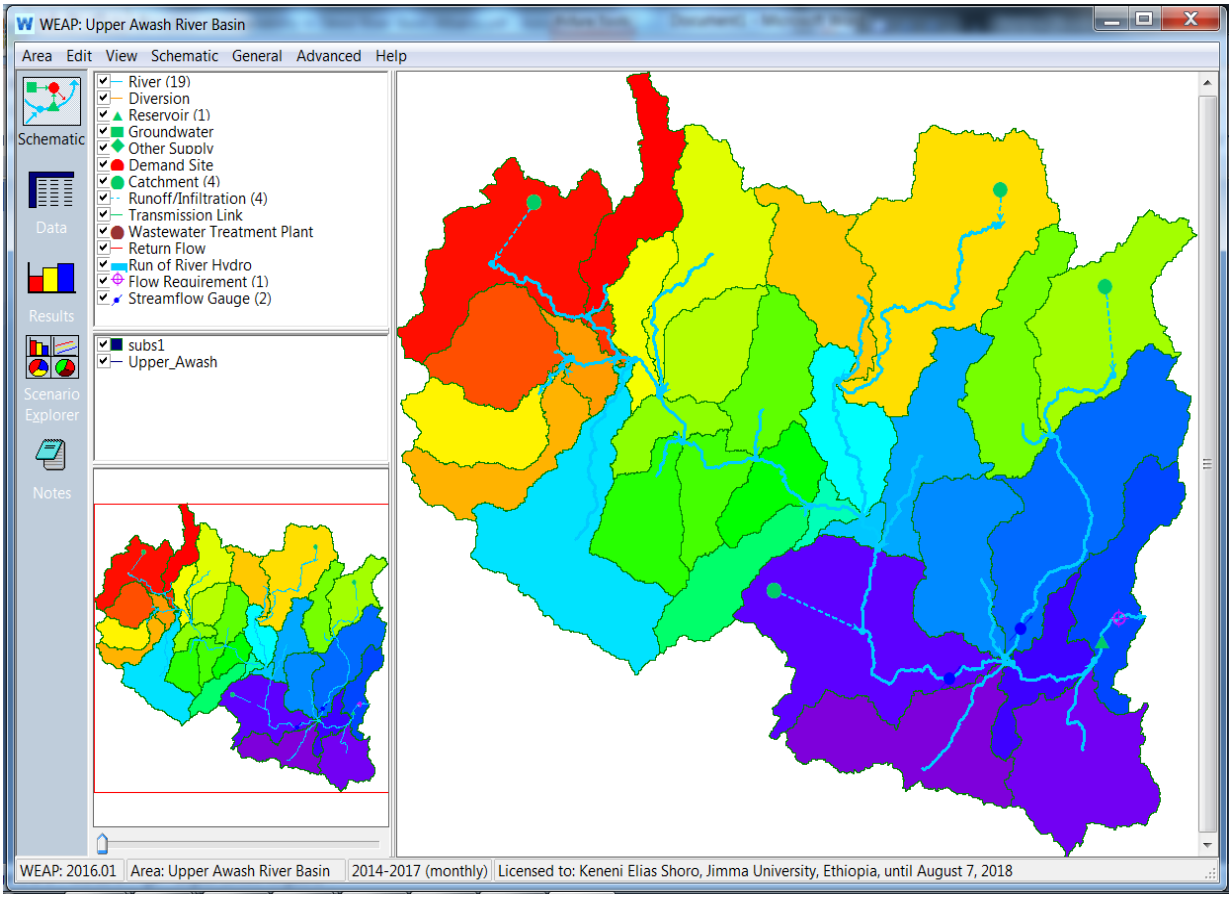

Figure 3.13 UARB schematic views in WEAP interface

In WEAP model, hydroelectric generation is computed using the following equation:

$$E = \gamma_w \eta f Q H T \times 10^{-9} \quad (GWh) \qquad (3.14)$$

where

E = the electricity generated (GWh)

γ_w = specific unit weight of water given by ρg

where ρ = density of water (1000 kg/m^3)

g = acceleration due to gravity (9.81 m/s^2)

η = the total generating efficiency of the system (%)

Q = the flow passing through the turbine (m^3/s)

H = the effective head working on the turbine (m);

T = the time step (hours)

Several parameters are required to be defined for the reservoir for WEAP to work out the hydroelectric production. The volume-elevation curve should be established. This is used to determine the reservoir elevation for the time. The head, H, on the turbine is determined as the difference between the reservoir elevation and the tailwater elevation. Independent of what time step the model is running on, the plant factor, *f*, specifies the percentage of the time step the power plant is allowed to run. For example, if the plant runs for half a year, then f is equal to 0.5. For Koka Hydropower Plant a plant factor and generating efficiency of 55% and 70% are assumed. Other characteristics of Koka reservoir and hydropower for power production are presented in Table 3.5.

Table 3.5 Koka Reservoir and Hydropower input parameters into WEAP model

Hydropower		Physical		Operation			
Max Turb. Flow (CMS)	Tailwater Elevation (masl)	Stor. Cap. (Mm^3)	Net Evap. (mm)	Top of Cons. (Mm^3)	Top of Buffer (Mm^3)	Top of Inactive (Mm^3)	Buffer Coefficient
42.3	1584	1038.5	200	837.4	500	26.5	1.00

3.6.2 Scenario Definition for Koka Hydropower According to RCPs

Two scenarios were developed for Koka reservoir and hydropower in accordance with IPCC definition of RCPs. Here the two RCP scenarios, RCP4.5 and RCP8.5 were selected to define future projection of climate and hydropower generation. These are selected because RCP4.5 represents the medium emission of GWG whereas RCP8.5 the highest GHG concentrations. The future streamflow and the resulting hydropower generation were simulated using the output of these climate scenarios. Three periods of climate change were used under each of these scenarios. The periods are 2019 – 2040, 2041 – 2070 and 2071 – 2100. As discussed previously, for the two scenarios it is

assumed that the depth of Koka Reservoir will be the same as it is now at the end of the 21st century.

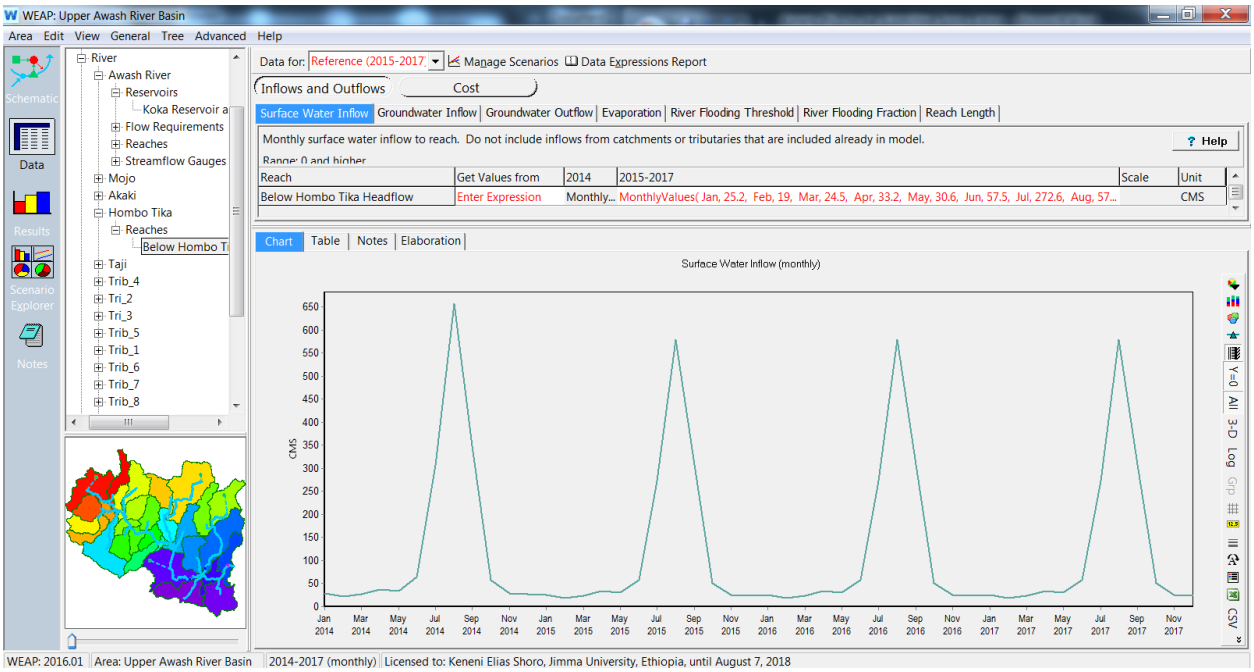

Figure 3.14 WEAP Print screen of monthly inflow into Koka Reservoir at Hombole gauging station of Awash River

The depth of the reservoir which is used by Ethiopian Electric Utility (EEU) and other institutions currently, and of course also by this research is about 60% of the original, the one at the time of the commencement of the hydropower plant in 1960. One limitation is that the sedimentation of the reservoir is not taken into account. It was proposed that the Koka dam will be raised by three meter. Even if it is invariance to reality, it was a must that the Koka reservoir depth remains the same in projection of future hydropower energy because of the nature of WEAP model.

CHAPTER 4

4. RESULTS

4.1 Performance of SDSM

Table 4.1 provides values for both R^2 and root mean square error (RMSE) for assessing model performance for monthly minimum and maximum temperatures for five stations. SDSM could simulate maximum and minimum temperatures for the stations. The model uses the coefficient of determination (R^2) to measure model performance. In fact in all the five stations, R^2 is found to be greater than 0.5, which of course could be taken as satisfactory.

Table 4.1 Performance of SDSM during calibration and validation periods

Predictands	Stations	Calibration			Validation		
		Year	R^2	RMSE	Year	R^2	RMSE
Precip.	Addis Ababa	1991-2000	0.53	12.91	2001-2010	0.52	11.98
	Debrezeit	1991-2000	0.51	13.34	2001-2010	0.50	13.41
	Guranda Meta	1991-2000	0.52	11.06	2001-2010	0.50	10.89
	Hombole	1991-2000	0.52	9.08	2001-2010	0.51	10.21
	Tulubolo	1991-2000	0.53	10.87	2001-2010	0.53	10.37
Temp.	Addis Ababa	1981-1995	0.68	0.8	1996-2010	0.67	1.0
	Debrezeit	1981-1995	0.59	1.12	1996-2010	0.60	1.03
	Guranda Meta	1981-1995	0.56	0.92	1996-2010	0.57	0.97
	Hombole	1981-1995	0.61	1.19	1996-2010	0.60	1.21
	Tulubolo	1981-1995	0.60	1.13	1996-2010	0.60	1.14

RMSE of the model was also measured and was found to be adequate as described by Moriasi et al. (2007).

As can be seen from the table, the performance of SDSM is relatively acceptable in downscaling both temperature and precipitation. It is adequate to work further with the model in order to deal with climate change impact assessments. To show more about the robustness of the state of the art decision support tool, SDSM, the comparison between observed and modelled minimum temperature at Addis Ababa meteorology station is presented in Figure 4.1. Figure 4.2 shows the comparison between the observed and modelled monthly total precipitation at Addis Ababa weather station located at Bole. Addis Ababa is located in UARB.

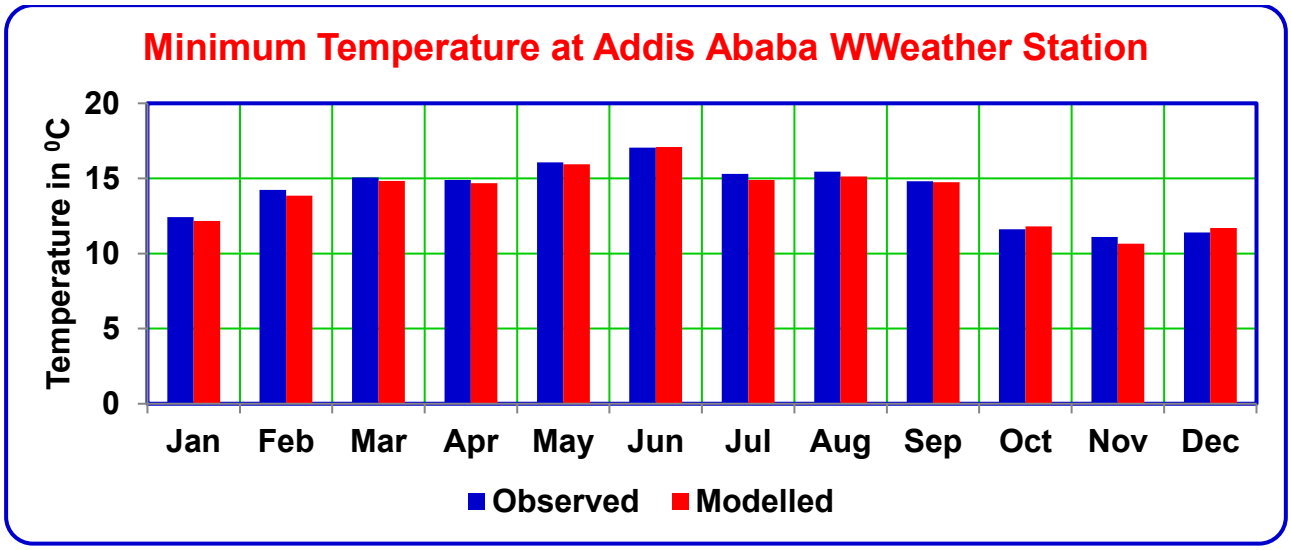

Figure 4.1 Comparison of observed and modelled mean minimum monthly temperature (^{0}C) for the period 1981 - 2001 at Addis Ababa weather station

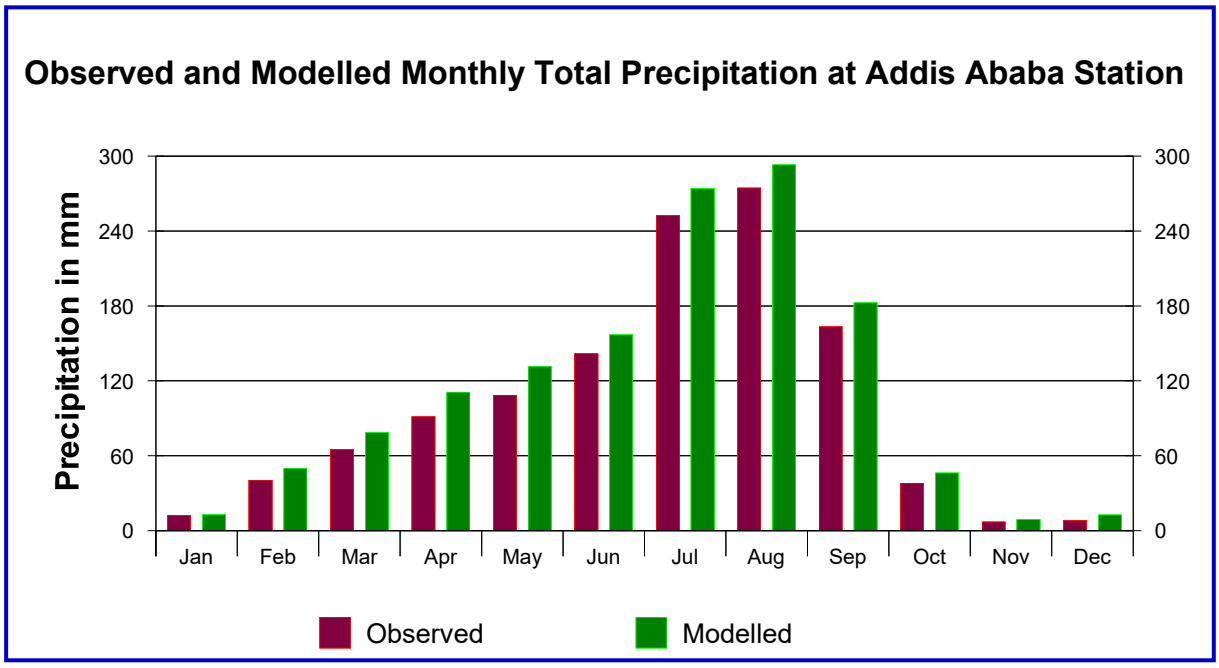

Figure 4.2 Comparison of observed and modelled mean total precipitation (mm) for the period 1985 - 2000 at Addis Ababa weather station

SDSM model slightly overestimated monthly total precipitation as compared to the measured precipitation at the meteorology station, as can be seen from Figure 4.2. However, the model can reproduce the observed precipitation to so that it is possible to deal with the climate change impact assessment.

In spite of the fact that the SDSM decision support tool can adequately help in the projection of future climate and for the assessment of climate change impacts for the purpose of decision making, the issue of the very coarse resolution of the GCMs should

be addressed well. For this purpose, it was found essential to compare the future projection of climate variables from HadCM3 A2a GCM experiment with those of the CMIP5 RCPs (Figure 4.3). Furthermore, the river discharge simulated using SWAT model through the use of projected climate variables as inputs should also be compared with the discharge modelled by using RCP emission scenarios as inputs. The latter will be dealt with after hydrologic modelling is presented. The comparison is really useful to justify that the new scientific experiments associated with CMIP5 models make any difference, especially for Ethiopia.

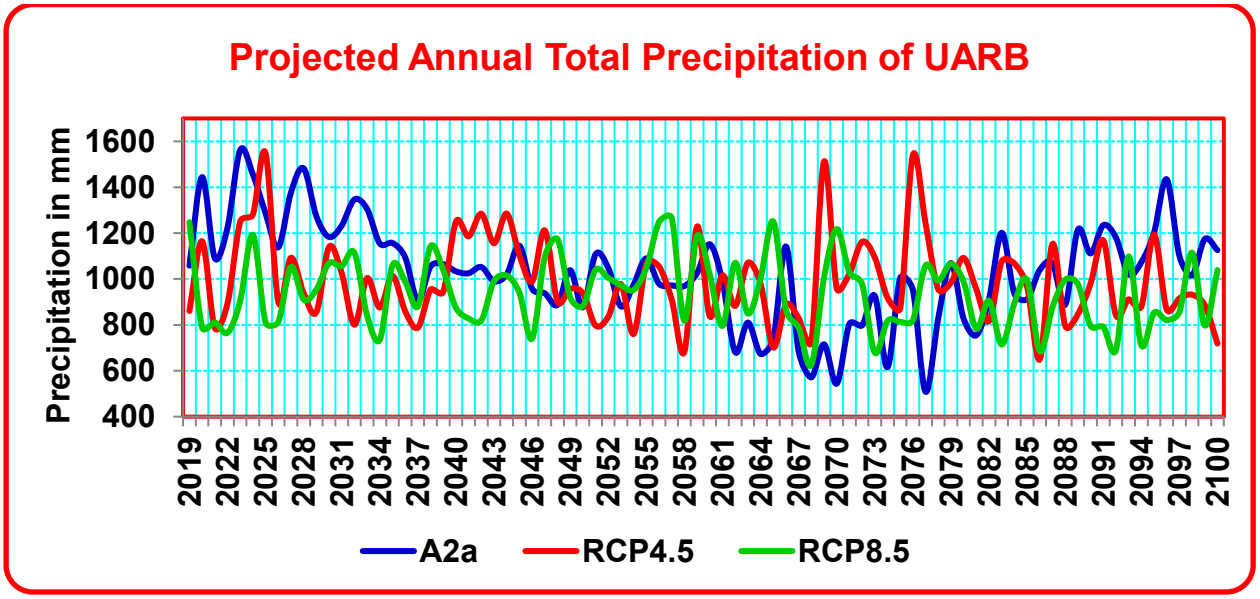

Figure 4.3 Comparison of projected future precipitation: blue for the one downscaled from GCM A2a output; red for RCP4.5 emission scenario and green for RCP8.5 emission scenario run for Addis Ababa weather station of UARB

The average annual total precipitations for these 82-years period from HadCM3 A2a, RCP4.5 and RCP8.5 scenarios respectively are 1031.0 mm, 993.5 mm and 940.6 mm. The temporal variation of precipitation pattern is somewhat difficult to explain. In the figure above, the projection of future precipitation shows that RCP4.5 and RCP8.5 have comparatively similar pattern, except that there are peak rainfall events in RCP4.5 emission scenario. For example, it seems that there will be huge storms in 2025, 2069 and 2076 as projected using the RCP4.5 emission scenario. The total annual precipitation projected for these three years according to RCP4.5 emission scenario are 1548.4 mm, 1512.0 mm and 1539.7 mm respectively. These are large values as compared to the total annual average precipitation of about 994.0 mm. Because the CMIP5 RCP emission scenarios are projected on relatively finer grid resolution, RCP4.5 and RCP8.5 emission scenarios are used for further analysis in this research.

4.2 Hydrologic Modelling

4.2.1 Sensitivity Analysis

Modelling climate change impact on water resources in general and on hydropower generation in particular requires in part or in full the knowledge of hydrological processes leading eventually to streamflow. This necessitates evaluation of sensitivity of flow output to selected parameters with hydrologic models. SWAT hydrologic model was used to fulfil this purpose. After the pre-processing of the data and set up of SWAT model, simulation was performed for the data period of 1981 – 2010, the first two years being considered as the warm-up period. Here, nineteen parameters that are considered to be most related to flow were used for sensitivity analysis with SWAT, as presented in Table 3.2.

The sensitivity analysis results showed that the eight most sensitive parameters for flow in Hombole subbasin in descending order were SCS runoff CN for moisture condition II (CN2), groundwater recharge to deep aquifer (RCHRG_DP), threshold depth of water in the shallow aquifer for return flow to occur (GWQMN), available water capacity of the soil layer (SOL_AWC), soil evaporation compensation factor (ESCO), threshold depth of water in the shallow aquifer for 'revap' to occur (REVAPMN), soil depth (SOL_Z) and plant uptake compensation factor (EPCO) (Table 4.2).

Table 4.2 The eight most sensitive parameters, their rank and relative sensitivity

S. No	Parameters	Description	Relative sensitivity	Rank
1	CN2	SCS runoff CN for moisture condition II	1.6500	1
2	RCHR_DP	Groundwater recharge to deep aquifer (mm)	0.6310	2
3	GWQMN	Threshold depth of water in the shallow aquifer for return flow to occur (mm)	0.1890	3
4	SOL_AWC	Available water capacity of the soil layer (mm/mm soil)	0.1790	4
5	ESCO	Soil evaporation compensation factor	0.1240	5
6	REVAPMN	Threshold depth of water in the shallow aquifer for 'revap' to occur (mm)	0.1070	6
7	SOL_Z	Soil depth (mm)	0.0810	7
8	EPCO	Surface runoff lag coefficient	0.0675	8

SWAT estimates and displays relative sensitivities along with the ranks of the sensitive parameters. The display of the relative sensitivity of the parameters is useful in comparing the effects that the different parameters have on the target variable, in this case the flow. According to Lenhart et al. (2002), the relative sensitivity of parameters is classified into

four classes (Table 4.3). Based on this system, as is shown in the table, the relative sensitivity of SCS runoff CN for moisture condition II (CN2) was found to be very high. The Groundwater recharge to deep aquifer (RCHRG_DP) was high, but not as high as CN2, while the rest six flow parameters have medium relative sensitivity. The relative sensitivity of the parameters is shown in Figure 4.4.

Table 4.3 Sensitivity index (Lenhart, 2002)

Class	Index	Sensitivity
1	0.00 ≤ I ≤ 0.05	Small to negligible
2	0.05 ≤ I ≤ 0.20	Medium
3	0.20 ≤ I ≤ 1.00	High
4	≥ 1.00	Very high

Therefore, CN2 was very critical, followed by RCHRG_DP in the occurrence of flow in UARB. The higher influence of CN2 could be attributed to the dense population and settlement of the basin that may lead to more overland flow rather than infiltrating into the ground. On the other hand, the RCHRG_DP is associated with ground water recharge to deep aquifer, and the 11% groundwater that boosts the overland flow could be the effect of this parameter. In general, all the eight parameters govern the surface and subsurface hydrological processes and also flow routing.

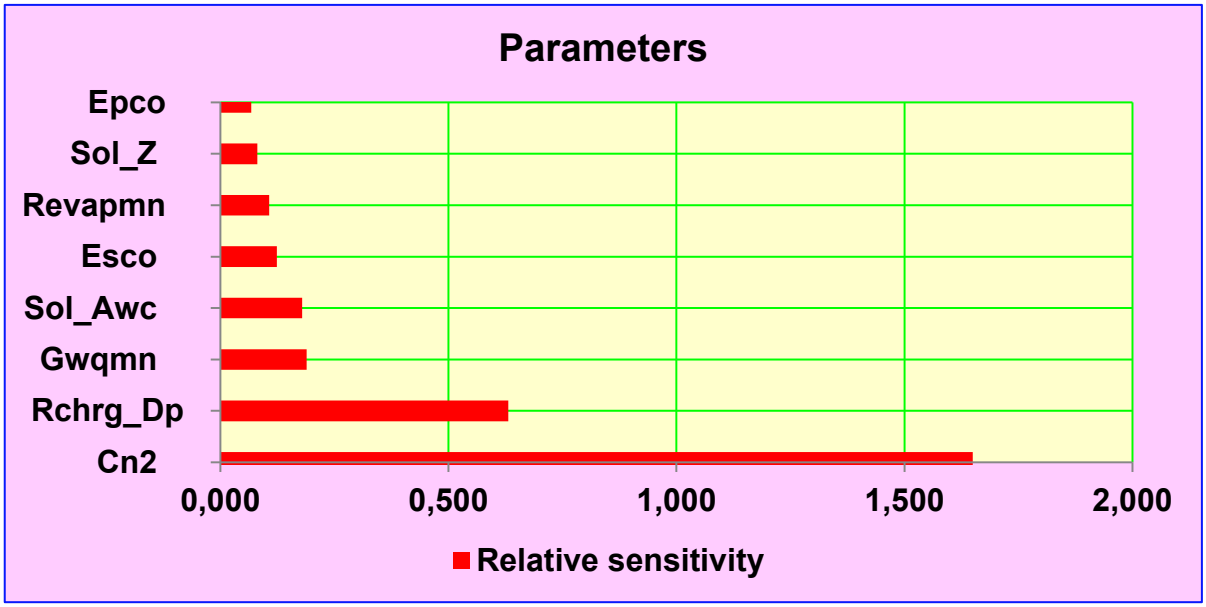

Figure 4.4 Relative sensitivity mean values of the most sensitive parameters

4.2.2 Calibration and Validation

Once the most sensitive parameters have been identified using SWAT model, the next step was calibration, validation and uncertainty analysis. A SWAT-CUP component, SUFI-2 algorithm, was applied for this purpose. The last decade of the data period was used for calibration and validation. The calibration year covers the period 2001 – 2006, the remaining four data years of 2007 – 2010 being used for validation. In this SUFI-2 algorithm, 2000 simulations were carried out in the final iteration. The decade used for calibration and validation was the recent one compared with the other two (1981 – 2000) and there were relatively very few or nearly no missing values. The calibration and validation results are presented in Table 4.4.

Table 4.4 Calibration and validation results for flow in UARB

	Period	R^2	NSE	p-factor	r-factor	PBIAS
Calibration	2001 – 2006	0.90	0.90	0.43	0.42	-8.6
Validation	2007 - 2010	0.91	0.88	0.42	0.46	-24.6

Table 4.4 shows that SUFI-2 performed very well both in calibration and validation; with R^2 and NSE of 0.90 and 0.90 for calibration, and 0.91 and 0.88 for validation respectively. Therefore, it can be inferred that the SFUI-2 algorithm is an effective one for flow calibration and validation in the study area. The PBIAS was also found to be acceptable as it is less than 25% and greater than -25%. Figure 4.5 shows the observed and modelled monthly river discharge for Hombole gauging station as simulated by SUFI-2. The figure also reveals that SUFI-2 is reliable in reproducing observed flow.

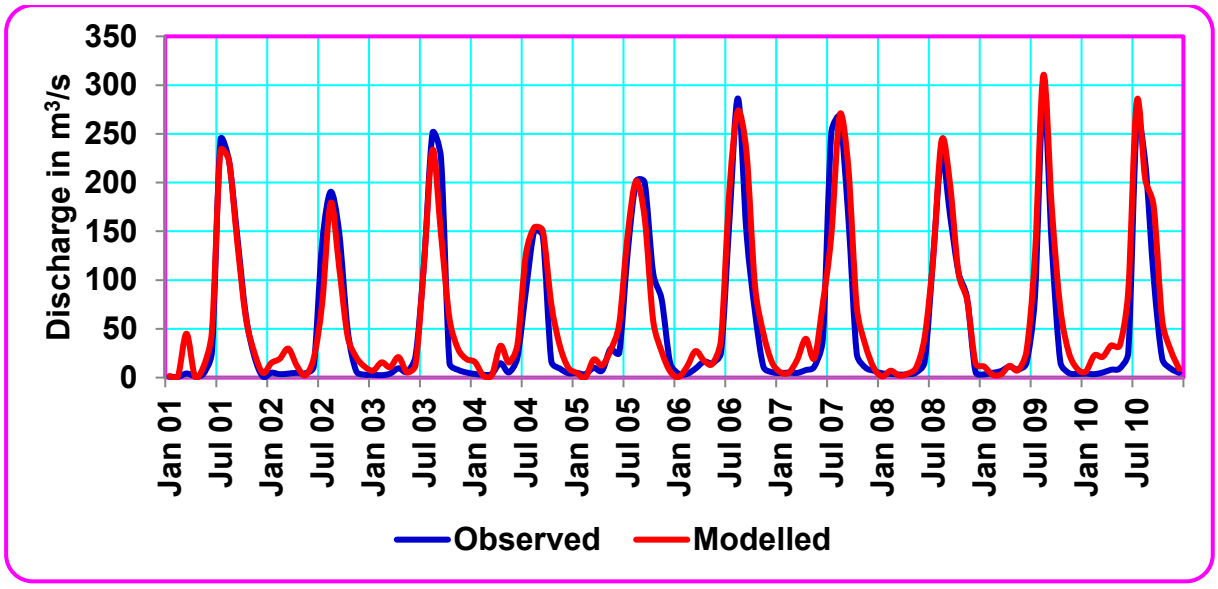

Figure 4.5 River discharge for Hombole station for the calibration and validation periods

4.2.3 Uncertainty Analysis

Model uncertainty analysis aims at a quantitative assessment of the reliability of model outputs. Several sources of modelling unknowns and uncertainties result in the fact that model predictions are not a certain value, but should be represented with a confidence range of values (Beven, 1993; Gupta *et al.*, 1998; Vrugt *et al.* 2003). These sources of uncertainty are often categorized as input uncertainties, such as errors in rainfall, model structure uncertainties, i.e., uncertainties caused by inappropriateness of the model to reflect the reality or the inability to identify the model parameters and uncertainties in the observations used to calibrate/validate the model outputs.

For the case at hand, uncertainty analysis was performed after sensitivity analysis, but simultaneously with calibration and/or validation processes using SUFI-2. SUFI-2 starts with large but meaningful ranges of sensitive parameters so that the measured data falls within the 95PPU. The uncertainty is then reduced step by step after several iterations. Uncertainty analysis result obtained using SUFI-2 during calibration and validation periods at Hombole gauging station is shown in Figure 4.6. The shaded region (95PPU) includes all sources of uncertainties. Even though the model performed very well with respect to the goodness of fit indices, it can be seen from the results of p-factor and r-factor that the uncertainties are relatively large both during calibration and validation. The p-factor was 0.43 during calibration, and it was 0.42 during validation period. Regarding the r-factor, it was 0.42 and 0.46 during calibration and validation periods respectively.

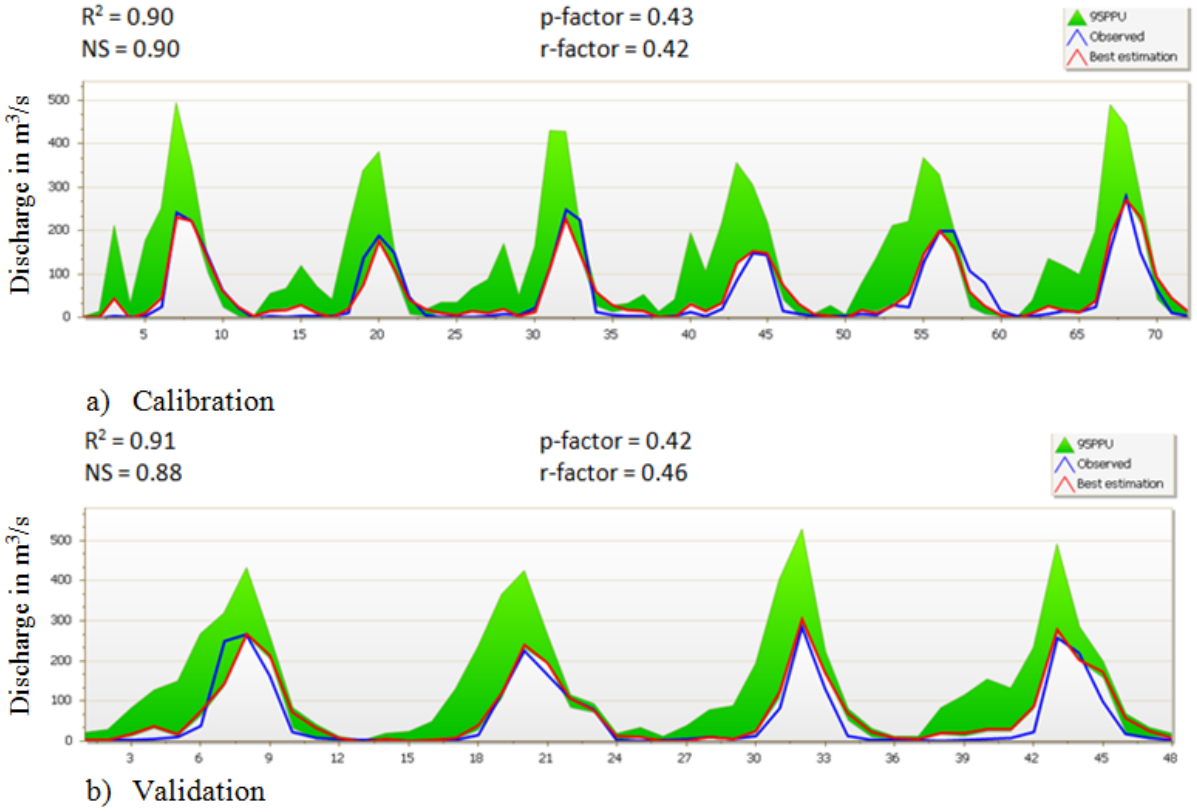

Figure 4.6 Monthly calibration (a) and validation (b) results showing the 95% prediction uncertainty (95PPU) intervals along with the observed flow

The course results of p-factor and r-factor led the 995PPU to be wide and the best simulation to be located out of the band in most of the cases. As all forms of uncertainties are reflected in the measured variables (e.g., discharge), the parameter uncertainties generating the 95PPU accounted for all uncertainties. Breaking down the total uncertainty into its various components is highly interesting, but quite difficult to do, and it is hardly possible to get reliable procedure so far (Abbaspour et al., 2007).

The scatter plot of monthly flow shows relatively good relationship between observed and modelled flows as can be seen in Figure 4.7. But because of the large uncertainty revealed by the p-factor and r-factor, the curves for the observed and modelled flows seem to appear mostly below the band.

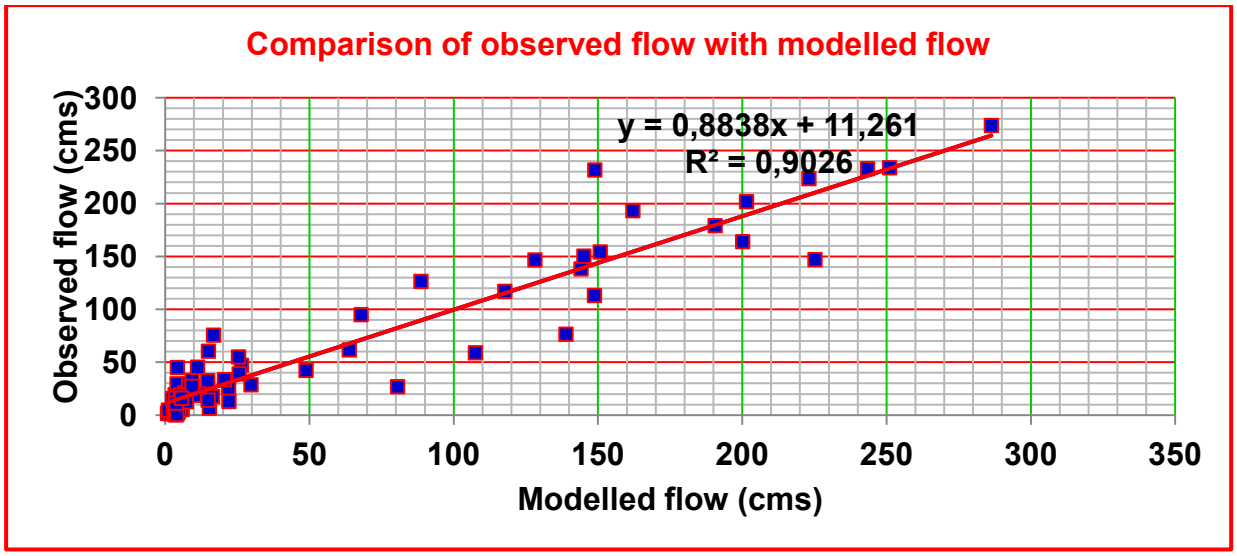

Figure 4.7 Scatter plot of monthly flow against modelled flow at Hombole station of UARB

The dotty plots for four of the parameters presented in Fig. 4.8 below shows that curve number CN2 has a very high influence on flow throughout its range. The dots are plots of parameter values against the objective function. The purpose of these graphs is to reveal the distribution of the sampling points and to give an insight of parameter sensitivity. In the figure, distribution of all the parameters is shown.

Table 4.5 Maximum, minimum and fitted values of parameters

Parameter Name	Fitted Value	Min VValue	Max Value
R__CN2.mgt	0.041000	0.040881	0.200000
V__GWQMN.gw	1.675065	1.668687	2.000000
R__REVAPMN.gw	7.736690	7.480312	10.000000
R__RCHRG_DP.gw	0.997802	0.996381	1.000000
R__ESCO.hru	0.996464	0.992924	1.000000
R__EPCO.hru	0.958980	0.769874	1.000000
R__SOL_AWC(..).sol	0.391969	0.390209	0.400000
R__SOL_Z(..).sol	0.998025	0.996894	1.000000

The eight parameters to which flow is sensitive are associated with land management (e.g., R_CN2.mgt), groundwater characteristics (e.g., V_GWQMN.gw, R_REVAPMN.gw and R_RCHRG.gw), hydrologic response units (e.g., R_ESCO.hru and R_EPCO.hru) as well as soil characteristics (e.g., R_SOL_AWC.sol and R_SOL_Z.sol). Discharge is sensitive to all of these parameters but management practices and groundwater characteristics do have the most influence on flow.

Yet, even though the calibration and validation of the model proved to be very good, the uncertainty couldn't be further minimized. The diversity of the type of parameters could lead to more uncertainty. In UARB, the parameters that affect discharge are not confined

to one or two. As pointed above, and as can be seen from Table 4.5 and Figure 4.8, the parameters vary from management to HRU, and from soil to groundwater characteristics.

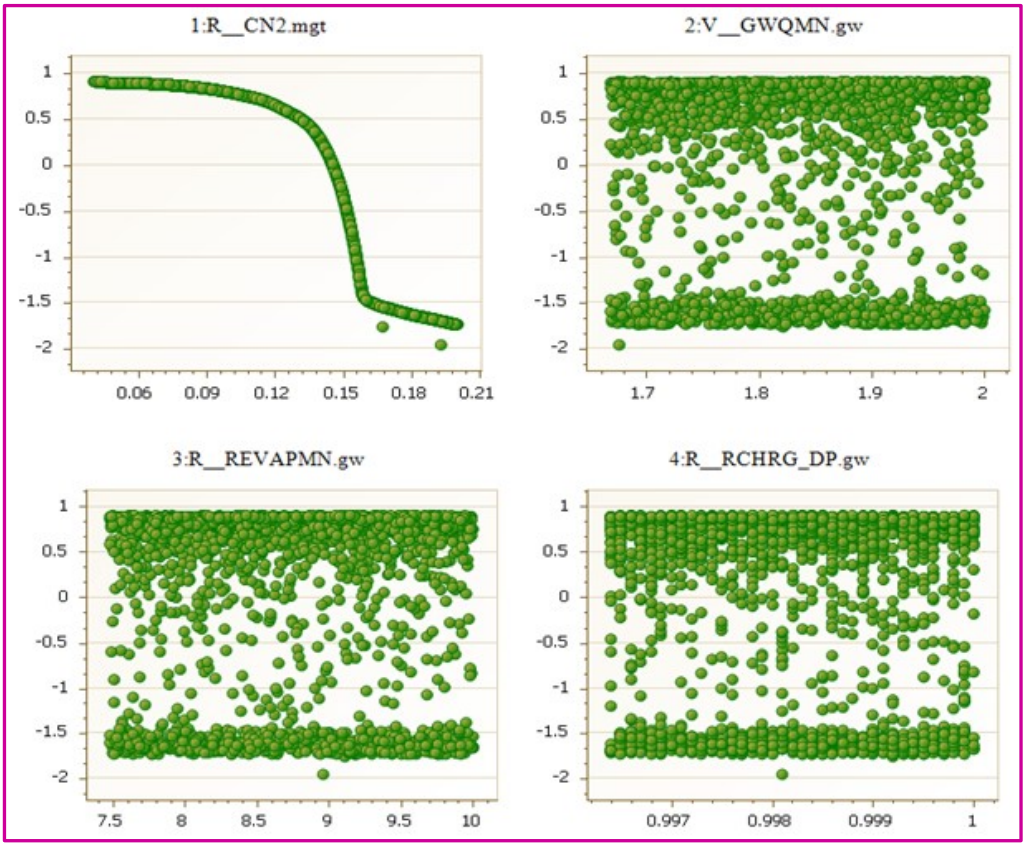

Figure 4.8 Dotty plots of uncertainty with SUFI-2

The SWAT run result shows that about 82% of the total water yield was contributed from surface runoff, while ground water flow contributes about 11%. Lateral flow contributes the rest 7% for total annual water yield. This indicates that the infiltration into the soil is less as compared to the surface runoff. The reason that most of water obtained from precipitation flows as surface runoff may be attributed to the land use land cover conditions of the study area.

4.3 Hydrologic Modelling from RCP Scenarios for Koka Reservoir

It was noted previously that the IPCC RCP data are available from 2006 onwards. Moreover, Koka hydropower production data for this particular study is available for the period 2006 – 2014. The streamflow data for the two rivers, Hombole and Mojo; that feed Koka Reservoir were also available for the period 1981 – 2014. It was thus, necessary that the period 2006 – 2014 was considered as a reference period as far as hydropower and RCP are concerned.

WEAP model simulates evaporation from a reservoir, inflows into and outflow from a reservoir, hydropower and many other hydrological and meteorological elements. In the following subsections, simulation results of monthly evaporation, inflow volume, average storage and hydropower production will be presented. Then presentation of the projection of these elements till 2100 follows.

4.3.1 UARB Rainfall

The average monthly and annual total rainfall over UARB for the period 2006 – 2014 is shown in Figure 4.9 and Figure 4.10. Usually precipitation shows fluctuating pattern spatially as well as temporally. Compared with the observations, the same behaviour is simulated here as can be seen from the figure. Accordingly the peak rainfall was modelled and found to occur in July.

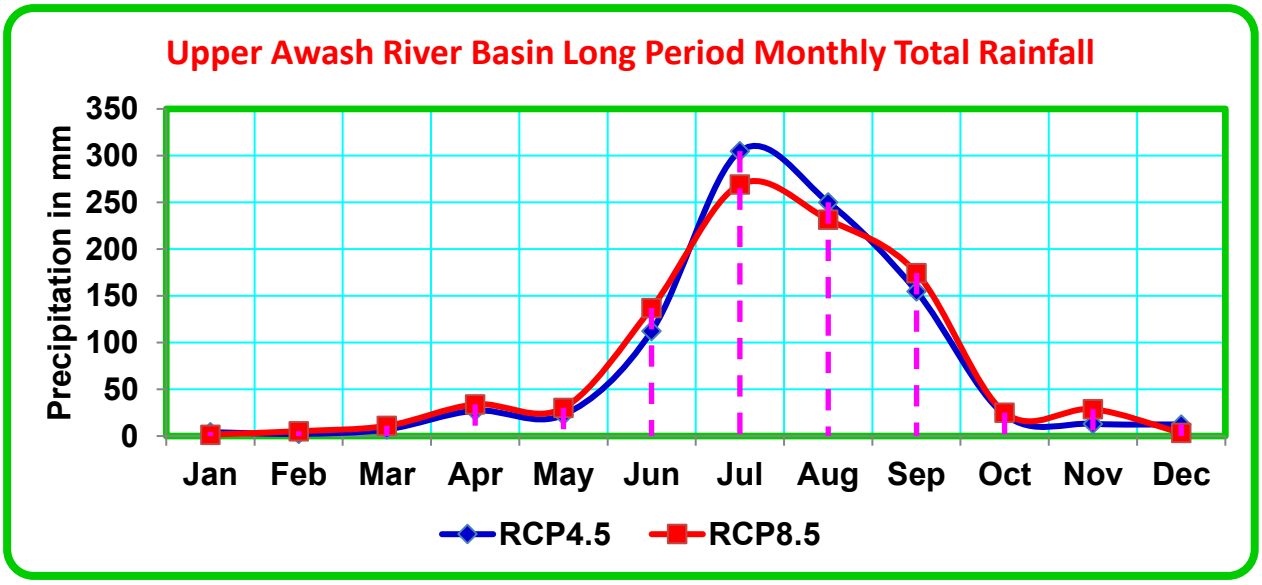

Figure 4.9 UARB mean monthly total precipitations under RCP4.5 and RCP8.5 emission scenarios for the period 2006 – 2014

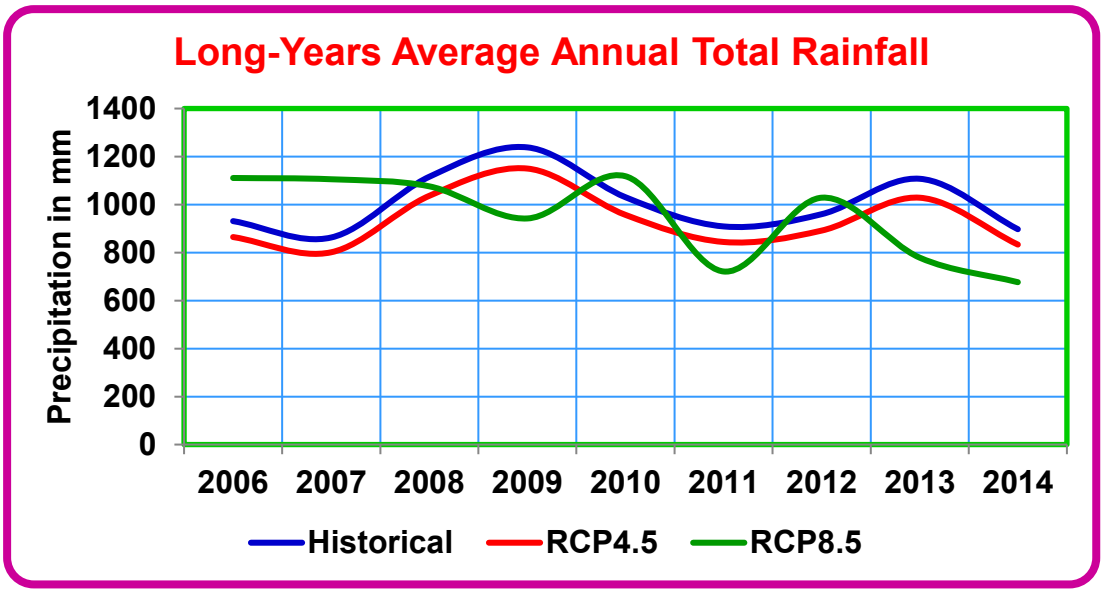

Figure 4.10 UARB mean annual total precipitation under RCP emission scenarios against the historical record for the period 2006 - 2014

Except the usual pattern that precipitation in general has, the magnitude of average annual precipitation in RCP4.5 and RCP8.5 is very comparable in the reference period. What unique characteristics RCP8.5 has is that it has a kind of frequent alternate zenith and nadir. However, the peaks and nadirs are often located very differently. For example, in Figure 4.10, RCP8.5 shows nadir (lowest point) in 2009, and then zenith (peak) in 2010, again nadir in 2011 etc. The peaks and nadirs in RCP4.5 are wide apart. In general terms, from the figure it can be seen that RCP8.5 has the characteristic leading to frequent extreme events of drought and floods than RCP4.5.

4.3.2 Inflow into Koka Reservoir

Model results from RCP4.5 and RCP8.5 were compared with historical data for the period 2006 - 2014. Figure 4.11 shows a line graph of modelled average annual inflow volume into Koka Reservoir from RCP4.5 and RCP8.5 against the historical flow. In general in all the three cases, a decreasing tendency can be seen from the graph from 2006 towards 2014. For this reference period, the inflow resulted from RCP4.5 tend to follow the pattern of historical inflow. The simulation result from RCP8.5 shows a fast rising and falling limbs as compared to the other two scenarios. It shows that the relationships, as could be expected for this case, become more and more irregular. The result is also shown in tabular form (Table 4.6).

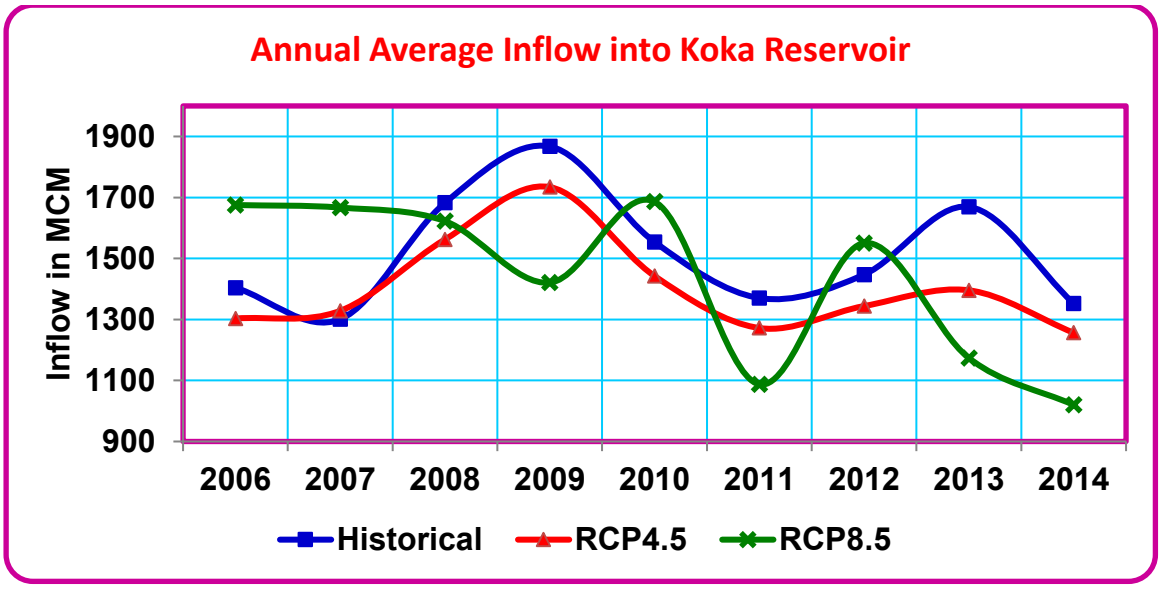

Figure 4.11 Annual inflow volume (MCM) into Koka Reservoir under RCP emission scenarios against the historical flow for the period 2006 – 2014

The historical flow in 2009 is the highest as can be seen from the figure as well as the table. But overall, the average annual flow simulated based on RCP8.5 emission scenario is the highest one, with a value of 1675.2 MCM. It followed the precipitation pattern. When precipitation increases, it is natural that inflow also increases.

Table 4.6 Annual inflow volume (MCM) into Koka Reservoir under RCP climate change scenarios for the period 2006 – 2014

Scenarios	2006	2007	2008	2009	2010	2011	2012	2013	2014	Avg.
Historical	1404.0	1300.8	1682.4	1867.2	1554.0	1370.4	1447.2	1669.2	1352.4	1404.0
RCP4.5	1303.2	1328.4	1562.4	1734.0	1442.4	1272.0	1344.0	1395.6	1256.4	1303.2
RCP8.5	1675.2	1666.8	1622.4	1420.8	1686.0	1087.2	1550.4	1173.6	1020.0	1675.2

As can be seen from the table, in the reference period, the averages of both RCP scenarios are different. But compared with the future conditions, they are relatively close to each other. The gap increases so widely as time proceeds toward the end of the 21st century as will be covered in subsequent subsections.

It is also important to consider the annual distribution of the average monthly inflow into Koka Reservoir. As expected, the peak for all scenarios occurs in August (Figure 4.12). In the figure it is even hardly possible to differentiate between the curve of RCP4.5 and RCP8.5. This shows that during the beginning of the experiment period, the scenarios have very similar pattern. This is in fact reflection of the current condition of the globe.

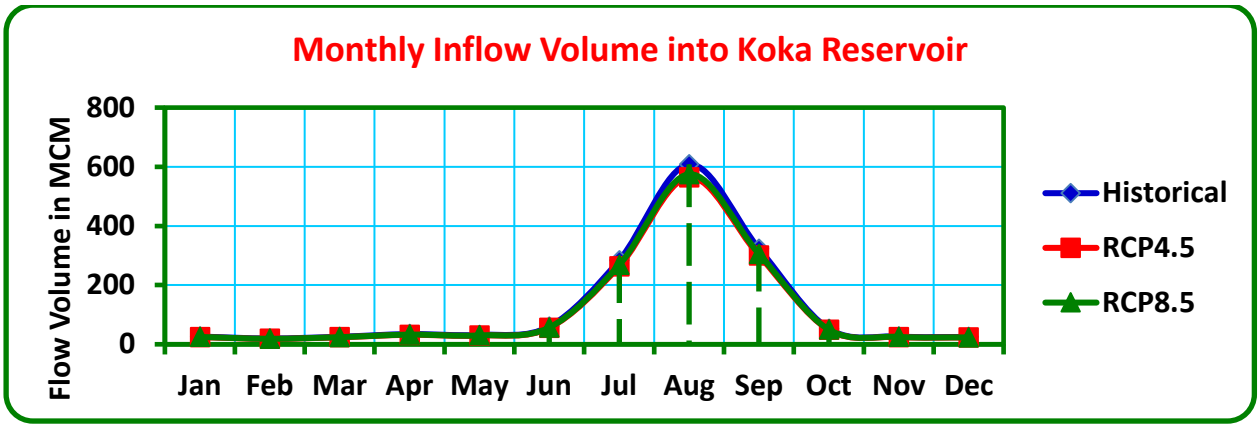

Figure 4.12 Monthly average inflow volume (MCM) into Koka Reservoir under RCP emission scenarios compared with historical flow for the period 2006 – 2014.

4.3.3 Evaporation from Koka Reservoir

The historical distribution of monthly evaporation from Koka Reservoir shows variation from month to month. Due to the behaviour of sunshine, temperature, wind speed and precipitation, the lowest evaporation is in the month of August where as the highest one is in October.

Table 4.7 Monthly average evaporation from Koka Reservoir under RCP4.5 and RCP8.5 emission scenarios for the period 2006 – 2014

Scenarios	Jan	Feb	Mar	Apr	May	Jun	Jul	Aug	Sep	Oct	Nov	Dec	Annual
Historical	27.9	24.2	32.6	24.3	32.6	31.0	21.0	13.3	31.3	44.1	29.6	30.7	342.6
RCP4.5	25.3	21.4	31.3	24.9	33.2	31.8	19.6	12.7	31.3	44.3	28.4	27.7	332.0
RCP8.5	25.0	22.1	31.6	24.7	32.9	31.5	20.4	12.8	31.1	43.3	27.1	28.6	331.0

The results are presented in volume, and shown in Table 4.7 and Figure 4.13. For comparison, the modelled evaporation, based on RCP4.5 and RCP8.5 scenarios for the period 2006 – 2014, is also presented and they are very similar and nearly equal compared with the historical one.

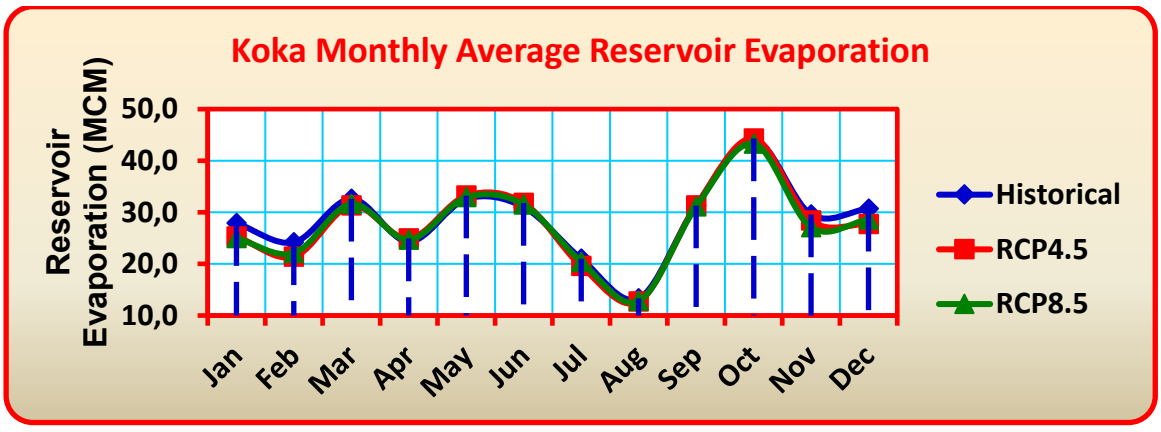

Figure 4.13 Monthly average evaporation from Koka Reservoir under RCP4.5 and RCP8.5 emission scenarios for the period 2006 - 2014

Here in evaporation also, the values modelled using the two RCP scenarios are almost equal: 333 MCM and 331 MCM for RCP4.5 and RCP8.5 respectively. In general terms, in the reference period, the monthly evaporation is high in March, May, Jun and October. Historical evaporation from the reservoir is a bit above the amount in the RCPs having average annual evaporation of 342.6 MCM. The reason could be the simulated lower temperature (see Figure 4.1)

It is worthwhile to notice that when evaporation in mm is input into WEAP, it displays in volume. Thus, the unit of volume is used here in representing its characteristics.

4.3.4 Koka Reservoir Storage

The average annual storage capacity of Koka Reservoir for the period 2006 – 2014 is shown in Table 4.8 and Figure 4.14. The long years average for the RCPs is, in similar manner as for the previous hydrological elements, are close to each other for the reference period. The storage capacity of Koka Reservoir for the Historical and RCP4.5 scenarios seem to follow similar pattern as can be seen from the figure. Moreover, the years 2008, 2009 and 2013 mark higher storage capacities for historical scenario with volumes 946 MCM, 879.8 MCM and 894 MCM respectively. The average Koka reservoir capacity according to both RCPs for the period is less than the observed capacity, as can be seen from Table 4.7.

Table 4.8 Koka Reservoir average storage capacity (MCM) under RCP4.5 and RCP8.5 emission scenarios for the period 2006 - 2014

Scenarios	2006	2007	2008	2009	2010	2011	2012	2013	2014	Avg.
Historical	751.8	696.6	946	879.8	832	697.1	775.1	894.1	811.4	809.3
RCP4.5	698.2	647	836.8	928.5	772.7	681.5	719.9	830.4	672.8	754.2
RCP8.5	852	892.5	868.8	760.7	902.7	582.3	830.5	660.1	546.2	766.2

It can further be noticed from the figure that in this reference period, the lowest Koka Reservoir capacity was recorded in 2007 and 2011. Regarding RCP8.5, the maximum storage capacity was observed in 2010 while the lowest capacity in 2014.

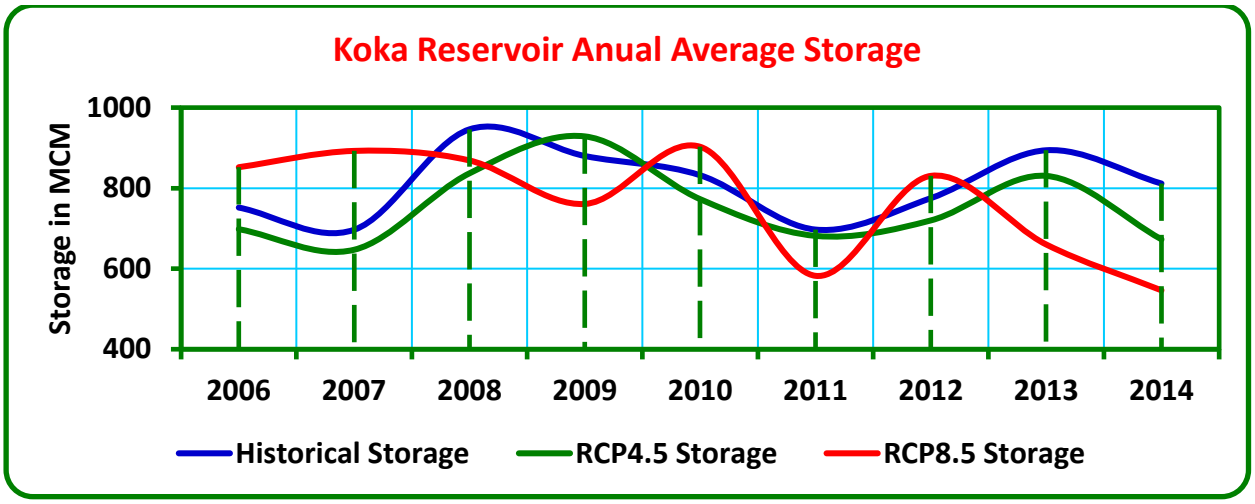

Figure 4.14 Koka Reservoir annual average storage capacity (MCM) under RCP scenarios for the period 2006 – 2014

4.4 Future Projections of Climate Change

4.4.1 Comparison of Streamflow modelled from downscaled GCM climate model and CMIP5 RCP climate scenarios

It is, as pointed out earlier, worthwhile to compare the amount of streamflow modelled from previous GCM outputs with the one simulated from CMIP5 RCP climate scenarios. Figure 4.15 shows the comparison of streamflow simulated by using as inputs, climate variables (precipitation and temperature) downscaled from previous GCM model (HadCM3 A2a) experiment using SDSM with CMIP5 RCP4.5 and RCP8.5 emission scenarios. The model was run for the period 2019 – 2030 for comparison.

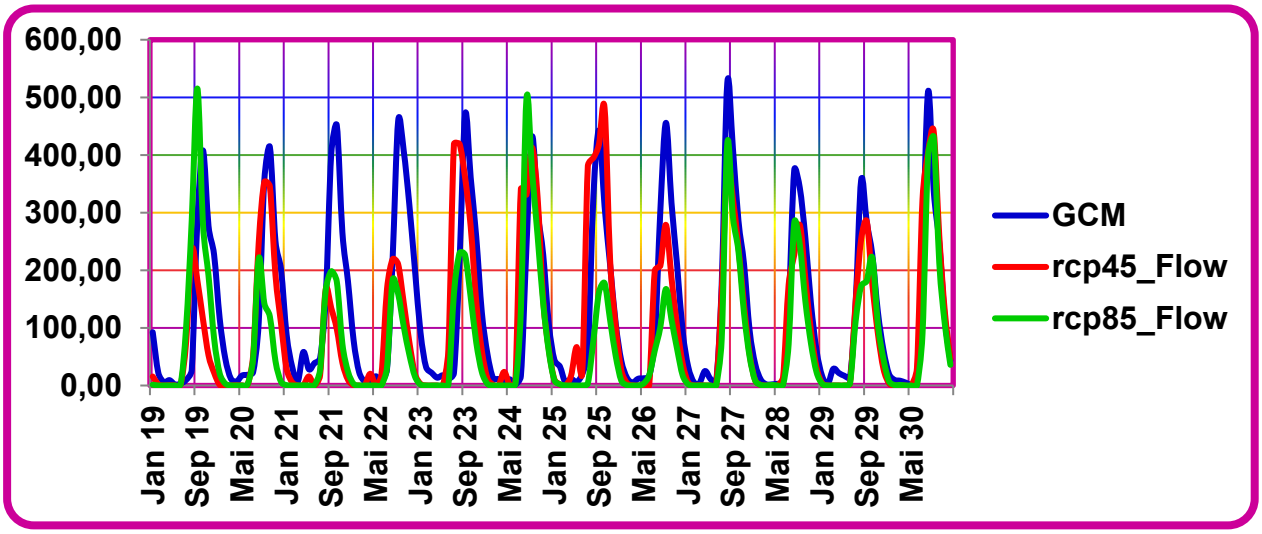

Figure 4.15 Comparison of projected streamflow for Hombole gauging station using previous GCM outputs and CMIP5 RCPs for the period 2019 – 2030

The SWAT hydrologic model simulated the observed annual river discharge reasonably well irrespective of the source of the inputs. In the figure, one can count about ten peak flow events. Six of them are peak flow events modelled from HadCM3 GCM climate outputs. Two peak flows were from RCP8.5 and other two peaks are from RCP2.6 and RCP8.5 emission scenarios. It can be clearly seen that the streamflow projected from HadCM3 A2a climate model output is higher. The higher streamflow according to previous GCM experiment may be attributed to the low spatial resolution.

In fact, the modelled streamflow is reflective of future precipitation modelled by SDSM. Virtually it can be said that the projected future precipitation, temperature and discharge are reasonable from the point of view of model capability.

However, in this study the core aim is the impact of climate change on hydropower generation. The focus is mainly on the most important variables that directly influence hydropower such as precipitation, temperature and streamflow. Many other factors requiring very fine resolution are ignored here. Since the RCPs available data from the year 2006 onwards is on grid distance of 0.44^0 (about 50 km x 50 km), as compared to the large grid distance of about 2.5^0 x 3.75^0 (277 km x 416 km) of previous GCMs, it is obvious that results obtained using the current RCP emission scenarios should better be used for the future climate change impact assessment.

4.4.2 UARB Temperature

The projected future temperatures according to the two RCP scenarios for UARB, from the five CORDEX stations that lie within the basin for the three periods of the 21st century are presented in Figures 4.16 – 4.18. In RCP4.5 scenario, a rise in temperature of 1.3 ^{0}C is projected even if there seem to be a decline beyond 2080s as stated by IPCC (2013). In RCP8.5, on the other hand, since the assumption is no climate policy, the rise in temperature of 3.7 ^{0}C is expected in UARB.

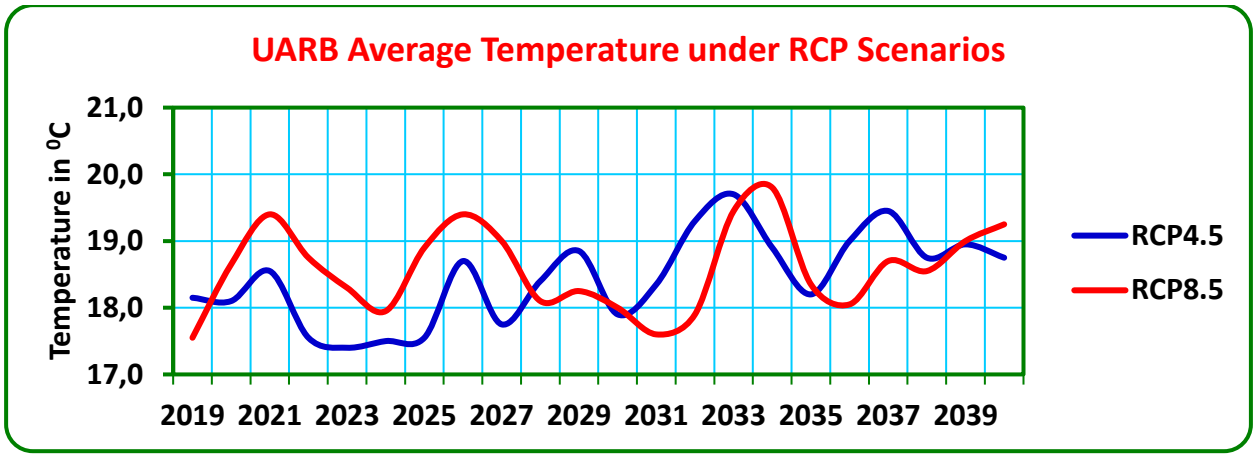

Figure 4.16 Projection of UARB annual average temperature under RCP scenarios for the period 2019 - 2040

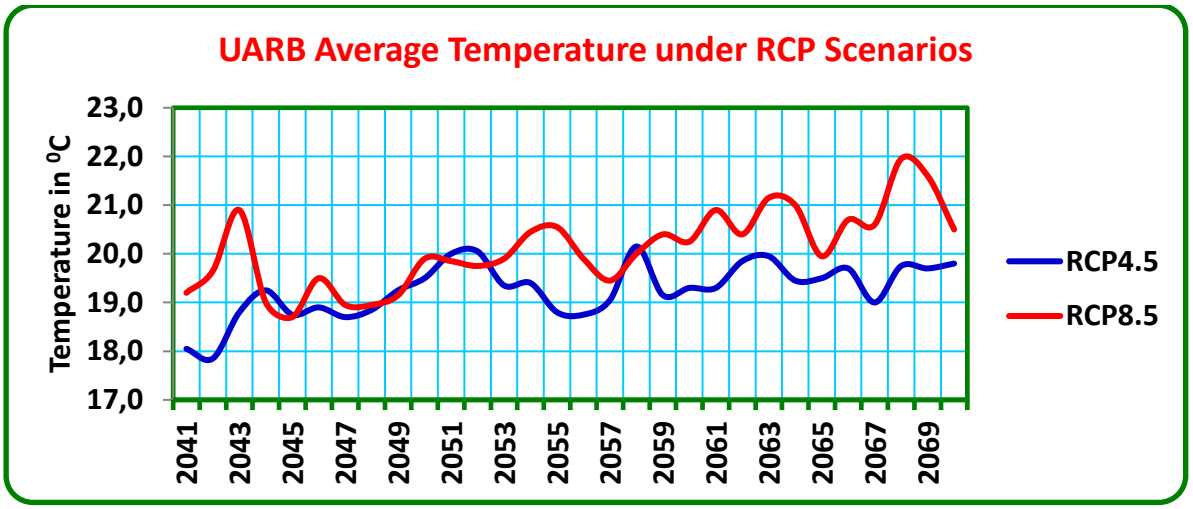

Figure 4.17 Projection of UARB average temperature under RCP scenarios for the period 2041 - 2070

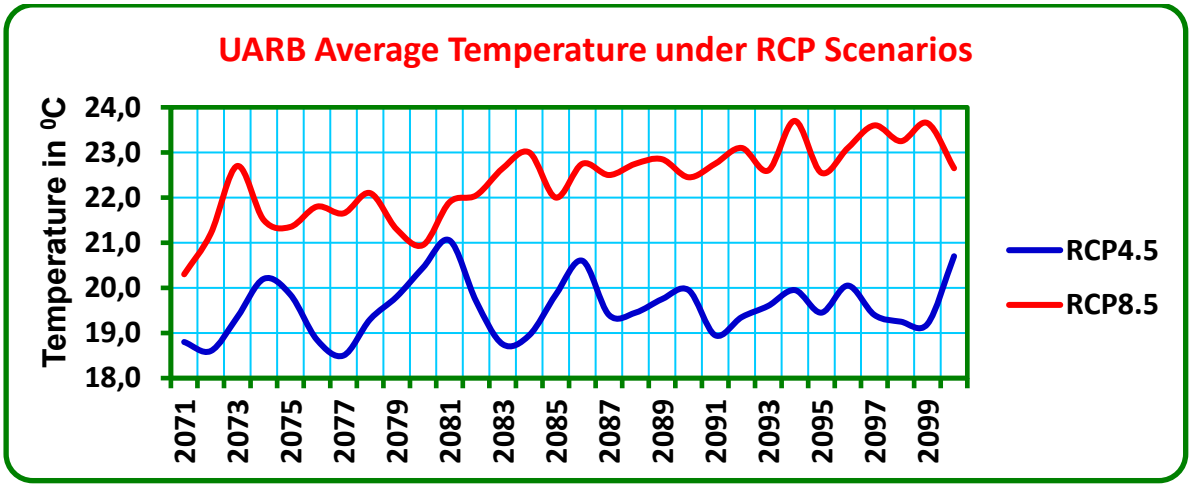

Figure 4.18 Projection of UARB annual average temperature under RCP scenarios for the period 2071 - 2100

From the three figures, one very obvious observation is that as time elapses towards the end of the century, the gap between RCP4.5 and RCP8.5 increases and increases. More tables are presented in Appendices.

4.4.3 UARB Precipitation

The projected rainfall for the period 2019 – 2040 is presented in Figure 4.19. It shows an increase for the first period of 2019 – 2040, compared to the period 2006 – 2014. The average total precipitation during the period 2006 – 2014 is 934 mm, while it increases to 1010 mm for the following period of 2019 – 2040. Again it shows a minor decrease for the period 2041 – 2070. The average total precipitation for this middle period is about 991 mm. Finally for the last decades of the century the average total rainfall for UARB will be 983 mm. Actually in all the three periods, the rainfall is greater than that for the reference period. These presented values are according to RCP4.5. All the figures and Tables are presented in Appendices.

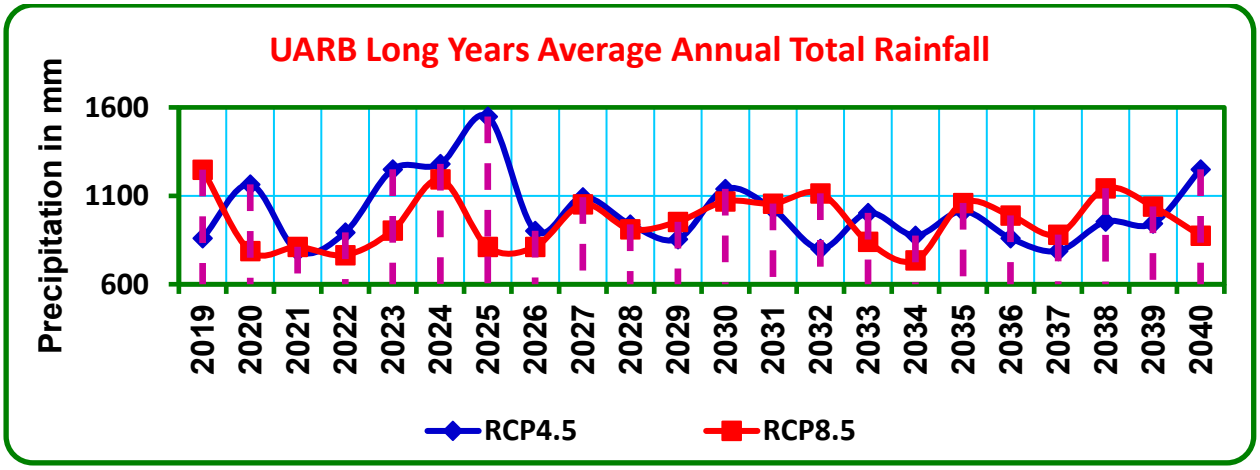

Figure 4.19 Projection of UARB annual average total rainfall under RCP scenarios for the period 2019 - 2040

Figure 4.20 shows the comparison between RCP4.5 and RCP8.5 in bar graph. The maximum rainfall that is projected for the period 2019 – 2040 occurs in 2025 for RCP4.5, with an amount 1548.4 mm. It nearly doubles the lowest projected precipitation of 787.4 mm that is expected to occur in 2021. This shows the fluctuation of rainfall.

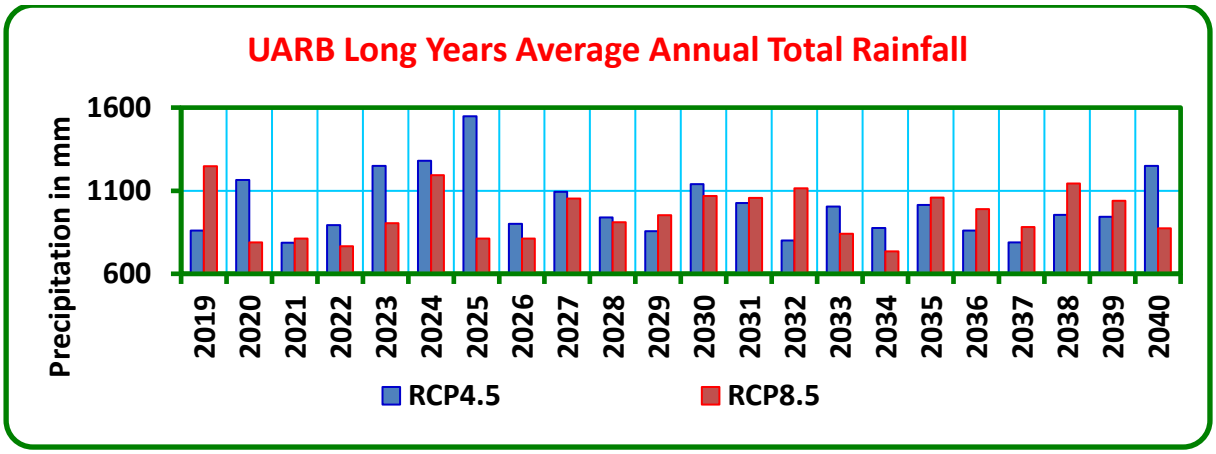

Figure 4.20 Bar graph showing projection of UARB annual total rainfall under RCP scenarios for the period 2019 - 2040

For all the three periods, the range of precipitation fluctuations according to RCP4.5 is greater than that for RCP8.5.

4.4.4 Koka Reservoir Evaporation

The monthly as well as annual average evaporation from the reservoir have been considered. Figure 4.21 shows average monthly evaporation from Koka Reservoir for the three future periods. Monthly as well as annual surface evaporation is projected to increase as temperatures rise over the river basin. Evaporation is maximum in October and minimum in August as modelled by WEAP.

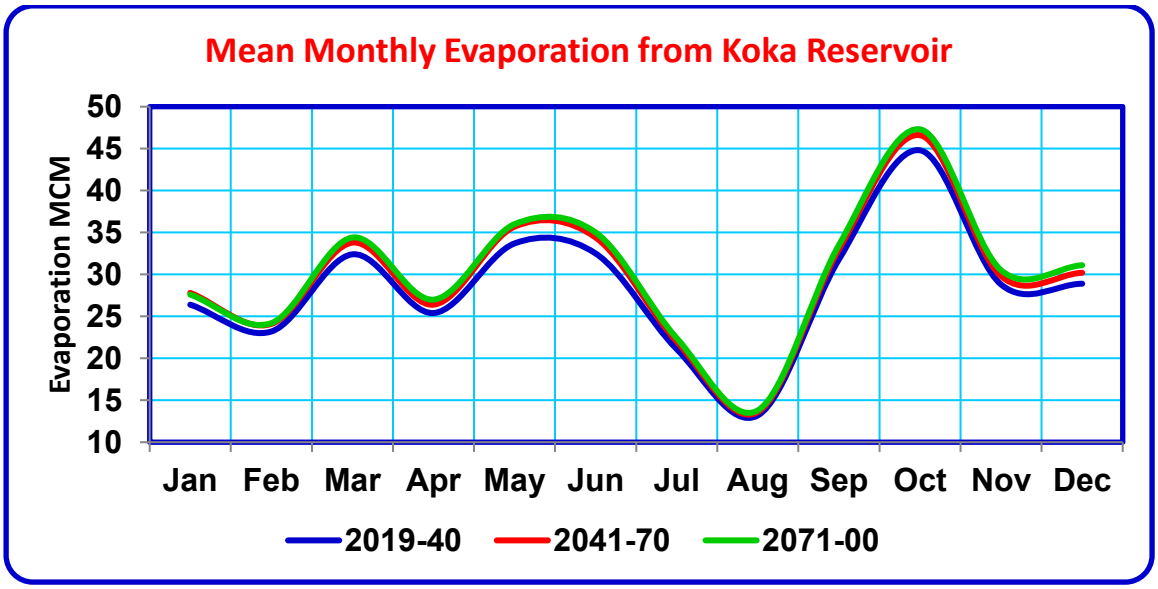

Figure 4.21 Projected mean monthly evaporation form Koka Reservoir under RCP4.5 emission scenario

The average annual reservoir evaporation shows increases in amount by 2.9% in the period 2019 - 2040, by 6.9% in 2041 – 2070 and by 9.0% in 2071 – 2100 for RCP4.5 emission scenario.

The increase in average annual evaporation for RCP8.5 is, as expected, more pronounced, since the temperature rises compared to RCP4.5. It increases in the periods 2019 – 2040, 2041 – 2070 and 2071 – 2100 by 4%, 10.5% and 23.2% respectively.

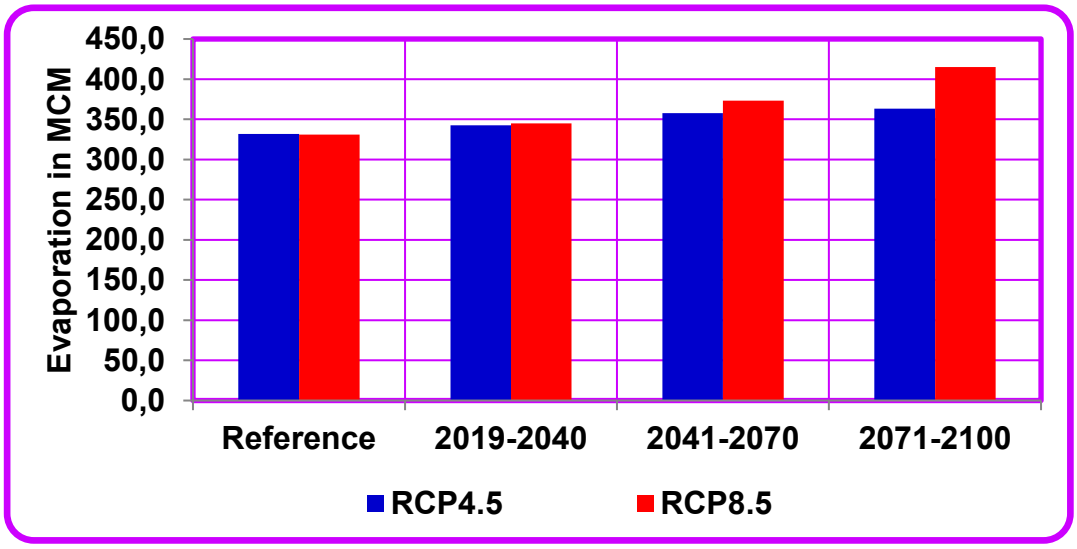

Figure 4.22 Bar graph showing projection of annual average evaporation from Koka Reservoir under RCP scenarios for the three future periods

The ever increasing rate of evaporation calls for special attention from decision makers. Much amount of water is lost every day, every month and every year from reservoirs. Remedy should be designed. Under discussion section, points reviewed from some literatures will be presented as to what should be done to reduce evaporation. Moreover, apart from annual evaporation, monthly evaporation as modelled by WEAP is presented in Appendix so as to alert decision makers.

4.4.5 Koka Reservoir Storage

The monthly average distribution of projected storage capacity for Koka Reservoir follows the normal reservoir characteristics during the current time. It is full in the rainy season and minimal at other months. The features of the reservoir for the future periods can be seen from Figure 4.23.

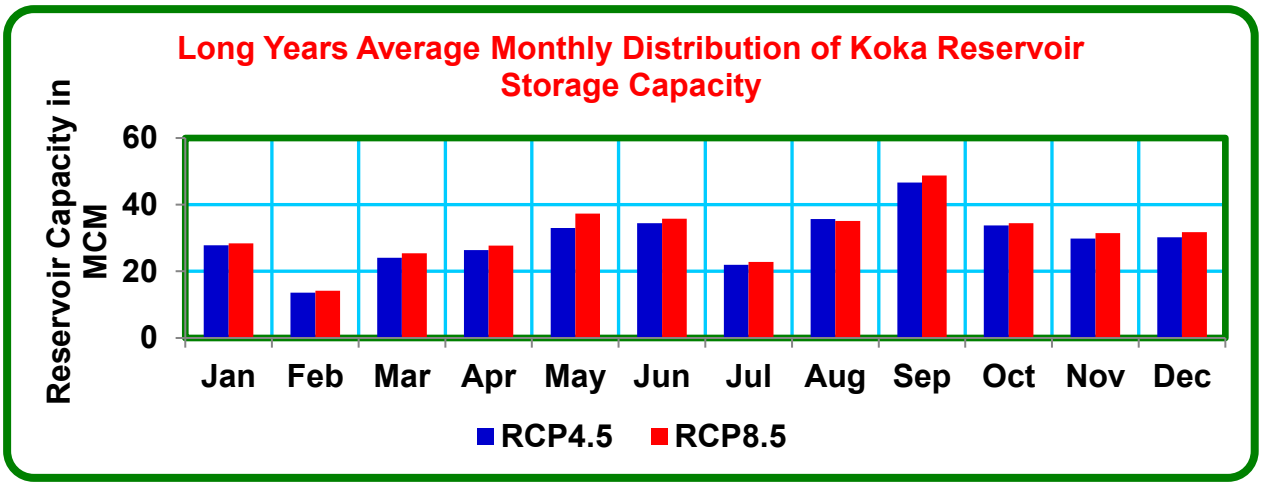

Figure 4.23 Long-years average monthly distribution of Koka Reservoir storage capacity under RCP emission scenarios

The maximum storage is projected to be the highest in the month of September for both RCPs. This is related to the time of concentration. While precipitation is peak in August, the highest storage capacity is projected to occur in September. This is a natural process. It takes time for the water to be stored in the reservoir. A large proportion of the Upper Awash River Basin is flat and gently sloping. The slope class of UARB presented in Figure 3.7 shows that slope range of 0 – 5% (legend in green colour) covers a large proportion of the basin. The flow of runoff to reach outlet is accordingly slow, and thus takes days and even weeks to reach the outlet at Koka Reservoir.

The long-term average annual storage capacity of the reservoir for the period 2019 – 2040 is shown in Figure 4.24. It is a reflection of the annual precipitation fluctuations. Just as the highest future precipitation projected to occur in 2025, so does the Koka Reservoir storage capacity.

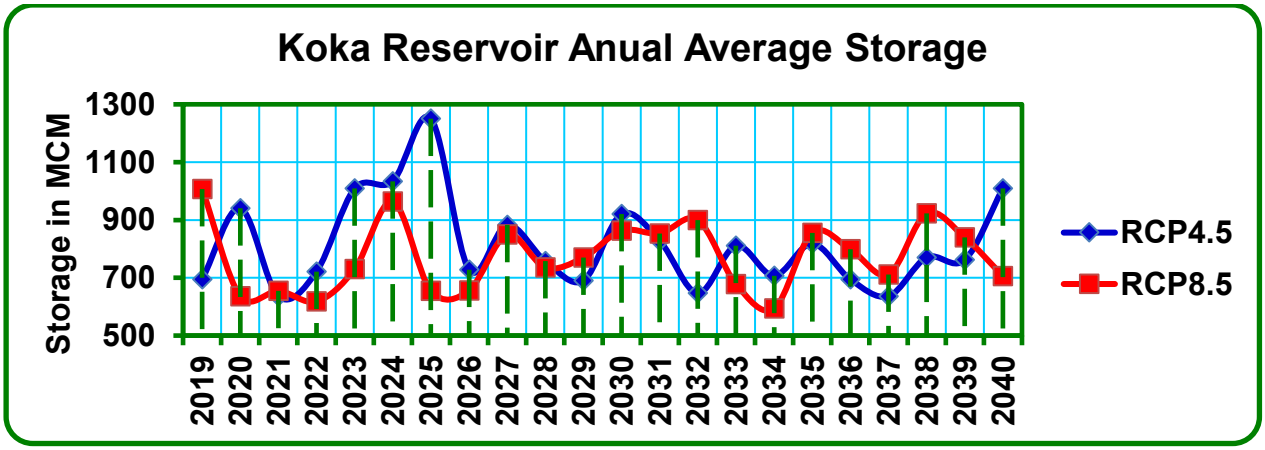

Figure 4.24 Line graph showing projection of Koka annual average storage capacity under RCP scenarios for the period 2019 – 2040

The summary of the projected average annual storage capacity for Koka Reservoir is shown in the bar graph of Figure 4.25. The graph clearly shows that the storage capacity diminishes near the end of 21st century and beyond, particularly for RCP8.5. Climate policy is a matter of “do” or “die”.

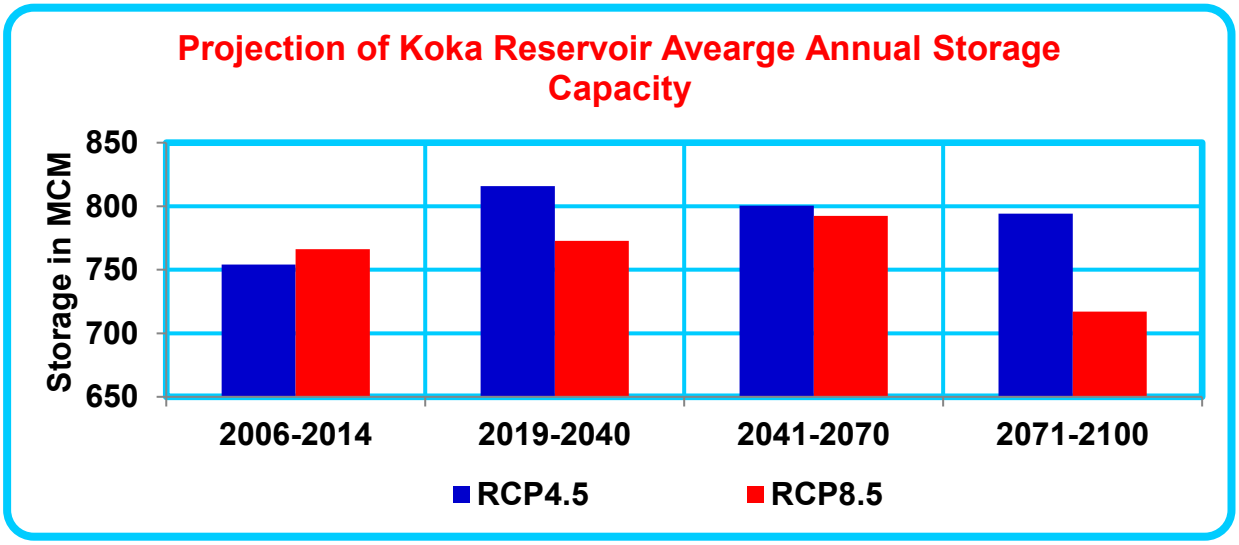

Figure 4.25 Bar graph showing the summary of the projection of average annual storage capacity for Koka Reservoir for the three future periods

4.5 Impact of Climate Change on Hydropower Generation

As stated so many times, precipitation, discharge and hydropower production are directly related. Monthly, seasonal and annual hydropower production as dictated by climate change impacts has been presented here. For the purpose of comparison, projections based on RCP4.5 and RCP8.5 emission scenarios have been presented frequently. However, assuming that climate change adaptation and mitigation policies will be enacted in the world in general and in Ethiopia in particular (in fact it should be the best option the country has), projections based on RCP4.5 (medium emission scenario that assumes emissions will reduce towards the end of the 21st century) are presented in some more figures.

There are limitations of hydropower functions in WEAP model. Detail analysis and optimization is quite difficult. Moreover, power production beyond maximum turbine flow is not possible in WEAP, especially for turbines having different capacities. Therefore, it is mandatory that some assumptions and simplifications be made. The assumptions and simplifications include working with generating efficiencies, plant factor and operating rules. Also, in allowing WEAP to simulate future hydropower generation, it is assumed that the decrease of the depth of the reservoir because of sediment is negligible to the

end of the century. The sediment deposition in the reservoir until this research is already taken into account, and thus nearly half the original height is input into the model. Having tolerated these uncertainties while modelling with WEAP, the hydropower productions for the reference and for the future periods have been simulated. A print-screen of hydropower simulation with WEAP for one of the simulations is presented in Figure 4.26. This figure shows the chart option and the tabular form is shown in Figure 4.27.

With regard to the projection of future hydropower generation of Koka Reservoir, it is actually observable that in the last three decades of the 21st Century, according to the results obtained, power generation declines to 88.1 GWh when modelled based on RCP8.5 emission scenario. Of course, this shows a decrease of energy by 15.1% as compared to the period of 2006 – 2014 for RCP8.5 scenario. The average annual energy actually produced from Koka Hydropower Plant for the reference period was 103.8 GWh. However, an increment of energy generation was projected in the period 2041 – 2070 for the same scenario.

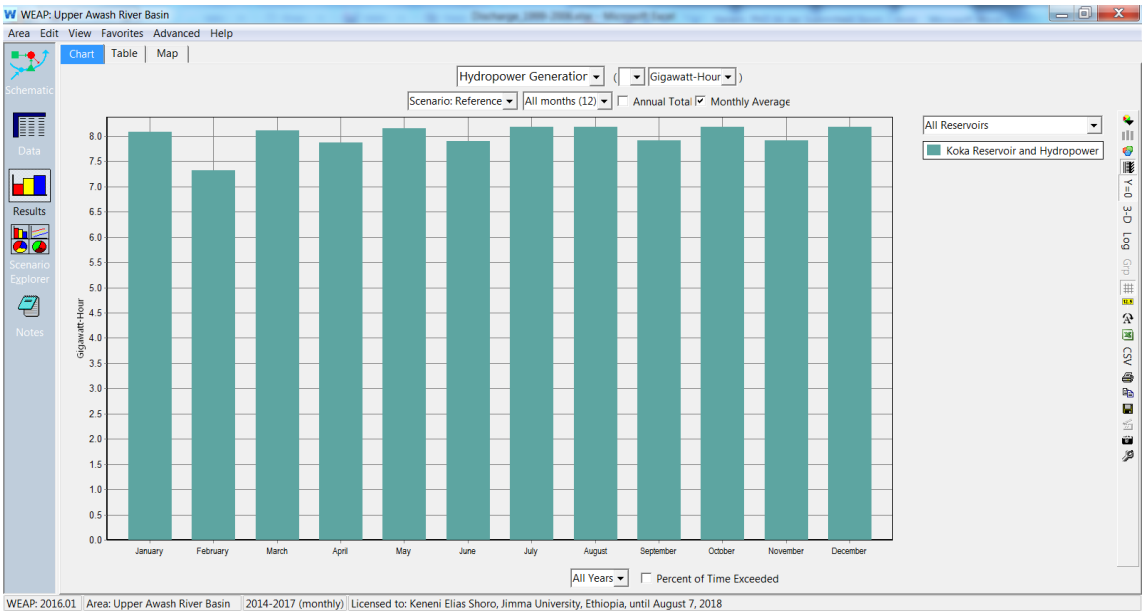

Figure 4.26 Print screen view of one of the hydropower simulation from Koka Reservoir with WEAP model

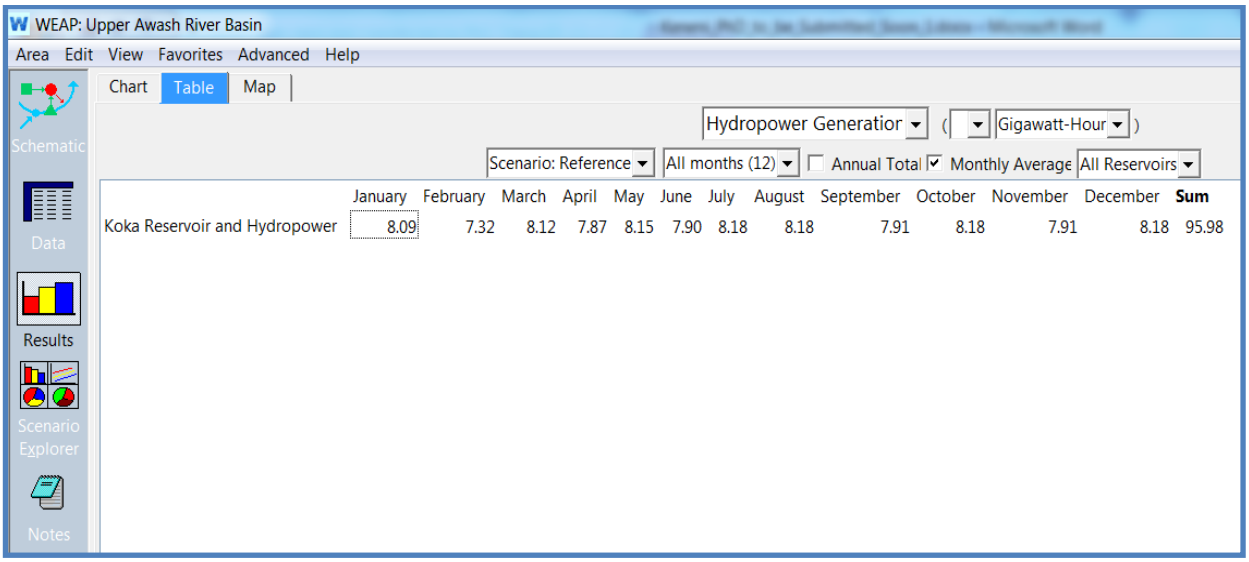

Figure 4.27 Print screen view of one of the hydropower simulations in tabular form from Koka Reservoir with WEAP model

This is attributed to the increase in precipitation in the period, leading to more runoff. The annual average precipitation projected for RCP8.5 scenario for the periods 2006 – 2014, 2019 – 2040 and 2041 – 2070 were found to be 950.7 mm, 956.9 mm and 981.2 mm respectively. There is an increase in precipitation by 3.2% in the period (2041 – 2070) compared with the first period of nine years according to RCP8.5 scenario. Figure 4.28 – Figure 4.30 show the average monthly, the annual total average and seasonal average of future projection of hydropower production that can be expected from Koka Reservoir for the three periods based on RCP4.5 emission scenario.

Driven under RCP4.5 scenario, though variable, it was seen that there will be an increase in energy production in all the three periods as compared to the reference period. The increase in energy for the periods 2019 – 2040, 2041 – 2070, and 2071 – 2100 was predicted to be respectively, 7.8%, 1.5% and 0.9%. But as can be seen from the percentages, the increment itself has decreasing tendency going further in the future even for this middle concentration scenario. This calls for more strict policy than the one considered in formulating RCP4.5 scenario, especially beyond the 21st Century. Table 4.9 shows the summary of projection of future hydropower energy from Koka Reservoir driven by RCP4.5 emission scenario.

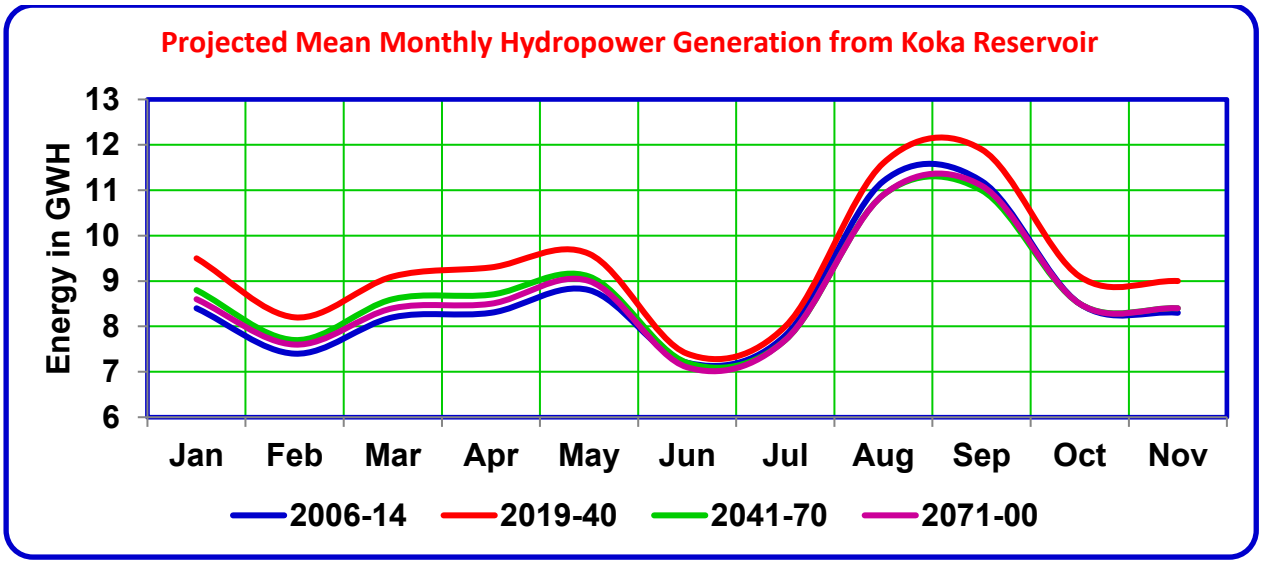

Figure 4.28 The reference and future projected monthly hydropower productions from Koka Reservoir under RCP4.5 emission scenario

The seasonal hydropower production was simulated for the period 2006 – 2014 according to CMIP5 RCP4.5 and RCP8.5 emission scenarios for the purpose of comparison with the actual production at the hydropower plant (not shown for RCP8.5, see Figure 4.30). The obtained results were reasonable and comparable with the actual hydropower production data of Koka Hydropower Plant.

Table 4.9 Summary of projection of hydropower production from Koka Reservoir under RCP4.5 and RCP8.5 emission scenarios for the future periods, compared with the current production

Period	Current	RCP4.5			RCP8.5		
	Energy (GWh)	Energy (GWh)	Change (GWh)	%	Energy (GWh)	Change (GWh)	%
2006 – 2014	103.8	–	–	–	–	–	–
2019 – 2040	–	111.9	8.1	7.8	102.2	–1.6	–1.5
2041 – 2070	–	105.4	1.6	1.5	106.2	2.4	2.3
2071 – 2100	–	104.7	0.9	0.9	88.1	–15.7	–15.1

Thus, in general terms it can be said that the RCP4.5 scenario may be taken as an ideal one for Ethiopia in the 21st century. At least there will be an increase in hydropower generation. The policy that restricts the concentration of GHGs under this scenario seems to work for the country.

On the other hand, the condition of future hydropower production under RCP8.5 scenario is even more complicated to generalize. A reduction of energy of 1.5% was projected for the period of 2019 – 2040. Next, there will be an increment in energy of 2.3% in the period 2041 – 2070, but then there will be a very sharp decline of 15.1% in the period 2071 –

2100. This implies that the climatic condition will in fact be very erratic. In this case extreme events which may cause unprecedented damages to life may happen, apart from the influence on hydropower. An unusual alternate increase and decrease of energy, that follows precipitation pattern, for RCP8.5 scenario may imply alternate events of drought and floods.

Figure 4.29 presents the comparison of hydropower generation for the three future periods with the hydropower data period of 2006 – 2014.

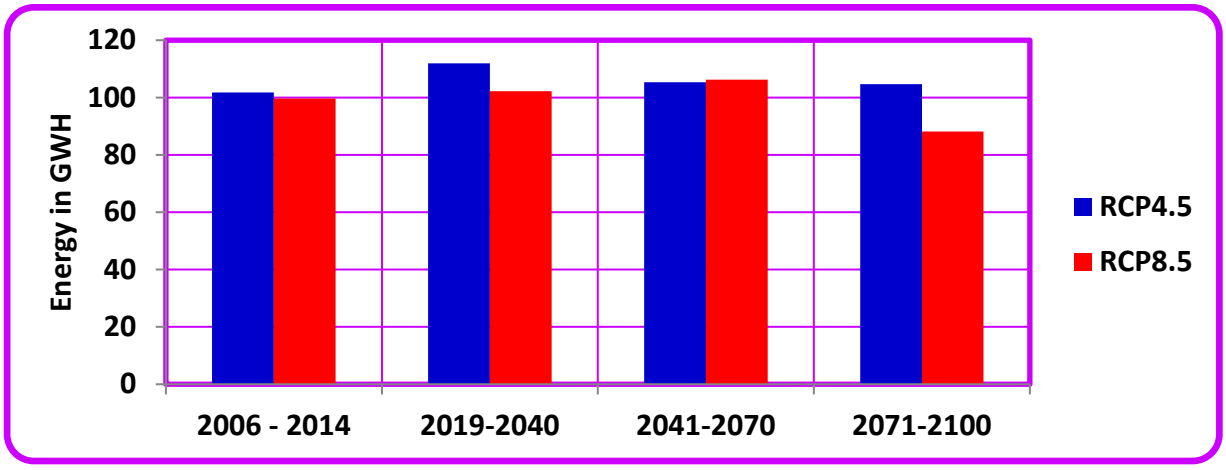

Figure 4.29 Projection of future annual hydropower production from Koka Reservoir under RCP emission scenarios

It is also important to see the seasonal pattern of the hydropower production as projected for the future periods. Figure 4.30 shows the summarized projected seasonal hydropower production from Koka Reservoir for the future periods against the current condition.

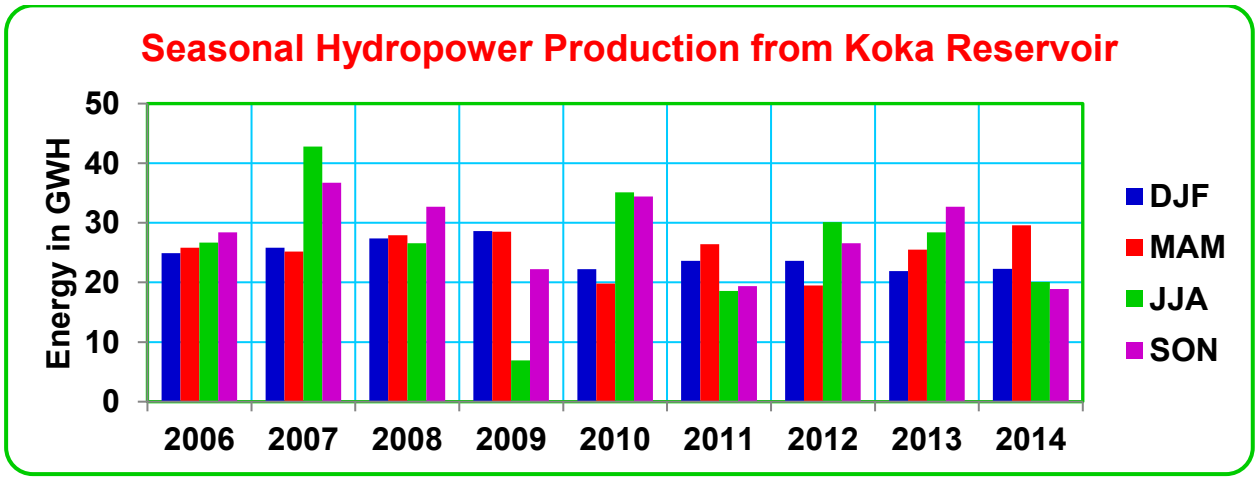

Figure 4.30 Seasonal hydropower production from Koka Reservoir for the period 2006 - 2014 under RCP4.5 emission scenario

The seasonal energy production for the period 2019 – 2040 is the highest in all the four seasons of the year (Figure 4.31). This fact is indeed in line with precipitation and streamflow amounts simulated in this period.

On the other hand, the seasonal energy production projected for the periods 2041 – 2070 and 2071 – 2100 are very comparable with each other and the amount of energy is less than that of the year 2019 – 2040. It can be inferred in relative terms that, like other time steps, the seasonal climate conditions have great implication on future hydropower production. This is indeed very important for decision makers to plan ahead.

From the obtained results and of course from the data available, there is one fact that should be raised with some justifications. Figure 4.31 shows the seasonal hydropower production for the period 2006 – 2014 and the projection for the three future periods, and figure 4.32 shows the projected seasonal hydropower production for the period 2041 – 2070. The uncertainty and an unexpected result which occur due to various factors are reflected in this projection. In Figure 4.32, it can be seen that in 2020, 2028 and 2039 the energy productions for rainy season of Ethiopia (JJA), are very low compared with the other seasons of the same years (compare it with the production of 2009, Figure 4.30). This is not the case under normal circumstances.

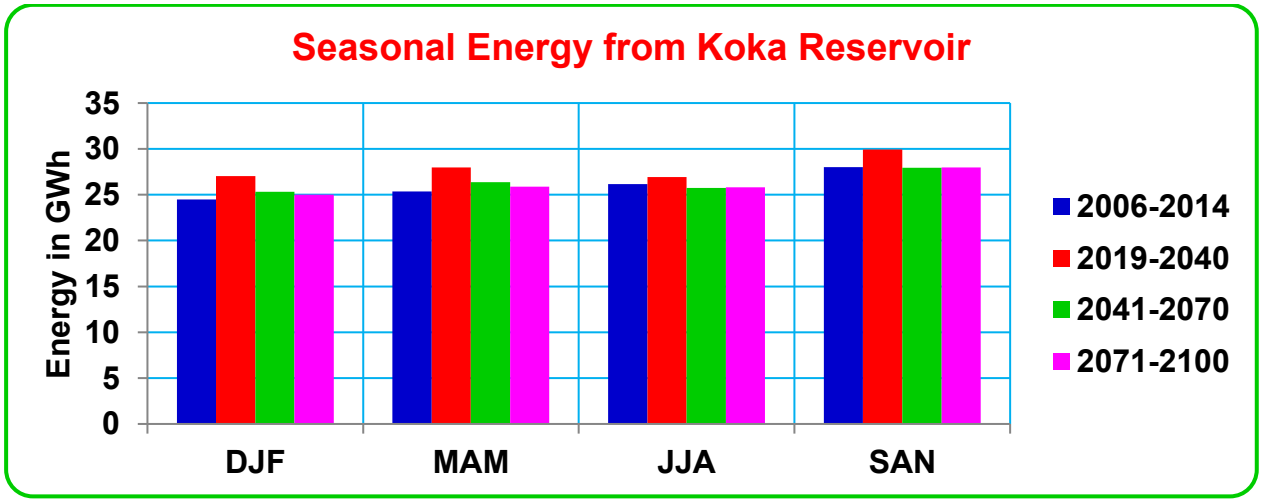

Figure 4.31 Projection of seasonal hydropower production form Koka Reservoir for the future periods under RCP4.5 emission scenario

In 2009, there was a shortage of water for hydropower production, not because of the decrease in rainfall, but because of the Koka Reservoir operation. Since the hydropower plant serves other purposes, there was frequent power shedding in Koka Hydroelectric

Plant in order to allow for other purposes of priority. That was the reason why the annual production of the year was reduced to 73 GWh.

As indicated above, the influence of this discrepancy was seen to reflect in rainy seasons of future period. It is inferred that this occurrence is attributed to the event that occurred in 2009.

The same scenario occurred in the next two periods (Tables presented in Appendix). According to the projection, the energy production for the year 2094 was found to be very low. This is very far from values in normal years. This calls for a strategy and techniques to correct for such problematic seasons with low energy production due to different factors.

One simple and of course crude way for doing this is taking the averages of the seasons of other unaffected years and periods for which the data is found in full and the operation of hydropower is normal. Unfortunately, bias correction as well as a technique for reducing uncertainty in this respect is not carried out in this research, except the uncertainty analysis carried out using SUFI-2 of SWAT-CUP. Future researches should consider these conditions for all existing, ongoing and planned hydropower productions in Ethiopia.

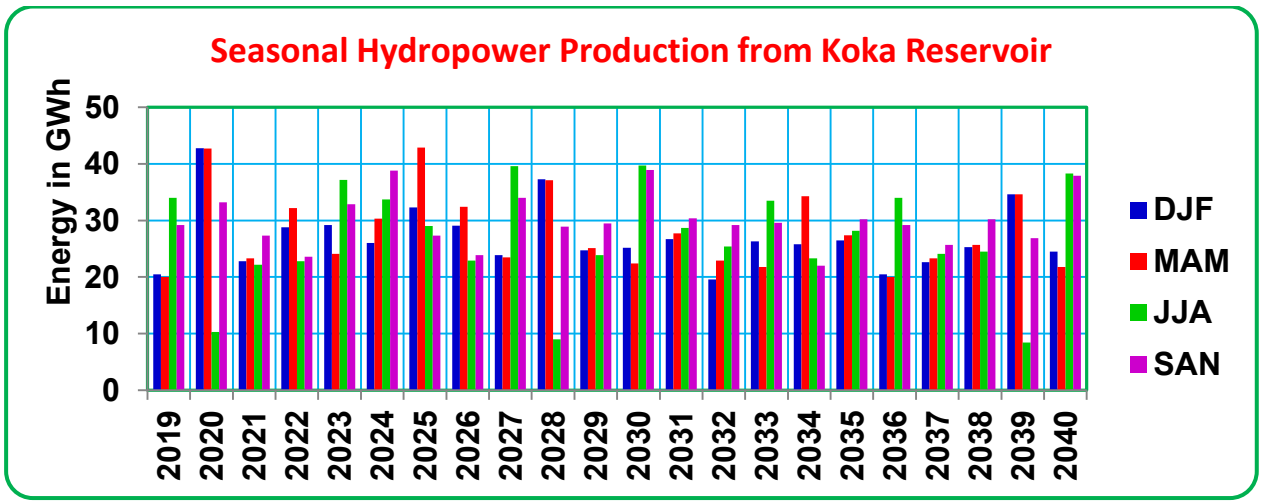

Figure 4.32 Projection of seasonal hydropower production from Koka Reservoir for the period 2019 - 2040 under RCP4.5 emission scenario

4.6 Discussion

It is reasonable to admit that all the models are not perfect and hence shall not be considered as the true reflection of hydrological processes, climate conditions and/or hydropower production of Upper Awash River Basin and the related Koka Hydropower

Plant. Especially with regard to hydropower modelling several assumptions were made. This and many other factors may affect the accuracy of the results.

4.6.1 Quality of Input Data

The starting points of all uncertainties in all the models used in this research are the input data. There are many missing gaps in meteorological and hydrological data that were the backbone of the whole research from the beginning to an end. When the missing gaps are filled using the available methodologies, it is obvious that there will be some distance away from the truth for the days without data. Even though the qualities of most of the streamflow data and of course of meteorological data are somewhat questionable, it was justifiable as well as mandatory to assume that the time series data of all meteorological and hydrological gauging stations are of adequate quality.

Moreover, among the data period, it was also imperative to select a range in which the uncertainties are negligible. Periods that may better represent the study period were selected for calibration and validation of hydrological modelling as well as for the analysis of hydropower generation modelling.

In most cases, the averages of all data were considered to show results in tabular form as well as for pictorial representation. In some cases, there may be circumstances in which a simple average is far away from the actual condition. For example, Thiessen polygon method was used to estimate the basin precipitation. The Thiessen polygon method may not represent the actual influence of the stations when extrapolated for the whole Upper Awash River Basin. To represent the basin temperature it was necessary that the averages of the meteorological stations were considered.

The integrated effects of all these, the uncertainties with the model themselves, errors in modelling and all other technical errors may result in fuzzy output. Nevertheless, it was possible to see some results that may serve as representatives of the real conditions on the river basin. Thus, truly speaking it can be concluded that for a really determined modeller or decision maker who is willing to exert some more efforts for the purpose of integrated water resource management and for future research, some useful guidance can be found from the obtained result.

4.6.2 Summary for Climate Change and Hydropower Projections

Because of the discrepancy in the availability of data period, it was found imperative that the reference period for meteorological and hydrological data was the period 1981 – 2010. On the other hand, hydropower generation data was found from Ethiopian Electric Utility (EEU) for the period 2006 – 2014. As a result the period 2006 – 2014 was considered as a reference period for the conditions in which modelling of hydropower production is involved. Furthermore, the IPCC CMIP5 RCP scenarios climate data start from the year 2006 and proceed till 2100, the extensions up to 2300. Therefore, to be consistent, in some case there are conditions in which the period 2006 – 2014 was taken as a reference period as far as the hydropower production modelling with WEAP is considered.

In dealing with hydrologic processes, five of the main variables that have more interrelation with reservoir and hydropower production were considered in this research both for the current period and in projections. These include basin temperature, basin rainfall, inflow to reservoir, reservoir evaporation and reservoir storage capacity.

Starting with evaporation, it was projected to increase over the reservoir surface. The average annual reservoir evaporation shows increases in amount by 2.9% in the period 2019 - 2040, by 6.9% in 2041 – 2070 and by 9.0% in 2071 – 2100 for RCP4.5 scenario. The increase in average annual evaporation for RCP8.5 is, as expected, more serious. This calls for special attention of decision makers. There is a silicon based liquid that is used to reduce evaporation from water bodies. This liquid, called Aquatain is spread in a very thin layer on top of bodies of water to form a barrier stopping contact between water and air and reducing the amount of loss to evaporation. Physical evaporation reduction methods are able to save a greater percentage of water, between 70 – 100% and entail a large capital cost and lower operations and maintenance costs (Benzaghta and Mohammad, 2009)

Inflow to reservoir and reservoir storage capacity are directly related to rainfall. But that the release from reservoir is regulated based on decision rules. Thus it can be said that future Koka Reservoir projection should consider the precipitation and evaporation projections. It should be noted that the average monthly distribution of the long-term reservoir capacity is seasonally very different. The lowest one was projected to be in February whereas the highest one is in September. Knowing the months helps reservoir operators and decision makers to make the pertinent water resources planning ahead.

With regard to long-term average annual storage capacity of the reservoir, the projection shows that the lowest annual storage of the near future will occur in 2020 for both RCP4.5 and RCP8.5. The projections were modelled to be 635 and 654 MCM respectively for that year. The storages are only about 61% of the maximum storage the reservoir can hold. Since evaporation and storage capacity are interrelated, this requires to also look for a method to reduce evaporation, as pointed earlier. The lowest capacity for the whole eighty two years was projected to occur in 2068 according to both RCP4.5 and RCP8.5 scenarios, with a value of 588 and 506 MCM respectively.

Apart from evaporation reduction, other biological and physical soil and water conservation practices are very useful in holding water that would be transported with rivers. The infiltration increases possibly groundwater recharge that would boost and homogenise the runoff. This also would increase reservoir storage.

The ultimate goal of the research was to assess the impact of climate change on hydropower generation. There is a fact to be admitted here also. First of all, currently the Koka Reservoir is meant significantly for irrigation rather than hydropower. Secondly, the study was done on an old hydropower plant with many of the features too old. This obviously has an impact on the output of the research. One basic truth is, however, that, as the result shows, the climate change has an impact on hydropower generation and the result can be extrapolated to other existing and ongoing large hydropower schemes. Of course, everything calls for great care. A reduction in energy generation of about 15% is projected according to the no policy RCP8.5 scenario after 2080s. Knowing this, assuming that the assumptions taken by IAM and CM experts hold, clearly warns the world community in general and developed countries in particular to look for their energy and climate policies. It forces them to design and implement strict policies. Otherwise, it will be playing with fire at the expense of their future generation.

CHAPTER 5

5. CONCLUSION AND RECOMMENDATIONS

5.1 Conclusion

Climate change is expected to be the result of increasing atmospheric concentrations of CO_2 and other greenhouse gases, due to anthropogenic emissions. Emissions of greenhouse gases have increased greatly since the start of the Industrial Revolution, primarily as a result of the burning of fossil fuels for electricity generation and transportation. In the absence of regulation, the continuing economic growth in developing countries suggests that emission levels will grow significantly over the 21st century.

The foremost technique of representing future climate change is from the use of General Circulation Models, and these complex mathematical models point out that temperature rises of around 2^0 C will occur, even though some models indicate considerably larger changes. Associated global warming will be accompanied with changes in regional and global precipitation patterns and other meteorological variables. The results of these changes will influence several areas of human activity, ranging from sea level rise and stress on water resources, to agriculture and human health. Overall, the consequences of the changes will have economic implications especially on developing nations.

As the electricity supply industry is in charge for around a third of all carbon releases a considerable level of emission decrease must occur here. To attain reductions, dependence on carbon-intensive technologies must be weakened, and low or no-carbon renewable resources utilized. Hydropower is the leading single renewable energy source used for electricity generation. In the current situation, it meets around a significant proportion of global electricity requirements and over the 21st century it is anticipated that hydropower production will increase considerably.

By the end of the 21st century, the temperature in the Upper Awash River Basin will be 1.3 ^{0}C to 3.7 ^{0}C more than the current temperature. It can be concluded that there will be an increase of about 0.5 ^{0}C per decade in UARB for no climate policy scenario. Even for the middle emission scenario of RCP4.5, with some climate effect mitigation policy, as projected for the river basin, there will be an increase in temperature of about 0.16 ^{0}C per decade till 2100. Even if there is an increase in precipitation in some cases, this couldn't

be a guarantee that streamflow and hydropower will increase. Increase in precipitation is followed by increase in evaporation. According to RCP8.5, in the period 2071 – 2100, a frightening increase in evaporation of about 23% was projected. The result is that there will be a decrease in power of about 15%.

Thus sticking to the climate policy is a matter of “do” or “die” for many countries including Ethiopia. Even the climate policy designed according to the medium scenario of RCP4.5 is not adequate, as could be seen from the result obtained. Of course a power increase is projected for the three periods. But the increase shows a fast decreasing tendency. The increases are 7.8%, 1.5% and 0.9% for the periods 2019 – 2040, 2041 – 2070 and 2071 – 2100, respectively. This shows that the policy should be stricter. Formulations of the policies are not enough. They should come into effect in all countries of the world.

The software models used for the realization of the research could capture the intended results, ranging from climate change and hydrology to hydropower generation. SWAT model could reproduce reasonable result in modelling hydrologic processes. SDSM could effectively generate daily precipitation and temperature using regression function the software is provided with. WEAP could simulate hydropower. The calibration and validation results obtained could produce confidence in proceeding with the models.

In fact it is reasonable to admit that there are different sources of uncertainties in almost all levels of usages of the models. Even the currently operational fine CORDEX grid of about 50 km x 50 km requires more refining. Within 50 km area, there are many local conditions that could alter weather and climate of an area. With respect to the previous 200 – 300 km grid on which the GCMs were previously based, CORDEX grid of about 0.44^0 is really very fine. Yet more refining is required for more dependable result. There are also many other uncertainties. Data quality matters the most. There were missing data that should be filled. This affects model results. Despite all these ups and downs, the intended results have been achieved. For further study, the following recommendations have been presented.

The SWAT run results shows that about 82% of the total water yield was contributed from surface runoff, while ground water flow contributes about 11%. Lateral flow contributes the rest 7% for total annual water yield. This indicates that the infiltration into the soil is less as compared to the surface runoff. The reason that most of water obtained from precipitation flows as surface runoff may be attributed to the land use land cover

conditions of the study area. This condition deserves special attention of decision makers. In order to ensure the sustainability of water resources, the landuse landcover condition of the area need to be managed effectively.

The contribution from lateral flow and groundwater flow may be improved by plantation and afforestation. Mixed agriculture and agro forestry can play both ways; they help in conservation of soil and water as well as in food production for human being and other animals. Therefore, long-term conservation of water is improved if infiltration is increased. Infiltration increases the proportion of groundwater flow and lateral flow.

5.2 Recommendations

- The increase in precipitation, if any, will not be a guarantee for increasing reservoir storage capacity, because the increase in evaporation excels the increase in precipitation. Therefore, a technique of reducing reservoir evaporation should be sought. The method of applying evaporation reduction for reservoirs obviously requires high initial cost but low operation cost. It is better that decision makers decide soon regardless of high initial cost. It can be seen that failing to take this decision results in more disaster than the money allocated for it.
- More accurate results would have been obtained if uncertainties with regard to land cover changes, downscaling methods, the hydrological simulation model, etc. were considered. Moreover, irrigation and other water schemes were not considered; had there been covered here, more representative results would have been obtained. Future doctoral and other purpose studies on the river basin are expected to include these and other related water resources projects.
- The downscaling of climate variables carried out used one GCM data from Hadley Center. In fact, for most modelling purposes, the CMIP5 RCP scenarios were used. In using downscaling methods especially for generating precipitation and temperature, it is advisable to use more than one model and model runs.
- Hydrological and climate data availability are very crucial for future development of any water resource projects. Hydropower production data is also very important to effectively plan for the future. Thus, the results of hydrological model (SWAT, SWAT-CUP) and hydropower simulation model (WEAP) will contribute to solving the challenge of water management problems to some extent. Tables are presented in Appendices. There may be a need to update the tables as necessary.

- Data quality should be highly considered while using distributed hydrological models. The applications with SWAT model were very challenging and a lack of suitable data was one of the prime concerns from the beginning to an end. Lacking appropriate data makes model execution very difficult and may affect the result obtained. Therefore, the databases should be extended and improved. Employing new data gathering systems should be devised especially in developing countries. This may require local and regional authorities to seriously take part in well managed and organized data compilation.

REFERENCES

Abbaspour, K. C. (2007). User Manual for SWAT-CUP, SWAT Calibration and Uncertainty Analysis Programs. Swiss Federal Institute of Aquatic Science and Technology, Eawag, Duebendorf, Switzerland, 93 pp.

Abbaspour, K. C., Yang, J., Maximov, I., Siber, R., Bogner, K., Mieleitner, J., Zobrist, J., and Srinivasan, R. (2007). Modeling hydrology and water quality in the pre-Alpine/Alpine Thur watershed using SWAT, J. Hydrol., 333, 413–430.

Abbaspour, K.C., Faramarizi, M., Ghasemi, S.S., and Yang, H. (2009). Assessing the impact of climate change on water resources in Iran, Water Resour. Res., 45, 1–16.

Abbott, M.B., and Refsgaard, C. (1996). Distributed Hydrological Modelling. ISBN 0792340426, 9780792340423, 321 pages

Albek, M., Bakır, O., and Albek, E., (2004). Hydrological modeling of Seydi Suyu watershed (Turkey) with HSPF. Journal of Hydrology 285 (2004) 260–271.

Allan, R. P., Soden, B. J., John, V. O., Ingram, W. and Good, P. (2010). Current changes in tropical precipitation. Environ. Res. Lett., 5, 025205.

Arnold, J. G., and Williams, J. R. (1987). Validation of SWRRB: Simulator for water resources in rural basins. *J. Water Resour. Plan. Manage. ASCE* 113(2): 243-256.

Arnold, J. G., Muttiah, R. S., Srinivasan, R. and Allen, P. M. (2000). Regional estimation of base flow and groundwater recharge in the upper Mississippi basin. *J. Hydrol.* 227(1-4): 21-40.

Arnold, J.G. and Allen, P.M. (1996). Estimating hydrologic budgets for three Illinois watersheds. J. Hydrology 176:57-77.

Arnold, J.G., Srinivasan, R., Muttiah, and Williams, J.R. (1998). Large area hydrologic modelling and assessment; part I: model development. J. of Amer. Water Res. Assoc. 34(1):73-89.

Benzaghta, M.A. and Mohammad, T.A. (2009). Evaporation from reservoir and reduction methods: An overview and assessment study, *International Engineering Convention*. Domascus, Syria and Medinah, Kingdom of Saudi Arabia, May 11-18, 2009

Bergman, M.J., and Donnangelo, L.J., (2000). Simulation of freshwater discharges from ungauged areas to the Sebastian River, Florida. *J. American Water Resources Assoc.* 36(5):1121−1132.

Beven, K. (1993) Prophecy, reality and uncertainty in distributed hydrological modelling. *Adv. Water Resour.* 16, 41–51.

Beven, K. and Binley, A. (1992). The Future of Distributed Models: Model Calibration and Uncertainty Prediction, Hydrological Processes, Vol. 6, 279-298

Beven, K. J. and Kirkby, M.J. (1979). A Physically Based Variable Contributing Area Model of Basin Hydrology. Hydrological Sciences Bulletin 24, 43-69.

Beven, K.J., Kirkby, M.J., Schofield, N. and Tagg A.F. (1984). Testing a physically based flood forecasting model (TOPMODEL) for three UK catchments. Journal of Hydrology 69, 119-143.

Bicknell, B.R., J.C. Imhoff, J.L. Kittle, A.S. Donigian, and R.C. Johanson. (2001). Hydrologic simulation program-FORTRAN. User‘s manual, v.11, Athens, GA., USEPA.

Blackshear, B., Crocker, T., Drucker, E., Filoon, J., Knelman, J. and Skiles, M. (2011). Hydropower Vulnerability and Climate Change, A Framework for Modelling the Future Hydroelectric Resources, Middlebury College Environmental Studies Scenior Seminar

Block, P., and Brown, C. (2008). Does Climate Matter? Evaluation the Effects of Climate Change on Future Ethiopian Hydropower; The Third Interagency on Research in Watersheds, Estes Park, CO

Borah D.K. and Bera M. (2003): Watershed Scale Hydrologic and Nonpoint Source Pollution Models, *American Society of Agricultural and Biological Engineers*, Vol. 46, pp. 1553-1566.

Brohan, P., J. J. Kennedy, I. Harris, S. F. B. Tett, and P. D. Jones, (2006). Uncertainty estimates in regional and global observed temperature changes: A new data set from 1850. J. Geophys. Res. Atmos., 111, DOI 10.1029/2005JD006548.

Brun, S. E. and Band, L. E. (2000). Simulating runoff behavior in an urbanizing watershed. Computers, Environment and Urban Systems, Vol. 24, 5-22.

Burrows, K. (2009). Climate Science – an Introduction

Chong-yu Xu (2002). Textbook of Hydrologic Models, Uppsala University, Department of Earth Sciences Hydrology, Villavägen 16, SE-752 36 Uppsala, Sweden

Chou, C., J. D. Neelin, C. A. Chen, and J. Y. Tu, 2009: Evaluating the “rich-get-richer’’ mechanism in tropical precipitation change under global warming. J. Clim., 22, 1982–2005.

Chow, V.T., Maidment, D.R. and Mays, L.W. (1988). Applied Hydrology, McGRAW-HILL INTERNATIONAL EDITORS, Civil Engineering Series, USA

Clarke, L.E., Edmonds, J.A., Jacoby, H.D., Pitcher, H., Reilly, J.M. and Richels, R. (2007). Scenarios of greenhouse gas emissions and atmospheric concentrations. Sub-report 2.1a of Synthesis and Assessment Product 2.1. Climate Change Science Program and the Subcommittee on Global Change Research, Washington DC

Collins, M., and Senior, C.A. (2002). Projections of future climate change, Weather Vol. 57.

Evans, J.P. (2011). CORDEX – An international climate downscaling initiative, 19th International Congress on Modelling and Simulation, Perth, Australia, 12-16 December 2011

Faramarzi, M., Abbaspour, K.C., Schulin, R., and Yang, H. (2009). Modelling blue and green water resources availability in Iran, Hydrol. Process., 23, 486–501.

Flato, G., J. Marotzke, B. Abiodun, P. Braconnot, S.C. Chou, W. Collins, P. Cox, F. Driouech, S. Emori, V. Eyring, C. Forest, P. Gleckler, E. Guilyardi, C. Jakob, V. Kattsov, C. Reason and M. Rummukainen (2013): Evaluation of Climate Models. In: Climate Change 2013: The Physical Science Basis. Contribution of Working Group I to the Fifth Assessment Report of the Intergovernmental Panel on Climate Change [Stocker, T.F., D. Qin, G.-K. Plattner, M. Tignor, S.K. Allen, J. Boschung, A. Nauels, Y. Xia, V. Bex and P.M. Midgley (eds.)]. Cambridge University Press, Cambridge, United Kingdom and New York, NY, USA.

Fohrer, N., and Frede, H.G. (2002). An integrated modeling approach to sustainable land use concepts in a low mountain range area. Proceedings of the World Congress of Soil Science: August Paper no. 136.

Fohrer, N., Haverkamp, S., and Frede, H.G. (2005). Assessment of the effects of land use patterns on hydrologic landscape functions: development of sustainable land use concepts for low mountain range areas. Hydrol Process 19:659–672.

Fohrer, N., Haverkamp,S., Eckhardt,K.S., and Ferde,H.G., (2001). Hydrological response to land use changes on the cathement scale. Physics and Chemistry of the Earth, Part B: Hydrology, Oceans and Atmosphere, 26, 577-582.

Fujino, J., Nair, R., Kainuma, M., Masui, T. and Matsuoka, Y. (2006). Multigas mitigation analysis on stabilization scenarios using aim global model. The Energy Journal Special issue #3:343–354

Gao, H., Tang, Q., Shi,X., Zhu, C., Bohn,T. J., Su,F., Sheffield,J., Pan,M., Lettenmaier,D.P and Wood,E.F. (2010). Water Budget Record from Variable Infiltration Capacity (VIC) Model. In Algorithm Theoretical Basis Document for Terrestrial Water Cycle Data Records.

Garen, D.C. and Daniel S. M., (2005). Curve Number Hydrology in Water Quality Modeling: Uses, Abuses, and Future Directions. Journal of the American Water Resources Association (JAWRA) 41(2):377-388.

Gassman, P.W., Reyes, M.R., Green, C.H., Arnold, J.G. (2007). The soil and water assessment tool: historical development, applications, and future research directions. Trans. ASABE 50, 1211–1250.

Gates, W.L., Rowntree, P.R. and Zeng, Q.-C. (1990). Validation of Climate Models. In Houghton, J.T., Jenkins, G.J. and Ephraums, J.J., editor, Climate Change, The IPCC Scientific Assessment, Chapter 4, Cambridge University Press

Gericke, O.J. Pretorius, Wagenaar1, E. D. and Loyd, C. (2004). Hydrological modelling of river basins Using HSPF model. Proceedings of the 2004 Water Institute of Southern Africa (WISA) Biennial Conference, Cape Town. ISBN: 1-920-01728-3

Gosain, A.K., Rao, S. and Basuray, D. (2006). Climate change impact assessment on hydrology of Indian River basins. *Current Sci.* 90(3): 346-353.

Gosain, A.K., Rao, S. Srinivasan, R. and Gopal N. (2005). Return-flow assessment for irrigation command in the Palleru River basin using SWAT model. *Hydrol. Process.* 19(3): 673-682.

Govender, M. and Everson, C.S. (2005). Modelling streamflow from two small South African experimental catchments using the SWAT model. *Hydrol. Process.* 19(3): 683-692.

Green, W.H. and Ampt, G.A. (1911). Studies in Soil Physics, I: The Flow of Air and Water through Soils. Journal of Agricultural Sciences 4:1-24.

Gupta, H. V., Sorooshian, S. and Yapo, P. O. (1998). Toward improved calibration of hydrologic models: multiple and non-commensurable measures of information. *Water Resour. Res.* 34, 751–763.

Harrison, P.H. (2001). An Assessment of the Impact of Climate Change on Hydroelectric Power. Thesis submitted for the degree of Doctor of Philosophy, The University of Edinburgh

Held, I., and B. Soden, 2006: Robust responses of the hydrological cycle to global warming. J. Clim., 5686–5699.

Hibbard, K. A., Meehl, G., Cox, P. and Friedlingstein, P. (2007) A strategy for climate change stabilization experiments. Eos 88:217–221

Hijioka, Y., Matsuoka, Y., Nishimoto, H., Masui, T. and Kainuma, M. (2008). Global GHG emission scenarios under GHG concentration stabilization targets. J Glob Environ Eng 13:97–108

Houghton, J. (2004). Global Warming; The Complete Briefing, Third Edition, Cambridge University Press

Houghton, J.T., Jenkins, G.J. and Ephraums, J.J (1990). Climate Change. The IPCC Scientific Assessment, Cambridge University Press, Cambridge

IPCC (2007) Climate Change 2007: The Physical Science Basis. Contribution of Working Group I to the Fourth Assessment Report of the Intergovernmental Panel on Climate Change [Solomon, S., D. Qin, M. Manning (eds.)].

IPCC (2013) Climate Change 2013: The Physical Science Basis. In: Stocker, T. F., Qin D., Plattner; G.-K., Tignor, M. M. B., Allen, S. K., Judith, B., Nauels, A., Xia, Y., Bex, V.,

Midgle, P. M. (eds) Working Group I Contribution to the Fifth Assessment Report of the Intergovernmental Panel on Climate Change, Cambridge University Press, Cambridge

IPCC, 2013: Climate Change 2013: The Physical Science Basis. Contribution of Working Group I to the Fifth Assessment Report of the Intergovernmental Panel on Climate Change [Stocker, T.F., D. Qin, G.-K. Plattner, M. Tignor, S.K. Allen, J. Boschung, A. Nauels, Y. Xia, V. Bex and P.M. Midgley (eds.)]. Cambridge University Press, Cambridge, United Kingdom and New York, NY, USA, 1535 pp.

Izaurralde, R.C., Williams, J. R. McGill, W. B. Rosenberg, N. J. and Quiroga Jakas, M. C. (2006). Simulating soil C dynamics with EPIC: Model description and testing against long-term data. *Ecol. Model.* 192(3-4): 362-384.

Jacomino, V.M.F., and Fields, D.E., (1997). A Critical approach to the calibration of a watershed model. Journal of American Water Resources Association 33 (1), 43–154.

Jha, M., Gassman, P.W., Secchi, S., Gu, R. and Arnold, J. (2004). Effect of Watershed Subdivision on SWAT Flow, Sediment, and Nutrient Predictions, Journal of the Amenrican Water Resources Association

Jha, M., Pan, Z., Takle, E.S., and Gu, R. (2004). Impacts of climate change on stream flow in the Upper Mississippi River Basin: A regional climate model perspective, *J.Geophys. Res.*, *109*, D09105, doi:10.1029/2003JD003686.

Jones, C., Giorgi, F. and Asrar, Ghassem (2011). The Coordinated Regional Downscaling Experiment: CORDEX An international downscaling link to CMIP5, Special Issue, No. 56, Vol. 16, No.2, May 2011

Joshi, M., E. Hawkins, R. Sutton, J. Lowe, and D. Frame, (2011). Projections of when temperature change will exceed 2°C above pre-industrial levels. Nature Clim. Change, 1, 407–412.

Jung, G. (2006) Regional Climate Change and the Impact on Hydrology in the Volta Basin of West Africa, Garmisch-Partenkirchen

Kalin, L. and Hantush, M. H. (2006). Hydrologic modeling of an eastern Pennsylvania watershed with NEXRAD and rain gauge data. *J. Hydrol. Eng.* 11(6): 555-569.

Khan, M.S., Coulibaly, P. and Dibike, Y. (2006). Uncertainty analysis of statistical downscaling methods, Journal of Hydrology 319 (2006) 357–382

Klipsch, J.D. & Evans, T.A. (2007). Reservoir Operations Modelling with HEC-ResSIM, Hydrologic Engineering Center, U.S. Army Corps of Engineers, Davis, CA. 530-756-1104.

Klipsch, J. D. and Hurst, M. B. (2013). HEC-ResSim Reservoir System Simulation, User's Manual, Version 3.1, US Army Corps of Engineers, Institute of Water Resources, Hydrologic Engineering Center (HEC)

Knisel, W.G. (1980). CREAMS, a field-scale model for chemicals, runoff, and erosion from agricultural management systems. USDA Conservation Research Report No. 26. Washington, D.C.: USDA.

Kristensen, K.J. and Jensen, S.E. (1975). A model of estimating actual evapotranspiration from potential evapotranspiration. Nordic Hydrology. 6, 170-188.

Lambert, F. H., and Webb, M. J. (2008). Dependency of global mean precipitation on surface temperature. Geophys. Res. Lett., 35, L23803.

Laroche, A., J. Gallichand, R. Lagace, and A. Pesant. (1996). Simulating atrazine transport with HSPF in an agricultural watershed. *J. Environ. Eng.* 122(7): 622−630.

Leggett, J., Pepper, W., Swart, R.J. (1992). Emissions Scenarios for the IPCC: an Update. In: Houghton JT, Callander BA, Varney SK (eds) Climate change 1992. The Supplementary Report to the IPCC Scientific Assessment, Cambridge University Press, Cambridge, pp 71–95

Lenhart, T., Eckhardt, K., Fohrer, N., and Frede, H. G.: (2002). Comparison of two different approaches of sensitivity analysis, Phys. Chem. Earth, 27, 645–654.

Leonard, R.A., W.G. Knisel., and D.A. Still. (1987). GLEAMS: Groundwater loading effects of agricultural management systems. Trans. ASAE.30:1403-1418.

Lijalem Z. (2006). Climate Change Impact on Lake Ziway Watershed Water Availability, Ethiopia, Msc Thesis, Cologne, Germany.

Lijalem Z. (2006). Climate Change Impact on Lake Ziway Watershed Water Availability, Ethiopia, Msc Thesis, Cologne, Germany.

Lukman, A.P. (2003). Regional impact of climate change and variability of water resources (Case study, Lake Naivasha basin, Kenya). MSc. Thesis, International Institute for Aerospace Survey and Earth Science, Enschede, The Netherlands.

Lumb, A. M., McCammon, R. B., and Kittle, J. L., Jr. (1994). User's manual for an expert system (HSPEXP) for calibration of the hydrological simulation program - FORTRAN. Water-Resources Investigations Report 94-4168, U.S. Geological Survey, Reston, VA.

Mausbach, M.J., and Dedrick, A. R. (2004). The length we go: Measuring environmental benefits of conservation practices. *J. Soil Water Cons.* 59(5): 96A-103A.

McSweeney C, New M, Lizcano G (2008). UNDP Climate Change Country Profiles – Ethiopia 2008. Available from: http://countryprofiles.geog.ox.ac.uk.

McKay, M., Beckman, R., and Conover,W. (1979). A comparison of three methods for selecting values of input variables in the analysis of output from a computer code. *Technometrics*, 21:239–245.

Meehl, G.A. and Bony, S. (2011). Introduction to CMIP5, Special Issue, No. 56, Vol. 16, No.2, May 2011

Mimikou, M.A. and Baltas, E.A. (2009). Climate change impacts on the reliability of hydroelectric energy production. Department of Water Resources, Hydraulic and Maritime Engineering, Faculty of Civil Engineering, National Technical University of Athens, Iroon Polytechniou 5, 157 80 Athens, Greece

Monteith, J.L. (1965). Evaporation and the environment. p. 205-234. *In* The state and movement of water in living organisms. 19th Symposia of the Society for Experimental Biology. Cambridge Univ. Press, London, U.K.

Moriasi, D. N., Arnold, J. G., van Liew, M. W., Bingner, R. L., Harmel, R. D. & Veith, T. L. 2007. Model evaluation guidelines for systematic quantification of accuracy in watershed simulations. *Transactions of the ASABE,* 50**,** 885-900.

Moss, R.H., Edmonds, J.A., Hibbard, K.A., Manning, M.R., Rose, S.K., van Vuuren D.P., Carter T.R., Emori, S., Kainuma, M., Kram, T., Meehl, G.A., Mitchell, J.F.B., Nakicenovic, N., Riahi, K., Smith, S.J., Stouffer, R.J., Thomson, A.M., Weyant, J.P. and Wilbanks, T.J. (2010) The next generation of scenarios for climate change research and assessment. Nature 463:747–756

Muttiah, R.S. and Wurbs, R. A. (2002). Scale-dependent soil and climate variability effects on watershed water balance of the SWAT model. *J. of Hydrology*, 256 (2002):264-285.

Nakicenovic et al (2000) Special Report on Emissions Scenarios (SRES). Cambridge University Press, Cambridge

Nash, J. E & Sutcliffe J. V. (1970) River flow forecasting through conceptual models. Part I. A discussion of principles. *J. Hydrol*. 10 (1970), 282–290.

Ndaruzaniye, V. (2011). Water Security in Ethiopia: Risk and Vulnarabilities' Assessment, Africa, Climate Change, Environemnt, Security (ACCESS), Issue 2: 2011

Nederveen, S.C. (2013). Flood Recession Farming: An Overview and Case Study from the Upper Awash Catchment, Ethiopia, Master thesis Hydrology, code 450122, ECTS

Neitsch, S.L., J.G. Arnold, J.R. Kiniry, and J.R. Williams. (2005). Soil and Water Assessment Tool Theoretical Documentation - Version 2005. Grassland, Soil & Water Research Laboratory, Agricultural Research Service, and Blackland Agricultural Research Station, Temple, Texas at http://www.brc.tamus.edu/swat.

Neudecker, H. & Magnus, J. R. (1988). *Matrix Differential Calculus with Applications in Statistics and Econometrics*, 136. John Wiley & Sons, New York, USA.

Nippon, K. (1996). Feasibility study on the Becho plain agricultural development project; Final report, Volume II, Annex I and II.

Olsson, T., Kämäräinen, M., Santos, D., Seitola, T., Tuomenvirta, H., Haavisto, R. and Lavado-Casmiro, W. (2017). Downscaling climate projections for the Peruvian coastal Chancay-Huaral Basin to support river discharge modeling with WEAP, Journal of Hydrology: Regional Studies 13 (2017) 26–42

Peoples Democratic Republic of Ethiopia (PDRE) (1989). Master plan for the Development of Surface Water Resources in the Awash Basin: Ethiopian Valleys Development Studies Authority, Final Report Volume 6, Halcrow

Priestley, C.H.B. and R.J. Taylor. (1972). On the assessment of surface heat flux and evaporation using large-scale parameters. Mon. Weather Rev. 100:81-92.

Refsgaard, J.C. and Storm, B. (1995). MIKE SHE. In: Singh, V.P. (Ed.), Computer Models of Watershed Hydrology. Water Resource Publications, CO, USA, 806-846.

Riahi, K., Grübler, A and Nakicenovic, N. (2007). Scenarios of long-term socio-economic and environmental development under climate stabilization. Technol Forecast Soc Chang 74:887–935

Rosenberg, N.J., Brown, R.A. Izaurralde, R.C., and Thomson, A.M.. (2003). Integrated assessment of Hadley Centre (HadCM2) climate change projections in agricultural productivity and irrigation water supply in the conterminous United States: I. climate change scenarios and impacts on irrigation water supply simulated with the HUMUS model. *Agricultural and Forest Meteorology* 117(1-2):73-96.

Saleh, A., J.G. Arnold, P.W. Gassman, L.M. Hauck, W.D. Rosenthal, J.R. Williams, A.M.S. McFarland. (2000). Application of SWAT for the Upper North Bosque River Watershed. Trans. ASAE 43(5):1077-87.

Santhi, C., J.G. Arnold, J.R. Williams, W.A. Dugas, and L. Hauck. (2001). Validation of the SWAT model on a large river basin with point and nonpoint sources. *J. of the American Water Resources Association* 37(5):1169-1188.

Santhi, C., Muttiah, R. S. Arnold, J. G. and Srinivasan. R. (2005). A GIS-based regional planning tool for irrigation demand assessment and savings using SWAT. *Trans. ASABE* 48(1): 137-147.

Sieber, J. and Purkey, D. (2016). Water Evaluation and Planning System (WEAP), User Gude, Stockholm Environment Institute

Simmons, A. J., Willett, K. M. Jones, P. D. Thorne, P. W. and Dee, D. P. (2010). Low-frequency variations in surface atmospheric humidity, temperature, and precipitation: Inferences from reanalyses and monthly gridded observational data sets. J. Geophys. Res. Atmos., 115, D01110, doi:10.1029/2009JD012442.

Singh, J., H. V. Knapp, J. G. Arnold, and M. Demissie. (2005). —Hydrologic modeling of the Iroquois River watershed using HSPF and SWAT.‖ *Journal of the American Water Resources Association,* vol.41, no.2, pp.343-360.

Skahill, B. E. (2004). Use of the Hydrological Simulation Program – FORTRAN (HSPF) Model for Watershed Studies, System-wide Modelling, Assessment, and Restoration Technologies (SMART), ERDC/TN-04-1

Smith, S.J. and Wigley, T.M.L. (2006). Multi-Gas forcing stabilization with minicam. The Energy Journal Special issue #3:373–392

Smith, T. M., R. W. Reynolds, T. C. Peterson, and J. Lawrimore, (2008). Improvements to NOAA's historical merged land-ocean surface temperature analysis (1880– 2006). J. Clim., 21, 2283–2296.

Srinivasan, R. and J.G. Arnold. (1994). Integration of a basin-scale water quality model with GIS. *Water Resources Bulletin* (30)3:453-462.

Stouffer, R.J., Taylor, K.E. and Meehl, G.A. (2011). CMIP5 Long-term experimental Design, Special Issue, No. 56, Vol. 16, No.2, May 2011

USDA, Soil Conservation Service (1972). National Engineering Handbook, Section 4: Hydrology. U.S. Government Printing Office, Washington, DC

USDA, Soil Conservation Service (1985). National Engineering Handbook, Section 4: Hydrology. U.S. Government Printing Office, Washington, DC

Van Griensven, A., Breuer, L., Di Luzio M., Vandenberghe, V., Goethals, P., Meixner, T., Arnold, J. and Srinivasan. R. (2006a). Environmental and ecological hydroinformatics to support the implementation of the European Water Framework Directive for river basin management. *J. Hydroinformatics* 8(4): 239-252.

Van Liew, M. W., and Garbrecht, J. (2003). Hydrologic simulation of the Little Washita River experimental watershed using SWAT. *J .American Water Resour. Assoc.* 39(2): 413-426.

Van Vuuren, D.P., Den Elzen, M.G.J., Lucas, P.L., Eickhout, B., Strengers, B.J., Van Ruijven, B., Wonink, S. and Van Houdt, R. (2007a). Stabilizing greenhouse gas concentrations at low levels: an assessment of reduction strategies and costs. Clim Chang 81:119–159

Veith, T.L. and L.T. Ghebremichael (2009). How to: applying and interpreting the SWAT Auto-calibration tools. In: Fifth International SWAT Conference Proceedings. August 5-7, 2009(Proceedings).

Volk, M., Hirschfeld, J., Schmidt, G., Bohn, C., Dehnhardt, A., Liersch, S. and Lymburner, L. (2007). A SDSS-based ecological-economic modeling approach for integrated river basin management on different scale levels: The project FLUMAGIS. *Water Resour. Mgmt*.

Vrugt, J. A., Gupta, H. V., Bouten, W. & Sorooshian S. (2003). A shuffled complex evolution metropolis algorithm for estimating posterior distribution of watershed model

parameters. In: *Calibration of Watershed Models* (ed. by Q. Duan, S. Sorooshian, H. V. Gupta, A. N. Rousseau & R. Turcotte). American Geophysical Union, Washington DC, USA. doi:10.1029/006WS07.

Water Works Design and Supervision Enterprise (2008). Evaluation of water resources of Ada'a and Becho plains groundwater basin for irrigation development project; Annex I, Vol I and II.

Wilby, R. L., Hay, L. E. and Leavesly G. H. (1999), A comparison of downscaled and raw GCM output: implications for climate change scenarios in the San Juan river basin, Colorado, J. Hydrol., 225, 67– 91.

Williams, J.R. (1969). Flood routing with variable time or variable storage coefficients. Trans. ASAE 12(1): 100-103

Williams, J.R. (1990). The erosion productivity impact calculator (EPIC) model: A case history. *Phil. Trans. R. Soc. London* 329(1255): 421-428.

Williams, M (2016). Universe Today, What is the Earth's average temperature? Article updated: 26 Jul, 2016, http://www.universetoday.com/55043/earths-temperature/

Wise, M., Calvin, K., Thomson, A., Clarke L, Bond-Lamberty, B., Sands, R., Smith S.J., Janetos, A. and Edmonds, J. (2009). Implications of limiting CO_2 concentrations for land use and energy. Science 324:1183–1186

Yang, J., Reichert, P., Abbaspour, K.C., Xia, J. and Yang, H (2008). Comparing uncertainty analysis techniques for a SWAT application to the Chaohe Basin in China, J. Hydrol., doi: 10.1016/j.jhydrol.

Yates, D., Sieber, J., Purkey, D. and Huber-Lee, A. (2005). WEAP21 – A Demand-, Priority-, and Preference-Driven Water Planning Model, Part 1: Model Characteristics, International Water Association; Water International, Volume 30, Number 4, Pages 487 – 500, December 2005

Zhang, Z., Wang, S., Sun, G., McNulty, S. G., Zhang, H., Li, J. Zhang, M., Klaghofer, E. and Strauss P. (2008). Evaluation of the MIKE SHE Model for Application in Loess Plateau, China, Journal of the American Water Resources Association, Vol. 44, No. 5

Zhou, J., Liu, Y., Guo, H. and He, D. (2014). Combining the SWAT model with sequential uncertainty fitting algorithm for streamflow prediction and uncertainty analysis for the Lake Dianchi Basin, China, Hydrol. Process., 28, 521–533.

Thesis

The thesis consisted of five chapters, and related references and appendices. Chapter one introduced the core purpose of the research starting by exposing the problem that led to the initiation of the research, mainly the hazardous consequence of climate change.

In the effort to fulfilling the objectives, the hydrological aspects of climate change have been associated with hydroelectric power generation in the study area, Upper Awash River Basin. Further, the impact of climate change on Koka Reservoir has been dealt with and thus its projected future evaporation and storage capacity were developed. A number of tables have been presented in the document, and also more will appear in the appendices that follow.

Future hydropower generation from Koka Reservoir was developed till 2100 under two Representative Concentration Pathways (RCP) emission scenarios thereby revealing the impact of climate change in the 21st century. It is believed that the result will make decision makers aware of the serious issue.

It was such that, as pointed out above, the streamflow, reservoir storage, evaporation and hydropower, using the respective models, were modelled till 2100, dividing the century into three long periods, of course excluding the reference period. The three future periods were 2019 – 2040, 2041 – 2070 and 2071 – 2100. The results of modelling revealed that there will be a decrease in energy by 15.1% in the last two decades of the 21st Century under RCP8.5 scenario as compared to the reference period of 2006 – 2014. The RCP8.5 scenario is the extension of the business as usual scenario under which there is no policy for alleviating the harsh effect of climate change.

With regard to RCP4.5 scenario, though variable, it was seen that there will be an increase in energy production in all the three periods as compared to the reference period. The increases in energy for the periods 2019 – 2040, 2041 – 2070, and 2071 – 2100 were predicted to be respectively, 7.8%, 1.5% and 0.9%. Even then, as can be seen from the trend of the increase, the increment itself has a decreasing tendency going further in the future for this middle concentration scenario.

The rate of evaporation has significant influence on hydropower generation. As time proceeds towards the end of the 21st century, the difference between RCP4.5 and RCP8.5 becomes clearly visible from the model results of evaporation and power. The average annual reservoir evaporation shows increases in amount by 2.9% in the period 2019 - 2040, by 6.9% in 2041 – 2070 and by 9.0% in 2071 – 2100 for RCP4.5 emission scenario.

The increase in average annual evaporation for RCP8.5 is found to be more pronounced. It increases in the periods 2019 – 2040, 2041 – 2070 and 2071 – 2100 by 4%, 10.5% and 23.2% respectively. The research showed that in the last two decades of the century, according to RCP8.5, an increase in evaporation of 23.2% is reflected in a decrease of power by 15.1%.

In conclusion, the research has shown sufficiently the impact of climate change on hydropower generation in the country. It is envisaged that the finding can be extrapolated for other hydro power projects of Ethiopia. Indeed, it is necessary to admit that other related parameters are sought for more details. For example, landuse land cover research should be incorporated. Moreover, other projects such as irrigation water supply should be considered as well. In other words integrated approach in space and time is mandatory.

CURRICULUM VITAE

1. Personal Data

Name: Keneni Elias Shoro
Date of Birth: 25 October 1970
Birth Place: Wollega
Nationality: Ethiopian
Address: Jimma, Ethiopia

P.O.Box: 853
Mobile: +251911814064
Marital Status: Married
E-mail: eebbifamaa2100@gmail.com

2. Educational Background

PhD Fellow: Evaluation of the Impact of Climate Change on Hydropower Generation in Ethiopia, A Case of Upper Awash Basin, University of Rostock, Germany

MSc.: Hydraulic and Hydropower Engineering (Arba Minch University, Ethiopia, 2007)
BSc.: Soil and Water Conservation (Former Haromaya University of Agriculture, Ethiopia, 1993)
Advance Diploma: Civil Engineering (Jimma University, Ethiopia, 2004)

3. Work Experience

From January 2008 on: Lecturer, Jimma University, Jimma Institute of Technology, Hydraulic Engineering Chair

I am offering Hydraulic Structures I and II, Design and Analysis of Earth Dams and Hydrodynamics courses to Hydraulic Engineering MSc students in Jimma Institute of Technology

(September 2005 to September 2007: Attended Graduate School (Masters), Arba Minch University, Ethiopia)

November 1993 to August 2005: Worked in Agricultural Development, Environmental Protection, Irrigation Development, Forest Conservation and Development organizations)

(In the mean time, i.e., September 2000 to July 2004, I attended Advance Diploma in Civil Engineering, Jimma University, Ethiopia)

Papers (not yet published)

- "Potential Assessment of Micro Hydropower for Rural Electrification in Some Selected Sites of Genale – Dawa Basin, Ethiopia"
- "Assessment of future climate change impact on temperature and precipitation in the Upper Awash Sub-basin, Ethiopia, using statistical downscaling approach"

Published article (Monograph from the PhD Thesis)

- Assessment of the impact of climate change on future hydropower production from Koka Reservoir under two representative concentration pathways (RCP) emission scenarios

APPENDICES

Appendix 1: Tables

Table 1: Climate Change Projection

A) Upper Awash River Basin Temperature (^{0}C)

Year	Scenario		Year	Scenario		Year	Scenario	
	RCP4.5	RCP8.5		RCP4.5	RCP8.5		RCP4.5	RCP8.5
2019	18.2	17.6	2046	18.9	19.5	2073	19.4	22.7
2020	18.1	18.7	2047	18.7	19.0	2074	20.2	21.5
2021	18.6	19.4	2048	18.9	19.0	2075	19.9	21.4
2022	17.6	18.8	2049	19.3	19.2	2076	18.9	21.8
2023	17.4	18.3	2050	19.5	19.9	2077	18.5	21.7
2024	17.5	18.0	2051	20.0	19.9	2078	19.3	22.1
2025	17.6	18.9	2052	20.1	19.8	2079	19.8	21.3
2026	18.7	19.4	2053	19.4	19.9	2080	20.5	21.0
2027	17.8	19.0	2054	19.4	20.5	2081	21.1	21.9
2028	18.4	18.1	2055	18.8	20.6	2082	19.7	22.1
2029	18.9	18.3	2056	18.8	19.9	2083	18.8	22.7
2030	17.9	18.0	2057	19.1	19.5	2084	19.0	23.0
2031	18.4	17.6	2058	20.2	20.0	2085	19.9	22.0
2032	19.3	17.9	2059	19.2	20.4	2086	20.6	22.8
2033	19.7	19.5	2060	19.3	20.3	2087	19.4	22.5
2034	18.9	19.8	2061	19.3	20.9	2088	19.5	22.8
2035	18.2	18.4	2062	19.9	20.4	2089	19.8	22.9
2036	19.0	18.1	2063	20.0	21.2	2090	20.0	22.5
2037	19.5	18.7	2064	19.5	21.0	2091	19.0	22.8
2038	18.8	18.6	2065	19.5	20.0	2092	19.4	23.1
2039	19.0	19.0	2066	19.7	20.7	2093	19.6	22.6
2040	18.8	19.3	2067	19.0	20.6	2094	20.0	23.7
2041	18.1	19.2	2068	19.8	22.0	2095	19.5	22.6
2042	17.9	19.7	2069	19.7	21.6	2096	20.1	23.1
2043	18.8	20.9	2070	19.8	20.5	2097	19.4	23.6
2044	19.3	19.0	2071	18.8	20.3	2098	19.3	23.3
2045	18.8	18.7	2072	18.6	21.2	2099	19.2	23.7

B) Upper Awash River Basin Annual Rainfall (mm)

Year	Scenario		Year	Scenario		Year	Scenario	
	RCP4.5	RCP8.5		RCP4.5	RCP8.5		RCP4.5	RCP8.5
2019	860.6	1247.4	2046	989.3	740.5	2073	1093.4	679.1
2020	1164.5	788.2	2047	1212	1096.5	2074	918.5	817.1

2021	787.4	811.1	2048	901.2	1174	2075	872.5	813.4
2022	893.4	765.5	2049	957	920.1	2076	1539.7	819.9
2023	1249.5	904.5	2050	937.9	881.7	2077	1243.1	1058.3
2024	1280.5	1192.9	2051	797.5	1039.9	2078	955.5	992.8
2025	1548.4	811.1	2052	835.4	1004.9	2079	983.6	1066.7
2026	901.6	812.5	2053	977.8	972.3	2080	1091.7	988.1
2027	1092.7	1052.2	2054	760.5	952.3	2081	954.5	783.1
2028	938.3	910.8	2055	1068.6	1048.7	2082	816.3	905.3
2029	855.4	953.5	2056	1054.3	1248.9	2083	1076.3	714.1
2030	1139.4	1069	2057	910.2	1265.8	2084	1067.2	894.8
2031	1025	1056.5	2058	682.9	817.7	2085	965.5	995.4
2032	800.7	1114.4	2059	1228.6	1187.1	2086	649.9	685.3
2033	1003.8	840	2060	837.7	1018.9	2087	1152.7	877
2034	875.6	735.3	2061	1016.2	795.5	2088	796.3	996.4
2035	1013.5	1059.4	2062	882.8	1070.6	2089	846.3	978.3
2036	860	989	2063	1070.7	849.8	2090	979.7	795.8
2037	788.1	880.8	2064	979.3	1003.5	2091	1168.4	791.5
2038	954	1142.7	2065	701.5	1250.9	2092	841.7	690.9
2039	943.8	1039.5	2066	887.7	865.4	2093	911.5	1098.3
2040	1250	874.6	2067	829.5	787.9	2094	879.7	711.7
2041	1186.1	828.1	2068	727.8	626	2095	1194.2	852.9
2042	1284.6	819.6	2069	1512	1004.8	2096	867.3	820.8
2043	1155.8	991.2	2070	959.9	1217.7	2097	915.5	855.9
2044	1285.2	1014.9	2071	1023.9	1029.2	2098	931.5	1114.9
2045	1104.5	939.7	2072	1162.2	977.1	2099	885.9	797.3

Table 2: Projections Related to Koka Reservoir Elements

A. Annual Average Reservoir Evaporation (MCM)

Year	Scenario		Year	Scenario		Year	Scenario	
	RCP4.5	RCP8.5		RCP4.5	RCP8.5		RCP4.5	RCP8.5
2019	337.0	325.8	2046	350.9	362.1	2073	359.3	421.5
2020	336.1	346.3	2047	347.2	351.8	2074	375.0	399.2
2021	344.4	360.2	2048	350.0	351.8	2075	368.5	396.4
2022	325.8	348.1	2049	357.4	355.6	2076	350.0	404.8
2023	323.1	339.8	2050	362.1	369.5	2077	343.5	402.0
2024	324.9	333.3	2051	371.3	368.5	2078	358.3	410.3
2025	325.8	350.9	2052	372.3	366.7	2079	367.6	395.5
2026	347.2	360.2	2053	359.3	369.5	2080	379.7	389.0
2027	329.6	352.8	2054	360.2	379.7	2081	390.8	406.6
2028	341.6	336.1	2055	349.1	381.5	2082	365.8	409.4

2029	350.0	338.8	2056	348.1	369.5	2083	348.1	420.5
2030	332.3	334.2	2057	353.7	361.1	2084	351.8	427.0
2031	340.7	326.8	2058	374.1	371.3	2085	368.5	408.5
2032	358.3	332.3	2059	355.6	378.8	2086	382.5	422.4
2033	365.8	361.1	2060	358.3	376.0	2087	360.2	417.8
2034	350.9	367.6	2061	358.3	388.0	2088	361.1	422.4
2035	337.9	340.7	2062	368.5	378.8	2089	366.7	424.2
2036	352.8	335.1	2063	370.4	392.7	2090	370.4	416.8
2037	361.1	347.2	2064	361.1	389.9	2091	351.8	422.4
2038	348.1	344.4	2065	362.1	370.4	2092	359.3	428.9
2039	351.8	352.8	2066	365.8	384.3	2093	363.9	419.6
2040	348.1	357.4	2067	352.8	382.5	2094	370.4	440.0
2041	335.1	356.5	2068	366.7	407.5	2095	361.1	418.7
2042	331.4	364.8	2069	365.8	401.0	2096	372.3	428.9
2043	349.1	388.0	2070	367.6	380.6	2097	360.2	438.2
2044	357.4	352.8	2071	349.1	376.9	2098	357.4	431.7
2045	348.1	347.2	2072	345.3	393.6	2099	356.5	439.1

B. Monthly Reservoir Evaporation (MCM)

	Jan	Feb	Mar	Apr	May	Jun	Jul	Aug	Sep	Oct	Nov	Dec
2019	26	22.8	31.9	25	33.2	32	20.8	13	31.3	44.1	28.4	28.5
2020	25.9	22.8	31.8	24.9	33.1	31.9	20.7	13	31.2	44	28.3	28.4
2021	26.6	23.3	32.6	25.6	33.9	32.7	21.2	13.3	32	45.1	29	29.1
2022	25.1	22.1	30.9	24.2	32.1	30.9	20.1	12.6	30.3	42.7	27.4	27.5
2023	24.9	21.9	30.6	24	31.8	30.7	19.9	12.5	30	42.3	27.2	27.3
2024	25.1	22	30.8	24.1	32	30.9	20	12.5	30.2	42.5	27.3	27.4
2025	25.1	22.1	30.9	24.2	32.1	30.9	20.1	12.6	30.3	42.7	27.4	27.5
2026	26.8	23.5	32.9	25.8	34.2	33	21.4	13.4	32.3	45.5	29.2	29.3
2027	25.4	22.3	31.2	24.5	32.5	31.3	20.3	12.7	30.6	43.1	27.7	27.8
2028	26.4	23.2	32.3	25.4	33.6	32.4	21.1	13.2	31.7	44.7	28.8	28.9
2029	27	23.7	33.1	26	34.5	33.2	21.6	13.5	32.5	45.8	29.5	29.6
2030	25.6	22.5	31.5	24.7	32.7	31.6	20.5	12.8	30.9	43.5	28	28.1
2031	26.3	23.1	32.3	25.3	33.6	32.4	21	13.1	31.7	44.6	28.7	28.8
2032	27.6	24.3	33.9	26.6	35.3	34	22.1	13.8	33.3	46.9	30.2	30.3
2033	28.2	24.8	34.6	27.1	36	34.7	22.6	14.1	34	47.9	30.8	30.9
2034	27.1	23.8	33.2	26	34.6	33.3	21.6	13.5	32.6	45.9	29.5	29.6
2035	26.1	22.9	32	25.1	33.3	32.1	20.8	13	31.4	44.2	28.4	28.5
2036	27.2	23.9	33.4	26.2	34.7	33.5	21.8	13.6	32.8	46.2	29.7	29.8
2037	27.9	24.5	34.2	26.8	35.6	34.3	22.3	13.9	33.6	47.3	30.4	30.5

2038	26.9	23.6	33	25.8	34.3	33.1	21.5	13.4	32.4	45.6	29.3	29.4
2039	27.1	23.9	33.3	26.1	34.6	33.4	21.7	13.6	32.7	46.1	29.6	29.7
2040	26.9	23.6	33	25.8	34.3	33.1	21.5	13.4	32.4	45.6	29.3	29.4
2041	25.9	22.7	31.7	24.9	33	31.8	20.7	12.9	31.1	43.9	28.2	28.3
2042	25.6	22.5	31.4	24.6	32.6	31.5	20.4	12.8	30.8	43.4	27.9	28
2043	26.9	23.7	33	25.9	34.4	33.2	21.5	13.5	32.4	45.7	29.4	29.5
2044	27.6	24.2	33.8	26.5	35.2	33.9	22	13.8	33.2	46.8	30.1	30.2
2045	26.9	23.6	33	25.8	34.3	33.1	21.5	13.4	32.4	45.6	29.3	29.4
2046	27.3	23.7	33.2	25.9	35.1	33.8	21.6	13.4	32.4	45.8	29.3	29.7
2047	27	23.4	32.8	25.6	34.7	33.4	21.4	13.2	32.1	45.3	28.9	29.3
2048	27.2	23.6	33.1	25.9	35	33.7	21.5	13.3	32.3	45.6	29.2	29.6
2049	27.8	24.1	33.8	26.4	35.7	34.4	22	13.6	33	46.6	29.8	30.2
2050	28.2	24.4	34.2	26.7	36.2	34.8	22.3	13.8	33.4	47.2	30.2	30.6
2051	28.9	25	35.1	27.4	37.1	35.7	22.9	14.1	34.3	48.4	31	31.4
2052	29	25.1	35.2	27.5	37.2	35.8	22.9	14.2	34.4	48.5	31	31.5
2053	27.9	24.2	34	26.5	35.9	34.6	22.1	13.7	33.2	46.8	30	30.4
2054	28	24.3	34.1	26.6	36	34.7	22.2	13.7	33.3	47	30	30.4
2055	27.2	23.5	33	25.8	34.9	33.6	21.5	13.3	32.2	45.5	29.1	29.5
2056	27.1	23.5	32.9	25.7	34.8	33.5	21.4	13.2	32.1	45.4	29	29.4
2057	27.5	23.9	33.4	26.1	35.3	34	21.8	13.5	32.7	46.1	29.5	29.9
2058	29.1	25.2	35.4	27.6	37.4	36	23	14.2	34.5	48.8	31.2	31.6
2059	27.7	24	33.6	26.3	35.5	34.2	21.9	13.5	32.8	46.4	29.6	30
2060	27.9	24.2	33.9	26.5	35.8	34.5	22.1	13.6	33.1	46.7	29.9	30.3
2061	27.9	24.2	33.9	26.5	35.8	34.5	22.1	13.6	33.1	46.7	29.9	30.3
2062	28.7	24.9	34.9	27.2	36.8	35.5	22.7	14	34	48.1	30.7	31.1
2063	28.8	25	35	27.4	37	35.7	22.8	14.1	34.2	48.3	30.9	31.3
2064	28.1	24.4	34.2	26.7	36.1	34.8	22.2	13.7	33.3	47.1	30.1	30.5
2065	28.2	24.4	34.2	26.7	36.2	34.8	22.3	13.8	33.4	47.2	30.2	30.6
2066	28.5	24.7	34.6	27	36.5	35.2	22.5	13.9	33.8	47.7	30.5	30.9
2067	27.4	23.8	33.4	26.1	35.2	34	21.7	13.4	32.6	46	29.4	29.8
2068	28.5	24.7	34.7	27.1	36.6	35.3	22.6	14	33.9	47.8	30.6	31
2069	28.5	24.7	34.6	27	36.5	35.2	22.5	13.9	33.8	47.7	30.5	30.9
2070	28.6	24.8	34.8	27.2	36.7	35.4	22.6	14	33.9	47.9	30.7	31.1
2071	27.2	23.5	33	25.8	34.9	33.6	21.5	13.3	32.2	45.5	29.1	29.5
2072	26.9	23.3	32.7	25.5	34.5	33.2	21.3	13.1	31.9	45	28.8	29.2
2073	27.3	24	34.1	26.7	35.6	34.7	22.2	13.7	33.2	46.8	30.2	30.8
2074	28.5	25	35.6	27.9	37.2	36.2	23.2	14.3	34.6	48.9	31.5	32.1
2075	28	24.6	34.9	27.4	36.6	35.6	22.8	14	34	48	31	31.6
2076	26.6	23.3	33.2	26	34.7	33.8	21.6	13.3	32.3	45.6	29.4	30

2077	26.1	22.9	32.6	25.6	34.1	33.1	21.2	13.1	31.7	44.8	28.9	29.4
2078	27.3	23.9	34	26.7	35.6	34.6	22.1	13.6	33.1	46.7	30.1	30.7
2079	28	24.5	34.9	27.4	36.5	35.5	22.7	14	33.9	47.9	30.9	31.5
2080	28.9	25.3	36	28.3	37.7	36.6	23.4	14.4	35.1	49.5	31.9	32.5
2081	29.7	26.1	37.1	29.1	38.8	37.7	24.1	14.9	36.1	51	32.9	33.5
2082	27.8	24.4	34.7	27.2	36.3	35.3	22.6	13.9	33.8	47.7	30.7	31.4
2083	26.5	23.2	33	25.9	34.5	33.6	21.5	13.2	32.1	45.4	29.3	29.8
2084	26.8	23.5	33.4	26.2	34.9	33.9	21.7	13.4	32.5	45.9	29.6	30.2
2085	28	24.6	34.9	27.4	36.6	35.6	22.8	14	34	48	31	31.6
2086	29.1	25.5	36.3	28.5	38	36.9	23.6	14.5	35.3	49.9	32.2	32.8
2087	27.4	24	34.2	26.8	35.7	34.7	22.2	13.7	33.3	47	30.3	30.9
2088	27.5	24.1	34.2	26.9	35.8	34.8	22.3	13.7	33.3	47.1	30.4	31
2089	27.9	24.5	34.8	27.3	36.4	35.4	22.6	13.9	33.9	47.8	30.8	31.4
2090	28.2	24.7	35.1	27.6	36.8	35.7	22.9	14.1	34.2	48.3	31.1	31.8
2091	26.8	23.5	33.4	26.2	34.9	33.9	21.7	13.4	32.5	45.9	29.6	30.2
2092	27.3	24	34.1	26.7	35.6	34.7	22.2	13.7	33.2	46.8	30.2	30.8
2093	27.7	24.3	34.5	27.1	36.1	35.1	22.5	13.8	33.6	47.4	30.6	31.2
2094	28.2	24.7	35.1	27.6	36.8	35.7	22.9	14.1	34.2	48.3	31.1	31.8
2095	27.5	24.1	34.2	26.9	35.8	34.8	22.3	13.7	33.3	47.1	30.4	31
2096	28.3	24.8	35.3	27.7	36.9	35.9	23	14.2	34.4	48.5	31.3	31.9
2097	27.4	24	34.2	26.8	35.7	34.7	22.2	13.7	33.3	47	30.3	30.9
2098	27.2	23.8	33.9	26.6	35.5	34.5	22.1	13.6	33	46.6	30	30.6
2099	27.1	23.8	33.8	26.5	35.4	34.4	22	13.6	32.9	46.5	30	30.6

C. Annual Average Inflow into the Reservoir (MCM)

Year	Scenario		Year	Scenario		Year	Scenario	
	RCP4.5	RCP8.5		RCP4.5	RCP8.5		RCP4.5	RCP8.5
2019	107.8	156.7	2046	124	93.1	2073	137.0	85.3
2020	145.9	99	2047	151.9	137.8	2074	115.1	102.7
2021	98.7	101.9	2048	112.9	147.5	2075	109.3	102.2
2022	111.9	96.2	2049	119.9	115.6	2076	192.9	103.0
2023	156.6	113.7	2050	117.5	110.8	2077	155.7	133.0
2024	160.4	149.9	2051	99.9	130.7	2078	119.7	124.8
2025	194	101.9	2052	104.7	126.3	2079	123.2	134.0
2026	113	102.1	2053	122.5	122.2	2080	136.8	124.2
2027	136.9	132.2	2054	95.3	119.7	2081	119.6	98.4
2028	117.6	114.5	2055	133.9	131.8	2082	102.3	113.8
2029	107.2	119.8	2056	132.1	156.9	2083	134.9	89.7
2030	142.8	134.3	2057	114	159.1	2084	133.7	112.4
2031	128.4	132.8	2058	85.6	102.8	2085	121.0	125.1

2032	100.3	140	2059	153.9	149.2	2086	81.4	86.1
2033	125.8	105.6	2060	105	128	2087	144.4	110.2
2034	109.7	92.4	2061	127.3	100	2088	99.8	125.2
2035	127	133.1	2062	110.6	134.5	2089	106.0	122.9
2036	107.8	124.3	2063	134.1	106.8	2090	122.7	100.0
2037	98.7	110.7	2064	122.7	126.1	2091	146.4	99.5
2038	119.5	143.6	2065	87.9	157.2	2092	105.5	86.8
2039	118.3	130.6	2066	111.2	108.7	2093	114.2	138.0
2040	156.6	109.9	2067	103.9	99	2094	110.2	89.4
2041	148.6	104.1	2068	91.2	78.7	2095	149.6	107.2
2042	160.9	103	2069	189.4	126.3	2096	108.7	103.1
2043	144.8	124.6	2070	120.3	153	2097	114.7	107.6
2044	161	127.5	2071	128.3	129.3	2098	116.7	140.1
2045	138.4	118.1	2072	145.6	122.8	2099	111.0	100.2

D. Storage Capacity (MCM)

Year	Scenario		Year	Scenario		Year	Scenario	
	RCP4.5	RCP8.5		RCP4.5	RCP8.5		RCP4.5	RCP8.5
2019	694.9319	1007.252	2046	798.9	597.9	2073	882.9	548.4
2020	940.3303	636.4565	2047	978.7	885.4	2074	741.7	659.8
2021	635.8231	654.9478	2048	727.7	948	2075	704.5	656.8
2022	721.4178	618.1267	2049	772.8	743	2076	1243.3	662.1
2023	1008.968	730.3666	2050	757.4	712	2077	1003.8	854.6
2024	1034	963.2441	2051	644	839.7	2078	771.6	801.7
2025	1250.328	654.9478	2052	674.6	811.4	2079	794.3	861.3
2026	728.0393	656.0783	2053	789.6	785.1	2080	881.5	797.9
2027	882.352	849.6315	2054	614.1	769	2081	770.8	632.3
2028	757.6744	735.4537	2055	862.9	846.8	2082	659.2	731
2029	690.7329	769.9331	2056	851.3	1008.5	2083	869.1	576.6
2030	920.0621	863.1972	2057	735	1022.1	2084	861.8	722.5
2031	827.6844	853.1037	2058	551.4	660.3	2085	779.6	803.8
2032	646.5628	899.8568	2059	992.1	958.6	2086	524.8	553.4
2033	810.5655	678.284	2060	676.4	822.7	2087	930.8	708.2
2034	707.0444	593.7408	2061	820.6	642.4	2088	643	804.6
2035	818.3982	855.4454	2062	712.9	864.5	2089	683.4	790
2036	694.4474	798.5987	2063	864.6	686.2	2090	791.1	642.6
2037	636.3884	711.2293	2064	790.8	810.3	2091	943.5	639.1
2038	770.3521	922.7085	2065	566.5	1010.1	2092	679.7	557.9
2039	762.1157	839.3765	2066	716.8	698.8	2093	736	886.9
2040	1009.371	706.2229	2067	669.8	636.2	2094	710.4	574.7
2041	957.8	668.7	2068	587.7	505.5	2095	964.3	688.7
2042	1037.3	661.8	2069	1220.9	811.4	2096	700.3	662.8
2043	933.3	800.4	2070	775.1	983.3	2097	739.3	691.1

2044	1037.8	819.5	2071	826.8	831.1	2098	752.2	900.3
2045	891.9	758.8	2072	938.5	789	2099	715.4	643.8

Table 3: a) Annual Hydropower Production (GWh)

Year	Scenario		Year	Scenario		Year	Scenario	
	RCP4.5	RCP8.5		RCP4.5	RCP8.5		RCP4.5	RCP8.5
2019	103.7	129.3	2046	107.5	81.1	2073	117.9	67.3
2020	129	84.2	2047	130.7	120.1	2074	99	81
2021	95.6	86.7	2048	97.9	128.6	2075	94.1	80.7
2022	107.4	81.8	2049	104	100.8	2076	130.4	81.3
2023	123.4	96.6	2050	101.9	96.6	2077	129	105
2024	128.8	127.5	2051	86.7	113.9	2078	103	98.5
2025	131.5	86.7	2052	90.8	110.1	2079	106	105.8
2026	108.3	86.8	2053	106.3	106.5	2080	117.7	98
2027	121	112.4	2054	82.6	104.3	2081	102.9	77.7
2028	112.3	97.3	2055	116.1	114.9	2082	88	89.8
2029	103.2	101.9	2056	114.6	126.8	2083	116	70.8
2030	126.2	114.2	2057	98.9	128.7	2084	115	88.7
2031	113.5	112.9	2058	74.2	89.6	2085	104.1	98.7
2032	97.1	119.1	2059	123.5	130.1	2086	70.1	68
2033	111.2	89.8	2060	91	111.6	2087	124.3	87
2034	105.4	82.6	2061	110.4	87.2	2088	85.8	98.8
2035	112.3	113.2	2062	95.9	117.3	2089	91.2	97
2036	103.7	105.7	2063	116.4	93.1	2090	105.6	78.9
2037	95.7	94.1	2064	106.4	109.9	2091	125.9	78.5
2038	105.7	122.1	2065	76.2	127.1	2092	90.7	68.5
2039	104.5	111.1	2066	96.5	94.8	2093	98.3	108.9
2040	122.5	93.4	2067	90.1	86.3	2094	94.8	70.6
2041	128.9	90.7	2068	79.1	68.6	2095	128.7	84.6
2042	125.6	89.8	2069	129.3	110.1	2096	93.5	81.4
2043	125.6	108.6	2070	104.3	123.4	2097	98.7	84.9
2044	129.7	111.2	2071	110.4	102.1	2098	100.4	110.6
2045	120	103	2072	125.3	96.9	2099	95.5	79.1

b) Monthly Hydropower Production (GWh)

	2019	2020	2021	2022	2023	2024	2025	2026	2027	2028	2029	2030
Jan	6.4	18.1	7.6	10.5	9.8	7.5	11.9	10.6	7.4	15.8	8.2	7.6
Feb	6.4	12.6	6.8	9.5	10.0	8.4	8.5	9.6	7.5	10.9	7.4	6.5
Mar	6.8	13.3	7.2	10.4	8.7	9.1	15.8	10.5	8.0	11.6	7.7	6.4
Apr	6.2	16.8	8.2	9.5	6.9	9.4	13.2	9.6	7.3	14.6	8.8	7.9
May	7.0	12.6	7.9	12.3	8.5	11.8	13.9	12.3	8.2	10.9	8.6	8.1

Jun	7.1	3.7	4.1	7.6	9.8	12.8	12.3	7.6	8.3	3.3	4.4	8.3
Jul	9.7	2.5	5.9	7.8	11.1	10.1	8.2	7.9	11.3	2.2	6.4	13.2
Aug	17.2	4.1	12.2	7.4	16.3	10.8	8.5	7.4	20.0	3.5	13.1	18.2
Sep	14.1	11.1	12.0	7.4	14.5	15.1	7.1	7.5	16.4	9.6	13.0	16.6
Oct	7.3	11.2	7.7	7.8	9.1	14.0	9.5	7.9	8.5	9.8	8.3	11.0
Nov	7.8	10.9	7.6	8.4	9.3	9.7	10.7	8.5	9.1	9.5	8.2	11.3
Dec	7.7	12.1	8.4	8.8	9.4	10.1	11.9	8.9	9.0	10.6	9.1	11.1
	2031	2032	2033	2034	2035	2036	2037	2038	2039	2040	2041	2042
Jan	9.1	5.6	8.8	9.5	9.1	6.4	7.7	8.4	14.6	7.4	10.4	7.7
Feb	8.2	6.4	9.0	6.8	8.0	6.4	6.9	7.6	10.2	6.3	9.3	7.8
Mar	9.0	6.9	7.8	12.6	8.9	6.8	7.6	7.9	10.8	6.2	10.2	8.3
Apr	9.0	7.1	6.3	10.6	9.0	6.2	7.6	9.0	13.6	7.7	10.2	7.5
May	9.7	8.9	7.7	11.1	9.5	7.0	8.1	8.8	10.2	7.9	11	8.5
Jun	7.9	9.7	8.8	9.9	7.8	7.2	6.6	4.5	3.0	8.0	8.9	8.7
Jul	8.6	7.6	10.0	6.6	8.4	9.7	7.2	6.5	2.1	12.9	9.7	11.7
Aug	12.2	8.1	14.7	6.8	12.0	17.1	10.3	13.5	3.3	17.4	13.9	20.8
Sep	12.2	11.3	13.0	5.7	12.1	14.1	10.3	13.3	9.0	16.2	13.9	17
Oct	9.2	10.6	8.2	7.7	9.1	7.3	7.8	8.5	9.1	10.7	10.5	8.9
Nov	9.0	7.3	8.4	8.6	9.0	7.8	7.6	8.4	8.8	11.0	10.2	9.4
Dec	9.4	7.6	8.5	9.5	9.4	7.7	8.0	9.3	9.8	10.8	10.7	9.3
	2043	2044	2045	2046	2047	2048	2049	2050	2051	2052	2053	2054
Jan	10	18.1	7.2	10.5	10.3	5.8	9.4	8.2	7	5.6	8.4	11.6
Feb	9	12.6	6.1	9.5	10.6	6.4	6.8	7.3	6.2	5.6	7.6	8
Mar	9.4	13.4	6.2	10.4	9.2	6.9	12.3	8	6.9	6	8.1	8.5
Apr	10.7	16.9	7.5	9.5	7.3	7.1	10.4	8.1	6.9	5.5	9.1	10.7
May	10.4	12.6	7.7	12.3	9.1	8.9	11	8.6	7.4	6.1	8.8	8
Jun	5.4	3.8	7.9	7.6	10.3	9.7	9.7	7.1	6	6.3	4.5	2.4
Jul	7.8	2.6	12.6	7.8	11.8	7.7	6.5	7.7	6.6	8.5	6.6	1.7
Aug	16	4.1	17.3	7.4	17.3	8.2	6.8	11	9.3	15	13.5	2.6
Sep	15.7	11.1	15.8	7.5	15.3	11.5	5.6	11	9.3	12.3	13.4	7.1
Oct	10.1	11.3	10.4	7.8	9.7	10.6	7.6	8.3	7	6.4	8.5	7.2
Nov	10	11	10.8	8.4	9.8	7.4	8.5	8.1	6.9	6.8	8.4	7
Dec	11.1	12.2	10.5	8.8	10	7.7	9.4	8.5	7.2	6.7	9.4	7.8
	2055	2056	2057	2058	2059	2060	2061	2062	2063	2064	2065	2066
Jan	7	11.2	7.8	4.3	11.1	7.4	8.9	5.9	9.2	14.9	4.6	9.4
Feb	5.9	10.2	8	4.9	8	6.5	7.9	6	8.3	10.4	3.9	8.6
Mar	5.8	11.1	6.9	5.3	14.8	7.2	8.8	6.3	8.7	11	3.8	9.3
Apr	7.3	10.2	5.8	5.5	12.4	7.3	8.8	5.7	10	13.8	4.8	8.6
May	7.5	13	6.8	6.8	13.1	7.7	9.4	6.5	9.6	10.4	4.9	11.1
Jun	7.6	8.1	7.8	7.4	11.5	6.4	7.6	6.6	5.2	3.1	5.1	6.8

Jul	12.2	8.3	8.9	5.8	7.7	6.8	8.3	9	7.2	2.1	8	7
Aug	16.8	7.8	13.1	6.2	8	9.8	11.8	15.8	14.8	3.3	11	6.6
Sep	15.3	7.9	11.6	8.7	6.7	9.6	11.9	13	14.6	9.1	10	6.7
Oct	10.1	8.3	7.3	8.1	9	7.4	9	6.8	9.3	9.3	6.6	7
Nov	10.4	9.1	7.4	5.6	10.1	7.3	8.8	7.2	9.2	9	6.8	7.6
Dec	10.2	9.4	7.5	5.8	11.1	7.6	9.2	7.1	10.3	10	6.7	7.8
	2067	2068	2069	2070	2071	2072	2073	2074	2075	2076	2077	2078
Jan	7.1	4.6	11.7	8.4	8.9	7.7	9.4	13.9	5.7	12.7	10.2	6
Feb	7.3	5.2	8.4	7.7	7.9	7.8	8.4	9.6	4.8	11.6	10.5	6.7
Mar	6.3	5.6	15.5	8.2	8.8	8.3	8.8	10.2	4.7	12.6	9	7.3
Apr	5.1	5.8	12.9	8.3	8.8	7.5	10.1	12.9	5.9	11.6	7.3	7.5
May	6.2	7.2	13.7	8.8	9.4	8.4	9.8	9.6	6.1	15	8.9	9.4
Jun	7.1	7.8	12	7.2	7.6	8.6	5	2.9	6.2	9.2	10.2	10.2
Jul	8.1	6.2	8.1	7.8	8.3	11.7	7.3	2	9.9	9.4	11.6	8.1
Aug	11.9	6.6	8.4	11.2	11.8	20.7	15	3.1	13.5	8.9	17.1	8.6
Sep	10.6	9.3	7	11.2	11.9	17	14.8	8.5	12.4	9	15.1	12.1
Oct	6.7	8.6	9.4	8.5	9	8.9	9.5	8.6	8.2	9.5	9.6	11.2
Nov	6.8	6	10.5	8.3	8.8	9.4	9.4	8.4	8.4	10.2	9.7	7.8
Dec	6.9	6.2	11.7	8.7	9.2	9.3	10.4	9.3	8.3	10.7	9.8	8.1
	2079	2080	2081	2082	2083	2084	2085	2086	2087	2088	2089	2090
Jan	9.6	9.5	8.3	5.4	9.2	16.1	6.3	6.9	9.8	5	8.2	8.5
Feb	6.9	8.4	7.4	5.5	8.3	11.2	5.3	6.2	10.1	5.6	5.9	7.5
Mar	12.7	9.3	8.2	5.8	8.7	11.9	5.4	6.8	8.7	6.1	10.9	8.3
Apr	10.6	9.4	8.2	5.3	9.9	14.9	6.5	6.2	7.1	6.2	9.1	8.4
May	11.2	10	8.7	5.9	9.6	11.2	6.7	8	8.6	7.8	9.6	8.9
Jun	9.9	8.1	7.1	6.1	5	3.3	6.8	4.9	9.8	8.4	8.5	7.5
Jul	6.6	8.8	7.8	8.2	7.2	2.4	10.9	5.1	11.2	6.7	5.9	7.9
Aug	6.9	12.7	11	14.6	14.8	3.6	15	4.8	16.4	7.2	5.9	11.4
Sep	5.7	12.7	11.1	11.9	14.6	9.9	13.7	4.9	14.6	10	4.9	11.4
Oct	7.7	9.6	8.3	6.2	9.3	10	9.1	5.1	9.2	9.3	6.7	8.6
Nov	8.6	9.4	8.2	6.6	9.2	9.7	9.3	5.5	9.3	6.5	7.4	8.4
Dec	9.6	9.8	8.6	6.5	10.2	10.8	9.1	5.7	9.5	6.7	8.2	8.8
	2091	2092	2093	2094	2095	2096	2097	2098	2099	2100		
Jan	10.1	5.6	7.8	13.3	7.7	9.1	7.8	5.8	8.6	6.3		
Feb	9	5.6	7	9.2	6.6	8.3	8	6.6	6.2	5.5		
Mar	10	6	7.4	9.8	6.5	9	6.9	7.1	11.5	6.1		
Apr	10	5.4	8.4	12.3	8.1	8.3	5.5	7.3	9.6	6.2		
May	10.7	6.1	8.1	9.2	8.3	10.7	6.8	9.2	10.1	6.6		
Jun	8.7	6.3	4.2	2.7	8.4	6.6	7.8	10	8.9	5.4		
Jul	9.5	8.5	6.1	1.9	13.5	6.8	8.9	7.9	6	5.8		

Aug	13.6	15	12.5	3.2	18.6	6.4	13.1	8.4	6.2	8.3		
Sep	13.6	12.3	12.4	8.1	17	6.5	11.6	11.7	5.1	8.3		
Oct	10.2	6.4	7.9	8.2	11.2	6.8	7.4	10.9	6.9	6.3		
Nov	10	6.8	7.8	8	11.5	7.3	7.4	7.6	7.8	6.2		
Dec	10.5	6.7	8.7	8.9	11.3	7.7	7.5	7.9	8.6	6.5		

Appendix 2: Figures

a) Upper Awash River Basin Temperature

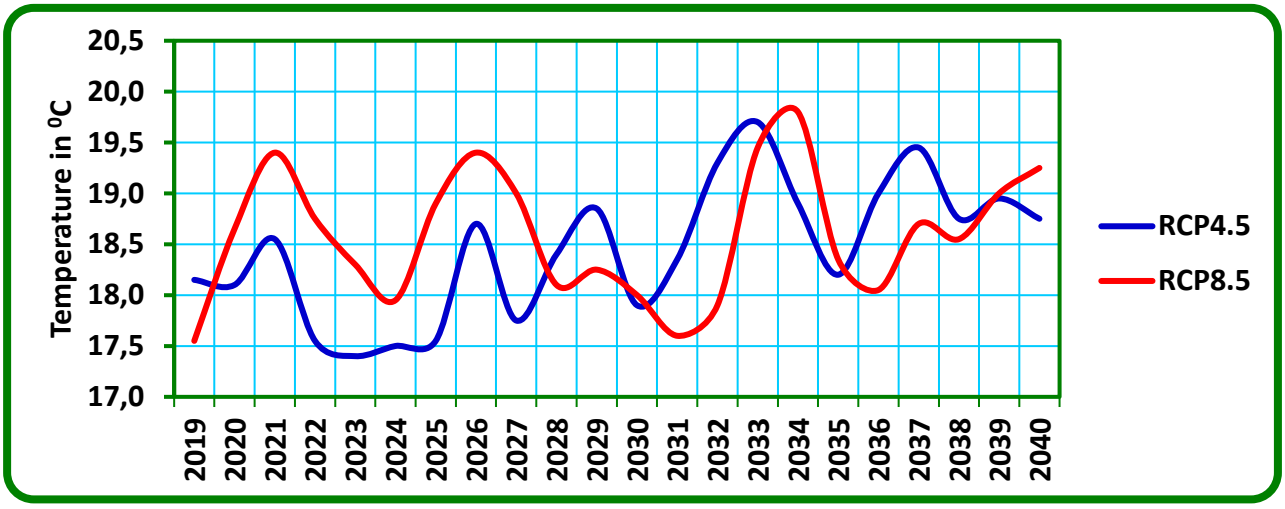

Figure a1: UARB Annual Average Temperature under RCP Scenarios for the Period 2019 – 2040

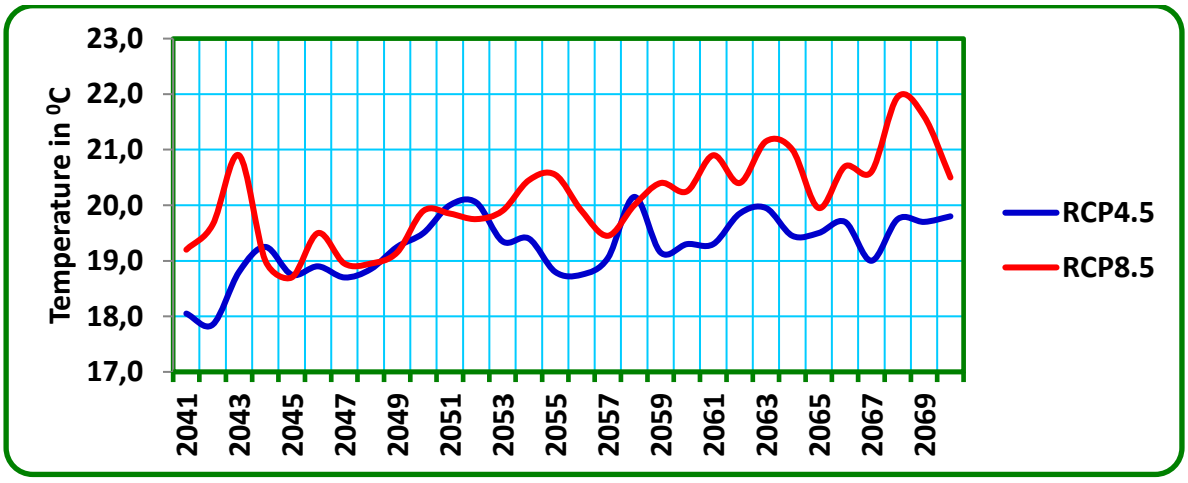

Figure a2: UARB Annual Average Temperature under RCP Scenarios for the Period 2041 – 2070

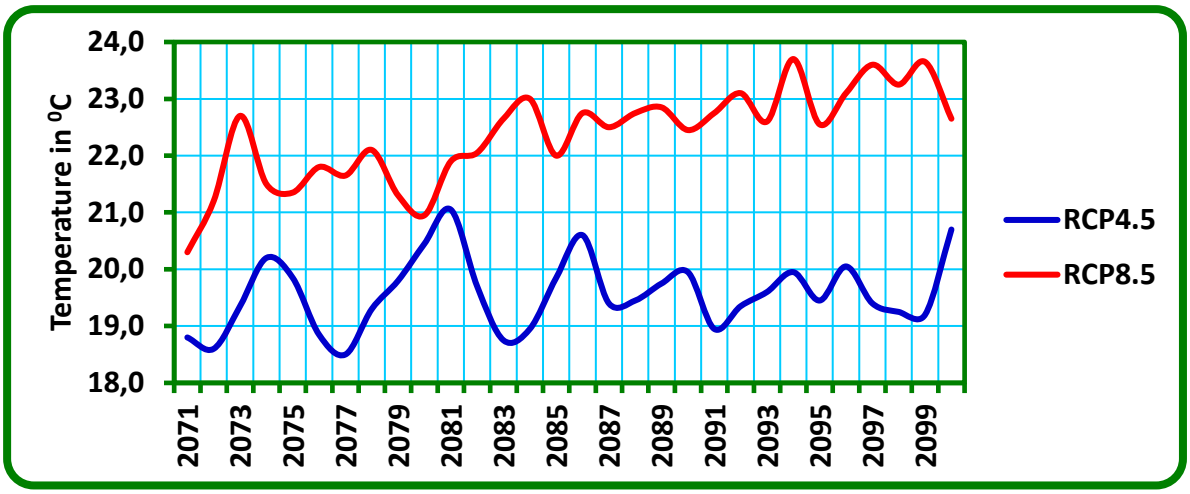

Figure a3: UARB Annual Average Temperature under RCP Scenarios for the Period 2071 - 2100

b) Upper Awash River Basin Rainfall

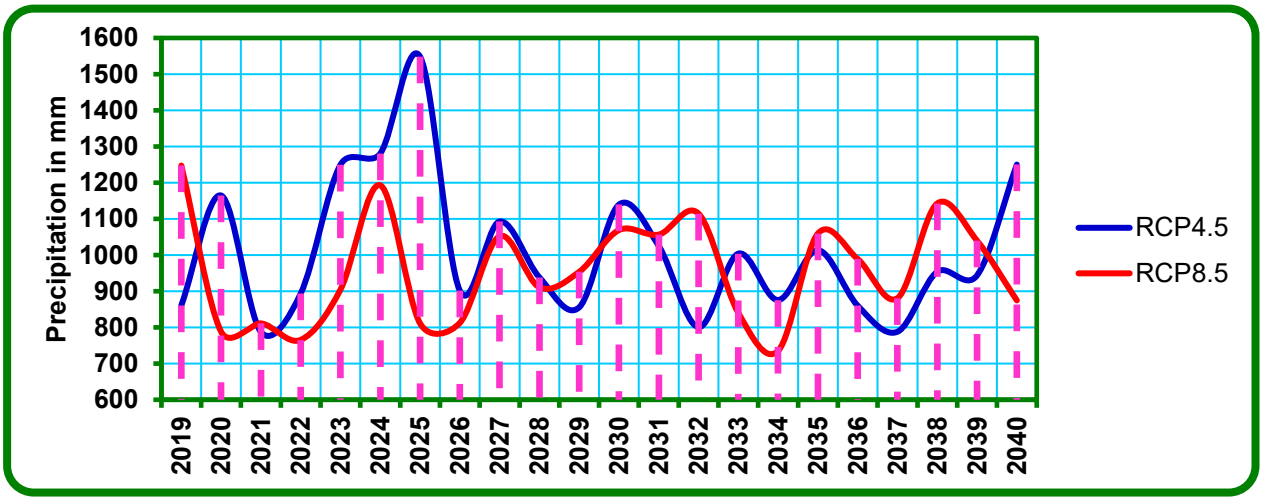

Figure b1: UARB Annual Average Rainfall under RCP Scenarios for the Period 2019 – 2040

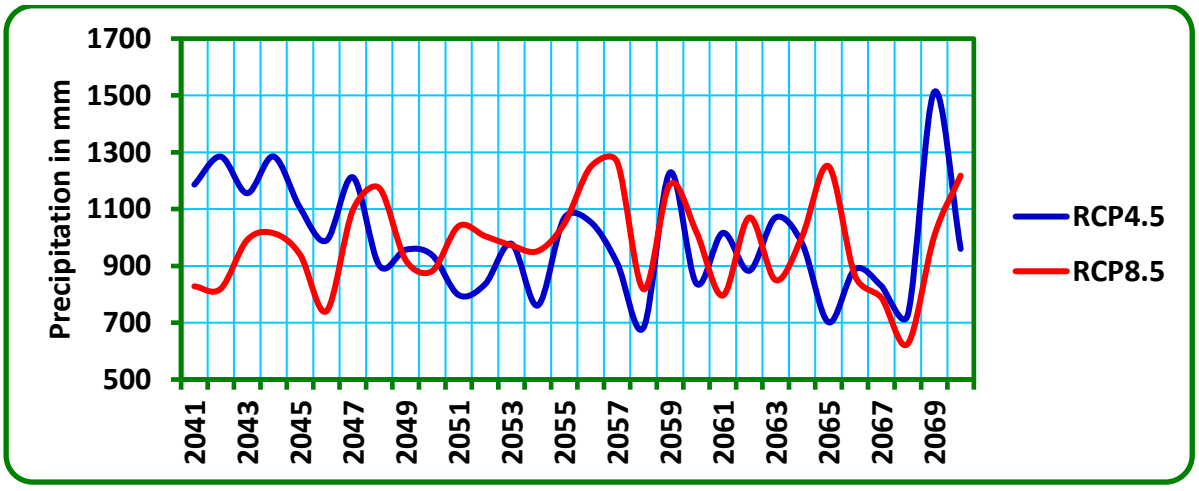

Figure b2: UARB Annual Average Rainfall under RCP Scenarios for the Period 2041 – 2070

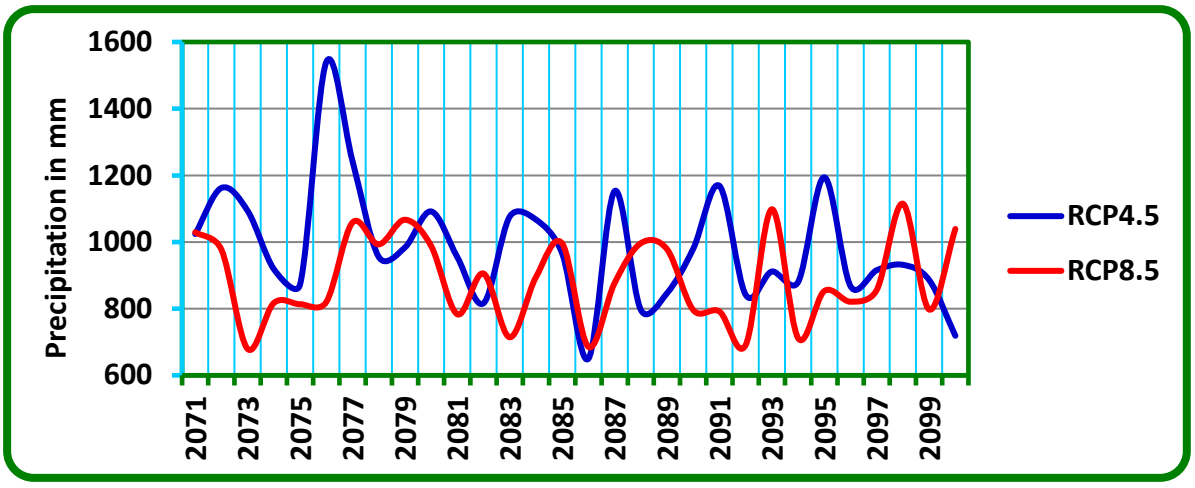

Figure b3: UARB Annual Average Rainfall under RCP Scenarios for the Period 2071 – 2100

C) Koka Reservoir Storage

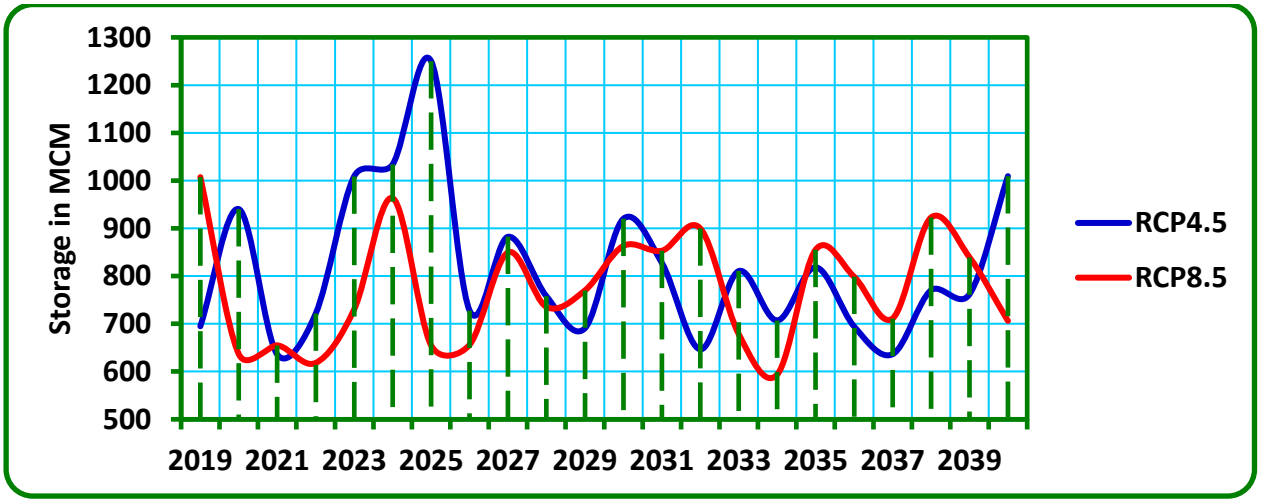

Figure c1: Koka Annual Average Storage under RCP Scenarios for the Period 2019 – 2040

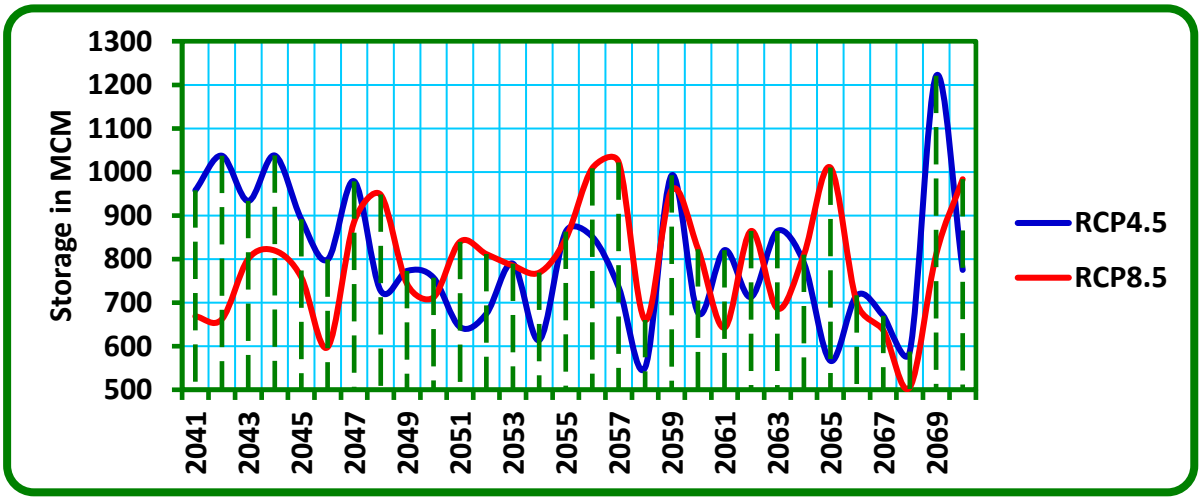

Figure c2: Koka Annual Average Storage under RCP Scenarios for the Period 2041 – 2070

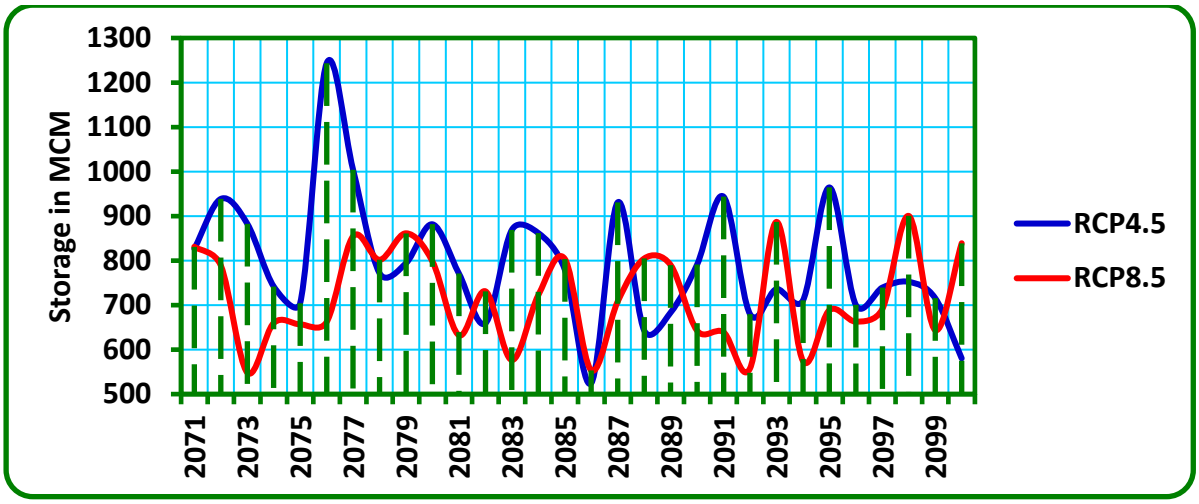

Figure c3: Koka Annual Average Storage under RCP Scenarios for the Period 2071 – 2100

d) Average Annual Inflow into Koka Reservoir

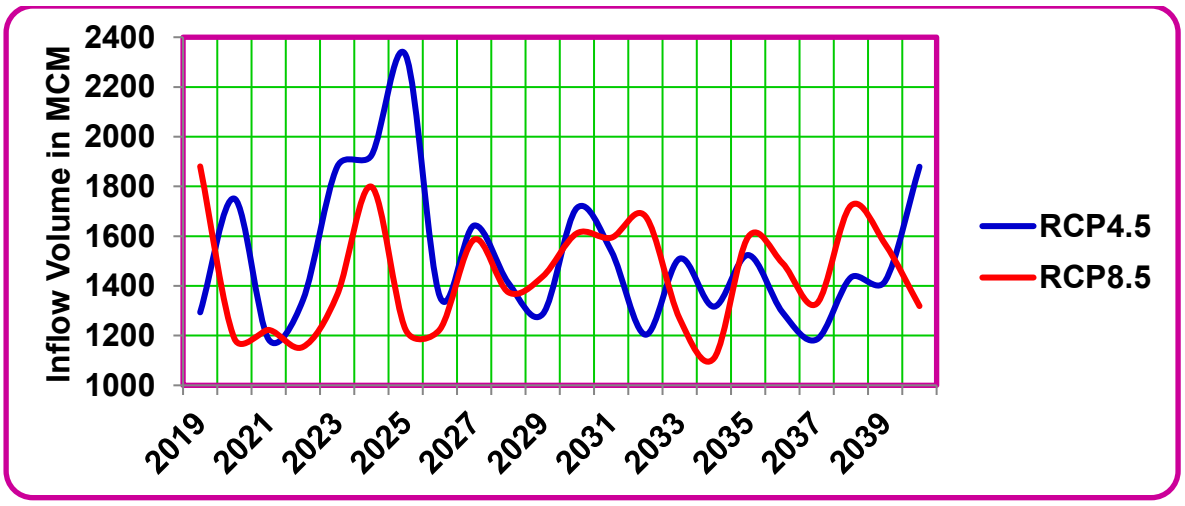

Figure d1: Annual Average Inflow Volume into Koka Reservoir under RCP Climate Change Scenarios for the Period 2019 – 2040

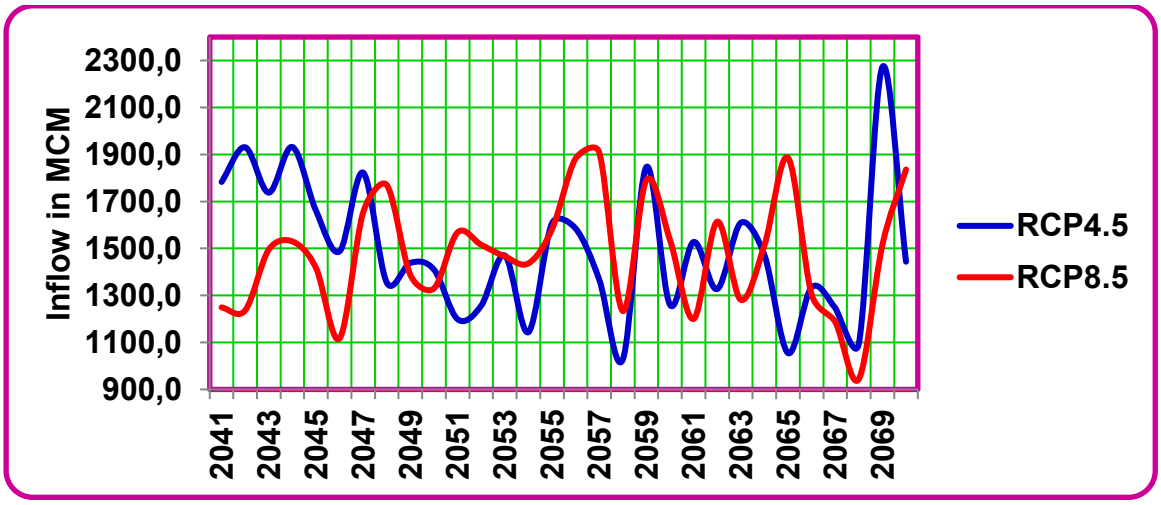

Figure d2: Annual Average Inflow Volume into Koka Reservoir under RCP Climate Change Scenarios for the Period 2041 – 2070

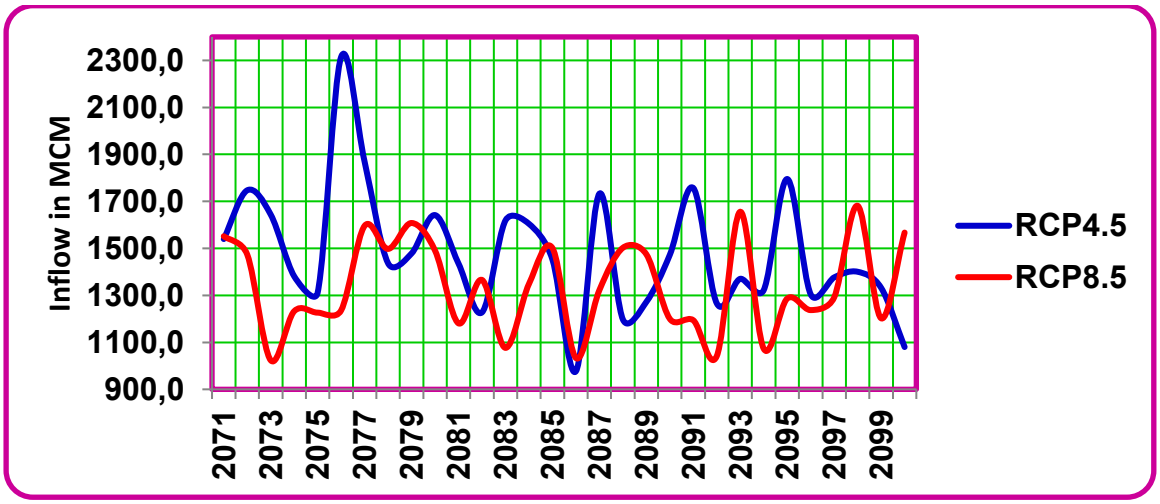

Figure d3: Annual Average Inflow Volume into Koka Reservoir under RCP Climate Change Scenarios for the Period 2071 – 2100

e) Average Annual Koka Reservoir Evaporation

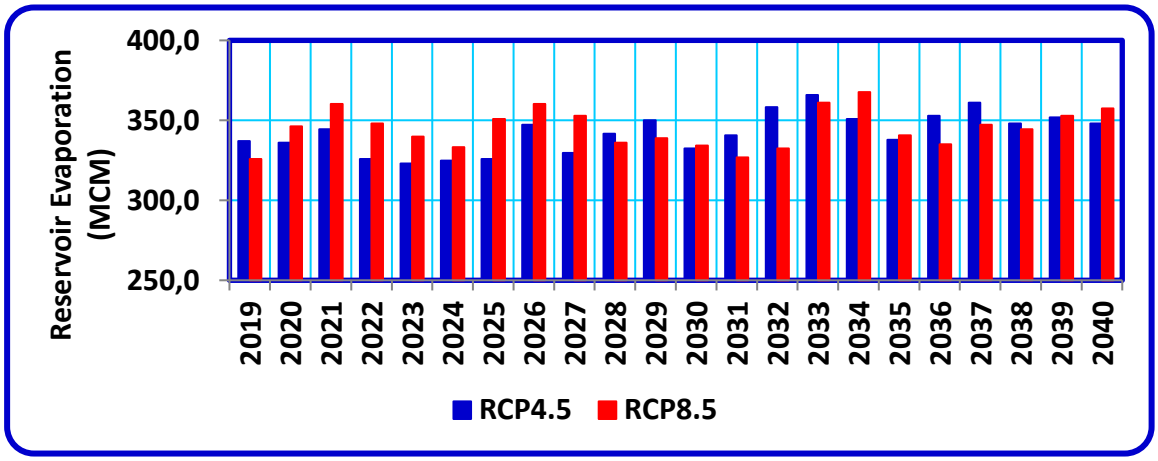

Figure e1: UARB Annual Average Evaporation under RCP Scenarios for the Period 2019 – 2040

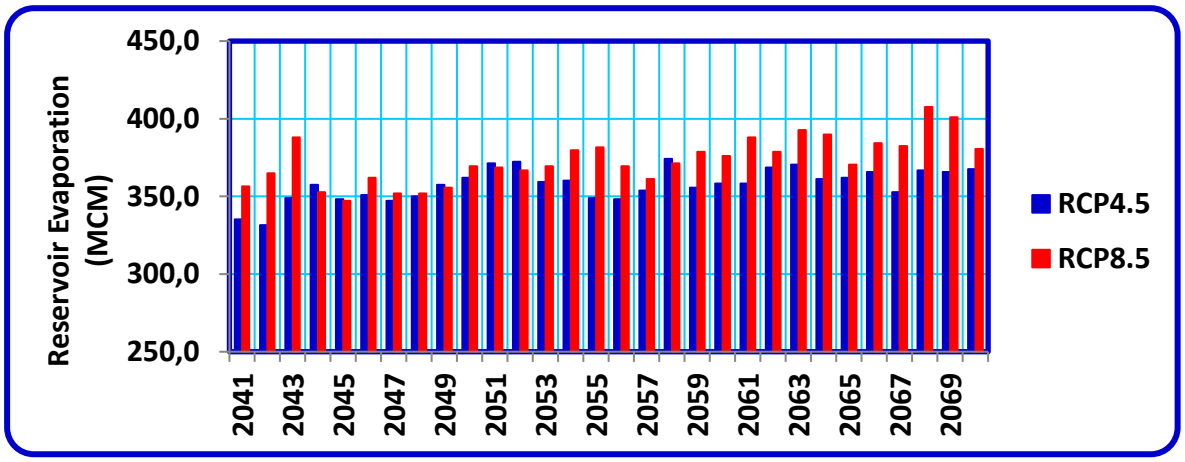

Figure e2: UARB Annual Average Evaporation under RCP Scenarios for the Period 2041 – 2070

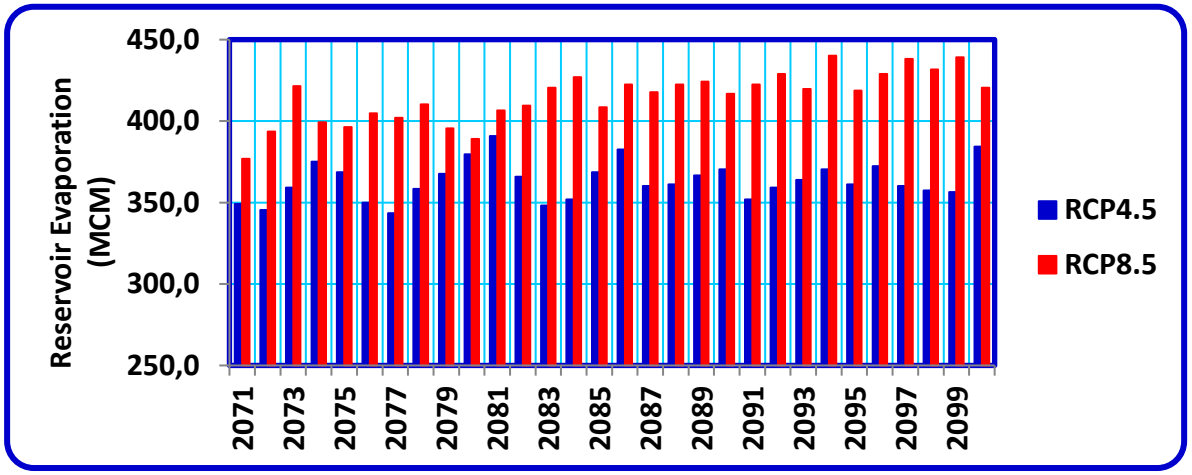

Figure e3: UARB Annual Average Evaporation under RCP Scenarios for the Period 2071 – 2100